



This is to certify that the

thesis entitled

*The Development of Salt Weathering
and Honeycomb Weathering in Carboniferous
Sandstones in the Mid-Western United States.*

presented by

John Barnes Sallman, III

has been accepted towards fulfillment
of the requirements for

M. S. degree in *Geological Sciences*

Michael Anthony Vellos

Major professor

Date *15 APRIL 1996*

LIBRARY
Michigan State
University

PLACE IN RETURN BOX to remove this checkout from your record.
TO AVOID FINES return on or before date due.

DATE DUE	DATE DUE	DATE DUE
JUL 05 1999	_____	_____
APR 12 2006	_____	_____
_____	_____	_____
_____	_____	_____
_____	_____	_____
_____	_____	_____
_____	_____	_____

THE DEVEL
WEATHERIN

**THE DEVELOPMENT OF SALT WEATHERING AND HONEYCOMB
WEATHERING ON CARBONIFEROUS SANDSTONES IN THE MID-
WESTERN UNITED STATES**

By

John Barnes Sallman, III

A THESIS

Submitted to
Michigan State University
in partial fulfillment of the requirements
for the degree of

MASTER OF SCIENCE

Department of Geological Sciences

1996

THE DEVELOPMENT OF
WEATHERING

Outcrops
sandstones or
determine whether
honeycomb
hypothesized
observations
weathering is
oxyhydroxid
outcrops su
controls hor

Iron
the develop
lichens and
hardening
The organi
cavities to
oxyhydrox
further we

ABSTRACT

THE DEVELOPMENT OF SALT WEATHERING AND HONEYCOMB WEATHERING OF CARBONIFEROUS SANDSTONES IN THE MID-WESTERN UNITED STATES

By

John Barnes Sallman, III

Outcrops exhibiting honeycomb weathering in Carboniferous sandstones of the temperate, mid-continental Midwest were studied to determine which outcrop characteristics may control the development of honeycomb weathering. Salt weathering of sandstone has long been hypothesized to control honeycomb formation. Field and laboratory observations suggest that salt weathering may be a precursor to honeycomb weathering in some cases. However, in the areas studied, the ubiquity of iron oxyhydroxide case-hardening and other characteristic iron structures in the outcrops suggest that the distribution/mobilization of iron in the rocks controls honeycomb development.

Iron diffusion is invoked as the basis for a new geochemical model for the development of honeycomb weathering. Organic acids from plants, lichens and other biota reduce and dissolve the ferric oxyhydroxide case-hardening on the sandstone surface, mobilizing the reduced ferrous iron. The organic acids then transport iron away from newly formed honeycomb cavities to honeycomb walls where the iron reprecipitates as ferric oxyhydroxides, strengthening the walls and making them more resistant to further weathering.

All praise
go to Jesus Christ
presence helped

Dr. Mich
to meet with me
comments add
made for a be
during our me

Next, I
Larson and D
made my job

My wife
when I was d
helped me to

My p
constant enc

Partia
Society and

ACKNOWLEDGEMENTS

All praise and thanks for this thesis and all of the work that went into go to Jesus Christ my Lord and Savior. His unconditional love and constant presence helped make this project a lot less stressful.

Dr. Michael A. Velbel also deserves thanks for always making the time to meet with me. His encouragement and ideas were appreciated. His comments added substantial data to this thesis and his editorial comments made for a better manuscript. I always enjoyed his sarcasm and cynicism during our meetings. Our long talks and discussions will be missed.

Next, I would like to thank my committee members, Dr. Grahame Larson and Dr. Duncan Sibley. Their helpful comments and suggestions made my job a lot easier.

My wife, Kelli, also deserves a lot of thanks. She always supported me when I was down and made me a much cheerier person. Her encouragement helped me to complete this project in two years.

My parents also deserve a word of thanks for their financial and constant encouragement.

Partial funding for this project was provided by the Clay Minerals Society and the Michigan Basin Geological Society.

CHAPTER 1 - INTRODUCTION

PURPOSE

PREVIOUS

History

Safety

Literature

Summary

HYPOTHESIS

METHODS

CHAPTER 2 - MATERIALS

MATERIALS

Introduction

History

Applications

LINCOLN

Virginia

VIRGINIA

CHAPTER 3 - CONCLUSIONS

INTRODUCTION

CONCLUSIONS

CHAPTER 4 - DISCUSSION

DISCUSSION

INTRODUCTION

DISCUSSION

CONCLUSIONS

TABLE OF CONTENTS

CHAPTER 1 - INTRODUCTION	1
PURPOSE AND SCOPE	4
PREVIOUS WORK.....	4
Honeycomb Weathering.....	4
Salt Weathering	12
Liesegang Banding.....	14
Surficial Geology	15
HYPOTHESIS.....	22
METHODS.....	22
CHAPTER 2 - SALT WEATHERING	24
MORRILL HALL	24
Introduction.....	24
Halite	30
Alunite.....	36
LINCOLN BRICK PARK AND FITZGERALD PARK.....	39
Introduction.....	39
Hydrous Iron Sulfate Efflorescence.....	42
VIRGINIA KENDALL LEDGES PARK	44
Introduction.....	44
Taranakite.....	44
Summary	46
CHAPTER 3 - HONEYCOMB WEATHERING.....	50
INTRODUCTION	50
COMPARISON OF HONEYCOMB WEATHERING.....	54
Salt Weathering	54
Iron Oxyhydroxides	57
Mineralogy and Clay Content	71
Aspect	71
Grain Size and Sorting.....	74
Bedding Characteristics.....	74
Presence of Lichen/ Algae.....	78
Discussion.....	80
CHAPTER 4 - GEOCHEMICAL MODEL FOR HONEYCOMB FORMATION	82
INTRODUCTION	82
DISCUSSION	83
Ion Sources for Iron Oxyhydroxides and Gypsum.....	83
Liesegang Banding and Self-Organization	84
Ground Water Ferricretes.....	86
Precipitation of Iron on the Rock Surface	
Ferruginization/Case-Hardening.....	87
Dissolution of Iron Oxides from the Rock Surface.....	89
Gypsum Efflorescence and Acid Environments.....	95
CONCLUSIONS	99

CHAPTER 5 -
SUMM
CONCI
SUGGE
APPENDICES
APPEN

APP

APP

APP

AP

AP

AP

AP

CHAPTER 5 - SUMMARY AND CONCLUSIONS.....	100
SUMMARY.....	100
CONCLUSIONS	101
SUGGESTIONS FOR FUTURE WORK.....	102
APPENDICES.....	104
APPENDIX A	
SANDSTONE DESCRIPTIONS	105
Michigan	
Eaton Sandstone, Fitzgerald Park and Lincoln Brick Park, Grand Ledge.....	105
Jacobsville Sandstone - Morrill Hall.....	107
Indiana	
Mansfield Sandstone, Turkey Run State Park.....	108
Illinois	
Pounds Sandstone, Ferne Clyffe State Park.....	109
Kentucky	
Caseyville Sandstone, Pennyrile State Park and Hawesville, Kentucky	111
Tar Springs Sandstone, Cloverport, Kentucky	113
Ohio	
Berea Sandstone, Holden Arboretum, Ohio.....	116
Black Hand Sandstone, Black Hand State Nature Preserve, Toboso, Ohio.....	117
Sharon Conglomerate, Cuyahoga Valley National Recreation Area, Ohio.....	119
APPENDIX B	
SITE LOCATIONS.....	123
APPENDIX C	
POINT COUNT DATA.....	135
APPENDIX D	
XRD AND EDS ANALYSIS RESULTS FOR SALT WEATHERING.....	136
APPENDIX E	
X-RAY DIFFRACTION DATA FOR HALITE AT MORRILL HALL	137
APPENDIX F	
X-RAY DIFFRACTION DATA FOR ALUNITE AT MORRILL HALL	139
APPENDIX G	
X-RAY DIFFRACTION DATA FOR HALOTRICHITE AT LINCOLN BRICK PARK AND FITZGERALD PARK.....	140
APPENDIX H	
X-RAY DIFFRACTION DATA FOR AMARANTITE AT LINCOLN BRICK PARK	142

APPEND

X-

LI

APPEND

X

V

APPEND

E

W

APPEND

X

E

APPEN

S

F

T

H

D

H

V

F

F

BIBLIOGRAP

APPENDIX I	
X-RAY DIFFRACTION DATA FOR ROZENITE AT LINCOLN BRICK PARK	143
APPENDIX J	
X-RAY DIFFRACTION DATA FOR TARANAKITE AT VIRGINIA KENDALL LEDGES PARK	144
APPENDIX K	
EDS AND XRD RESULTS FOR HONEYCOMB WEATHERING.....	145
APPENDIX L	
X-RAY DIFFRACTION DATA FOR GYPSUM EFFLORESCENCE.....	146
APPENDIX M	
SITE DESCRIPTIONS OF HONEYCOMB WEATHERING.....	149
Fitzgerald Park.....	149
Turkey Run State Park.....	151
Hawesville and Cloverport, Kentucky.....	152
Pennyrile State Park.....	153
Hocking Hills State Park.....	156
Virginia Kendall Ledges Park.....	158
Holden Arboretum.....	159
Black Hand Gorge	160
BIBLIOGRAPHY.....	162

Table 1 Previous
Table 2 Classific
Mottersh
Table 3 Point co
cavities.
the cavit
Table 4 Point co
Table 5 X-ray d
results f
Table 6 X-ray d
Table 7 X-ray d
Table 8 X-ray d
Brick Pa
Table 9 X-ray d
Brick Pa
Table 10 X-ray d
Park. ...
Table 11 X-ray d
Kendal
Table 12 X-ray d
results
Table 13 X-ray c
honeyc

LIST OF TABLES

Table 1	Previous hypotheses for the origin of honeycomb weathering.	52
Table 2	Classification of honeycomb weathering intensities used by Mottershead (1994).....	53
Table 3	Point count data for honeycomb walls versus honeycomb cavities. Iron cement is almost doubled in the walls relative to the cavities.....	70
Table 4	Point count data for figure 3. Data reported as number of count.....	135
Table 5	X-ray diffraction and energy dispersive spectroscopy analysis results for salts for present in occurrences of salt weathering.	136
Table 6	X-ray diffraction data for halite efflorescence at Morrill Hall.	137
Table 7	X-ray diffraction data for alunite efflorescence at Morrill Hall.....	139
Table 8	X-ray diffraction data for halotrichite efflorescence at Lincoln Brick Park and Fitzgerald Park.	140
Table 9	X-ray diffraction data for amarantite efflorescence at Lincoln Brick Park.....	142
Table 10	X-ray diffraction data for rozenite efflorescence at Lincoln Brick Park.	143
Table 11	X-ray diffraction data for taranakite efflorescence at Virginia Kendall Ledges Park.	144
Table 12	X-ray diffraction and energy dispersive spectroscopy analysis results for salts associated with honeycomb weathering.	145
Table 13	X-ray diffraction data for gypsum efflorescence associated with honeycomb weathering.....	146

Figure 1
Honeyc
Kentuck
Route 6

Figure 2
Locatio

Figure 3
Ternary
Carbon

Figure 4
Percent

Figure 5
Percent
studied

Figure 6
Weathe
the des
build u

Figure 7
Small i
salt eff

Figure 8
a) Larg
Hall.
uniform

Figure 9
Halite
solid a
rise of
mover
rise....

Figure 10
Erode
the sa
the m

Figure 11
SEM |
betwe
the gr

Figure 12
Aluni
Hall.

LIST OF FIGURES

Figure 1	Honeycomb weathered sandstone in west of Cloverport, Kentucky in the southwest corner of the intersection of U.S. Route 60 and Kentucky Route 144.	2
Figure 2	Location of study areas in the Mid-West.	3
Figure 3	Ternary diagram showing modal mineralogy of the Carboniferous sandstones.	19
Figure 4	Percent minerals present in the sandstones other than quartz.	20
Figure 5	Percent porosity and percent iron cement in the sandstones studied.	21
Figure 6	Weathered pillar base from Morrill Hall. The picture shows a) the destruction of the decorative sculpturing, b) the efflorescence build up and c) the grit/loess development.	25
Figure 7	Small indentations (incipient honeycomb weathering) created by salt efflorescence at Morrill Hall.	27
Figure 8	a) Large indentation weathered into a sandstone block at Morrill Hall. Note the depth of the indentation. b) Example of the non-uniform, convex fashioning of the sandstone blocks.	28
Figure 9	Halite infiltration and movement inside a sandstone block. The solid arrow indicates the infiltration and subsequent capillary rise of the water-halite solution. The striped arrow indicates the movement of the water-halite solution as temperatures begin to rise.	33
Figure 10	Eroded pillar showing the maximum height of capillary rise in the sandstone at Morrill Hall. The black line on the pillar marks the maximum height (approximately 8 inches).	34
Figure 11	SEM photograph showing halite efflorescence (a) growing between sand grains (b) at Morrill Hall. The halite is pushing the grains apart.	35
Figure 12	Alunite (A) replacing a potassium feldspar sand grain at Morrill Hall. Note the rhombohedral habit of alunite.	38

Figure 13
Efflorescence
portion
with a

Figure 14
Outcro

Figure 15
Fibrou

Figure 16
Outcro
Ledges
area in
over th
efflore
wide...

Figure 17
SEM p
Park.

Figure 18
Efflore
cavities

Figure 19
Efflore
in whi
in Hoc
honey

Figure 20
Groun
Illinoi
and br

Figure 21
Piece
Clyffe
sands

Figure 22
Sub-li
Park,

Figure 23
Conce

Figure 24
"Flam
struct
draw

Figure 25
Indiv
State

Figure 13	Efflorescence on the shale bed in Lincoln Brick Park. The lower portion of the picture contains the shale bed which is coated with a white crust or efflorescence.....	40
Figure 14	Outcrop area in Fitzgerald Park containing salt weathering.....	41
Figure 15	Fibrous crystal habit of halotrichite as seen under the SEM.	43
Figure 16	Outcrop photograph of area below the seep at Virginia Kendall Ledges. Note honeycomb cells in the picture. The buff colored area in the photograph is the area where the seep water washes over the rock face. The white substance on the stone is the efflorescence. The band of taranakite is approximately one inch wide.....	48
Figure 17	SEM photograph of taranakite from Virginia Kendall Ledges Park. Note the clay-like hexagonal sheet structure.	49
Figure 18	Efflorescence growing inside recently formed honeycomb cavities at Black Hand Gorge State Nature Preserve, Ohio.	55
Figure 19	Efflorescence growing on the walls of older honeycomb cavities in which the honeycomb walls are retreating at Old Man's Cave in Hocking Hills State Park. Note the black color of the honeycomb walls as compared to the honeycomb cavities.....	56
Figure 20	Groundwater ferricrete in Ferne Clyffe State Park in southern Illinois. The ferricrete is the dark band above the ground surface and below the red key ring in the picture.....	60
Figure 21	Piece of a ferricrete tube taken from the same outcrop in Ferne Clyffe State Park. Note the ironstone rim and the "clean" sandstone inside the tube.....	61
Figure 22	Sub-linear, sub-parallel Liesegang banding in Giant City State Park, southern Illinois.....	62
Figure 23	Concentric Liesegang banding in Giant City State Park.....	63
Figure 24	"Flame-type" Liesegang structures in Giant City State Park. The structures are most likely the result of iron-rich waters being drawn up in the capillary fringe in an ancient aquifer.....	64
Figure 25	Individual iron cemented circles in a sandstone in Giant City State Park.	65

Figure 26
Co.
hoi

Figure 27
Ho
pre
cav

Figure 28
Ho
in E

Figure 29
Sch
wal

Figure 30
Ros
wea

Figure 31
Hor
Clo
deve
the l

Figure 32
Hon
piece

Figure 33
Lich
on L
porti
weat
liche
cells
prev

Figure 34
A un
surfa

Figure 35
The
Repr
oxyh
repre
wher
arrov
the d

Figure 26	Coalescing iron-cemented rings that have weathered to create honeycomb-like cells in the rock face at Ferne Clyffe State Park.....	66
Figure 27	Honeycomb weathering occurring in iron oxyhydroxide precipitates at Turkey Run State Park, Indiana. Honeycomb cavity (a), honeycomb wall (b) and fracture (c).....	67
Figure 28	Honeycomb development along resistant bedding plane ridges in Black Hand Gorge State Nature Preserve, Ohio.....	68
Figure 29	Schematic cross section of a honeycomb cell, A) honeycomb walls, B) honeycomb cavity.	69
Figure 30	Rose diagram showing the range aspects of honeycomb weathered outcrops.	73
Figure 31	Honeycomb weathering in the roof of an overhang in west of Cloverport, Kentucky. Note the smaller honeycomb development within the larger honeycomb cavities. Also note the Liesegang banding in the sandstone.....	76
Figure 32	Honeycomb weathering development parallel to bedding in a piece of float in Ferne Clyffe State Park, Illinois.	77
Figure 33	Lichen/algae growth in association with honeycomb weathering on Little Mountain in Holden Arboretum. The left hand portion of the photo (a) contains excellent honeycomb weathering. The right hand portion of the photo (b) contains lichen/algae growth that appears to be destroying honeycomb cells. Rounded humps outlining degraded honeycomb walls are prevalent on the lichen covered side of the picture.	79
Figure 34	A uniformly thick case-hardened skin forming at the outcrop surface. The skin may also have a more undulatory expression. The dark stippled area represents the case-hardened zone.	88
Figure 35	Representation of preferential organic acid attack on iron oxyhydroxide case-hardened sandstone. The larger stipples represent the iron enriched zone. Honeycomb cavities form where instabilities are present at the iron-enriched zone. The arrows leading away from the newly forming cavities represent the diffusion of chelated iron from the forming cavities.....	93

- Figure 36
Diagra
breach
the fer
cavities
12 cm.
diame
- Figure 37
Lentic
substa
Ledge
- Figure 38
Elong
condit
- Figure 39
Locati
- Figure 40
Locati
Indian
- Figure 41
Locati
Illinoi
- Figure 42
Locati
Kentu
- Figure 43
Locati
Kentu
- Figure 44
Locati
Kentu
- Figure 45
Locati
- Figure 46
Locati
- Figure 47
Locati
Ohio.
- Figure 48
Locati
Ohio.
- Figure 49
Locati
Ohio..

Figure 36	Diagram showing iron concentrations after case-hardening is breached and honeycomb formation. The dark stipples represent the ferruginous honeycomb walls. The width of the honeycomb cavities is indicated by "d," which ranges in diameter from 5 to 12 cm. This width is representative of honeycomb cavity diameters.	94
Figure 37	Lenticular or tabular gypsum crystal habit resulting from organic substances acting as c-axis growth inhibitors at Virginia Kendall Ledges Park.	97
Figure 38	Elongate, prismatic gypsum crystal habit resulting from acid conditions at Stebbins Gulch in Holden Arboretum.	98
Figure 39	Location of Study Areas in Grand Ledge, Michigan.	123
Figure 40	Location of Study Area in Turkey Run State Park, West-Central Indiana.	124
Figure 41	Location of Study Area in Ferne Clyffe State Park, Southern Illinois.	125
Figure 42	Location of Study Area in Pennyryle State Park, Western Kentucky.	126
Figure 43	Location of Indian Lake Study Area East of Hawesville, Kentucky.	127
Figure 44	Location of Tar Springs Study Area West of Cloverport, Kentucky.	128
Figure 45	Location of Study Areas in Holden Arboretum, Ohio.	129
Figure 46	Location of Black Hand Gorge Study Area in Central Ohio.	130
Figure 47	Location of Old Mans Cave Study Area, Hocking Hills State Park, Ohio.	131
Figure 48	Location of Cedar Falls Study Area, Hocking Hills State Park, Ohio.	132
Figure 49	Location of Ash Cave Study Area, Hocking Hills State Park, Ohio.	133

Figure 50
Location
Cuyahoc

Figure 50

**Location of Virginia Kendall Ledges Park Study Area in
Cuyahoga Falls National Recreation Area, Ohio.....134**

This is
distinctive w
occurring in
(Figure 2).
coastlines (Mottershead
weathering p
honeycomb
coastal envi
types includ
Other exampl
Hawaiian pa
weathering,
1982).

Report
throughout t
more than c
honeycomb
where the h
areas, little
problematic

CHAPTER 1 - INTRODUCTION

This investigation examines salt weathering and a geomorphologically distinctive weathering pattern known as honeycomb weathering (Figure 1), occurring in Carboniferous sandstones of the Mid-Western United States (Figure 2). These features typically occur at the edges of deserts and along coastlines (Mustoe, 1982 and 1984; Gill et al., 1979; McGreevy, 1984; Mottershead, 1994). However, many examples of these characteristic weathering patterns do occur in temperate, humid and Arctic climates, thus honeycomb weathering does not necessarily occur primarily in desert and coastal environments. Honeycomb weathering is reported in several rock types including sandstone, limestone, metamorphic and volcanic rocks. Other examples of honeycombs exist where erosion has enlarged vesicles in Hawaiian pahoehoe lave flows (Mustoe, 1982). Most examples of honeycomb weathering, however, occur in texturally homogenous sandstones (Mustoe, 1982).

Reports of honeycomb weathering from diverse environments throughout the world suggest that honeycomb weathering may result from more than one cause (Mustoe, 1982). The presence of salts within the honeycomb structures is a common occurrence in coastal and desert areas where the honeycombing is linked to salt weathering. However, in inland areas, little or no salt is found in the honeycombs, making their origin problematical (Robinson and Williams, 1994).

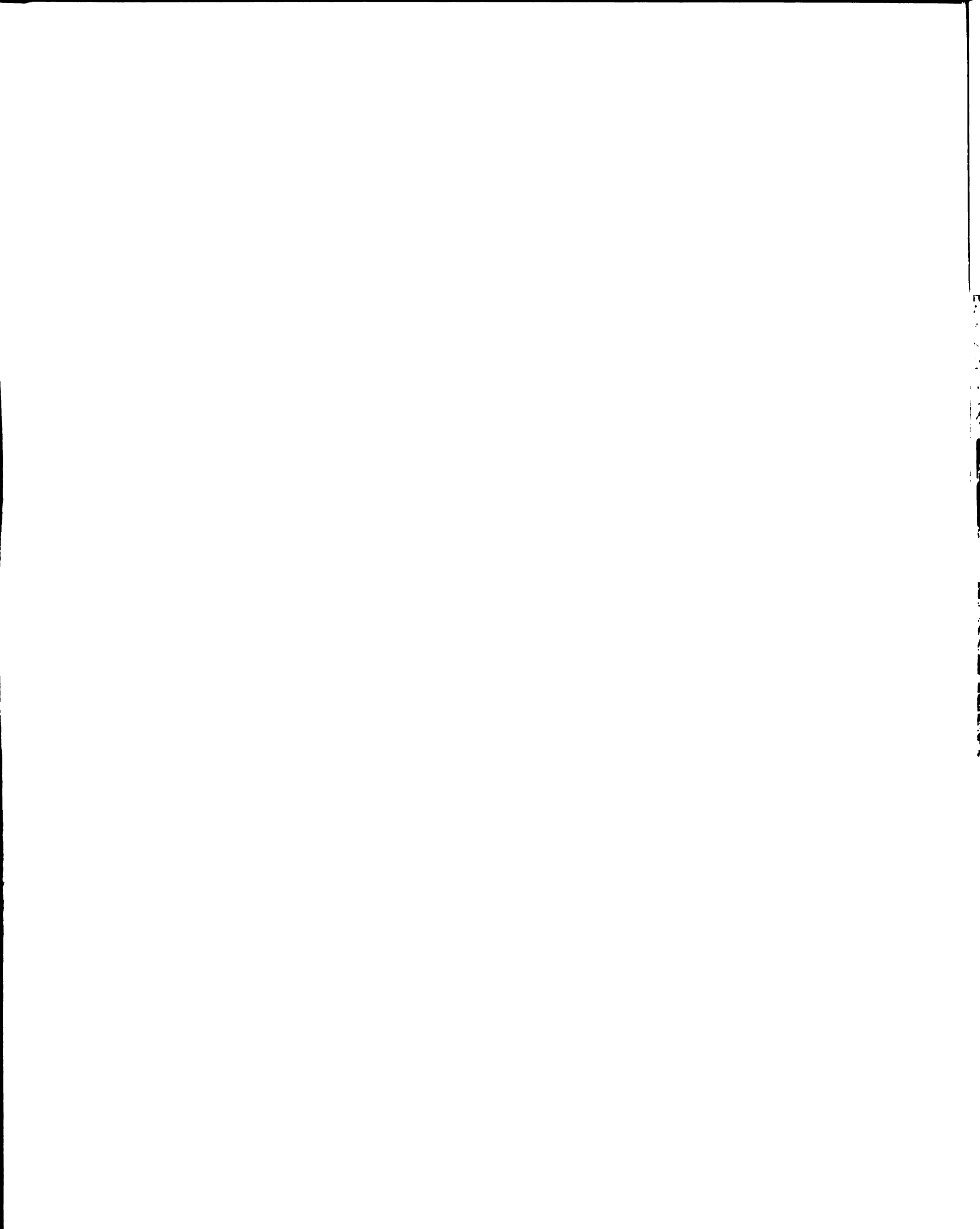


Figure 1

Honeycomb weathered sandstone in west of Cloverport, Kentucky in the southwest corner of the intersection of U.S. Route 60 and Kentucky Route 144.

Figure 2



Location of study areas in the Mid-West.

1. Fitzgerald Park and Lincoln Brick Park, Grand Ledge, Michigan.
2. Holden Arboretum, Kirtland, Ohio.
3. Virginia Kendall Ledges, Cuyahoga Valley National Recreation Area, Ohio.
4. Black Hand Gorge State Nature Preserve, Toboso, Ohio.
5. Hocking Hills State Park (Old Man's Cave, Ash Cave, Cedar Falls), Ohio.
6. Turkey Run State Park, Western Indiana.
7. Tar Springs Sandstone west of Cloverport, Kentucky.
8. Caseyville Sandstone east of Hawesville, Kentucky.
9. Pennyrile State Park, Western Kentucky.
10. Ferne Clyffe State Park, Goreville, Illinois.
11. Giant City State Park, southern Illinois.

The purp
at the outcrop th
salt weathering
weathering in c
to determine t
temperate regio
areas may form
Additionally, fe
proposed hypo
chemical or min

Honeycomb We

Sandston
surface, yet th
features has b
(Robinson and
regarded as c
sandstone wea
has become inc
in the near su
Williams, 199
environments

PURPOSE AND SCOPE

The purpose of this investigation is to determine the variables existing at the outcrop that influence the occurrence of honeycomb weathering and/or salt weathering. Many studies have been completed on honeycomb weathering in coastal and desert environments, but very few have attempted to determine the causes of honeycomb weathering in mid-continental, temperate regions. Honeycomb weathering in temperate, mid-continental areas may form by different mechanisms than in desert or coastal regions. Additionally, few attempts have been made to test any of the previously proposed hypotheses for the formation of honeycomb weathering using chemical or mineralogical studies (Mustoe, 1982).

PREVIOUS WORK

Honeycomb Weathering

Sandstone is estimated to occupy approximately 15% of the Earth's land surface, yet the systematic study of sandstone weathering and landform features has been largely overlooked, especially in temperate climates (Robinson and Williams, 1994). In the past, sandstones were traditionally regarded as chemically inert because of quartz's low solubility. Thus, sandstone weathering has typically been attributed to physical processes. It has become increasingly evident that quartz dissolution is far more important in the near surface environment than previously thought (Robinson and Williams, 1994). Weathering processes in the surface and sub-surface environments act on the sandstone to weaken and/or disintegrate the rock or

lead to a tough
and Williams,

Three g

cavernous we
weathering (al
weathering ten
hardened crust
the weathering
on the outer su
ground surface
Astor, 1987). A

the further deve
rock beneath th
hollows in cave
the hardened c
overhang as the
(Mabbutt, 1979).

rock structures
characteristic la
1979). Caverno
ground surface

Tafoni occ

weathering (me
meters above th
occur on smalle
Rossman, 1982).

characteristic of

lead to a toughening or hardening of the outer surface of the rock (Robinson and Williams, 1994).

Three geomorphic weathering patterns are often lumped together as cavernous weathering: cavernous weathering, tafoni and honeycomb weathering (also called alveolar weathering) (Mabbutt, 1979). Cavernous weathering tends to occur in arid, desert climates where the combination of a hardened crust and a weakened under-layer are critical for the formation of the weathering pattern (Mabbutt, 1979). After a case-hardened layer develops on the outer surface of the rock, infiltration of water into the rock from the ground surface weakens the rock beneath the case-hardened layer (Conca and Astor, 1987). At any point where the crust has been breached by weathering, the further development of a cavity is favored at the expense of the weakened rock beneath the case-hardened layer (Mabbutt, 1979). The growth of the hollows in cavernous weathering tends to be upwards and inwards beneath the hardened crust (Mabbutt, 1979). The crust often forms a canopy-like overhang as the growth of the cavity continues beneath the hardened crust (Mabbutt, 1979). Cavernous weathering tends to be controlled by large-scale rock structures such as joint zones and large-scale bedding, allowing the characteristic large hollows several meters in diameter to form (Mabbutt, 1979). Cavernous weathering is generally located in direct contact with the ground surface (Conca and Rossman, 1982).

Tafoni occur on the same scale and by the same processes as cavernous weathering (meters in diameter), but are typically located one to several meters above the soil surface (Conca and Rossman, 1982). Tafoni may also occur on smaller size scales on the order of tens of centimeters (Conca and Rossman, 1982). Honeycomb weathering, also termed alveolar weathering, is characteristic of sandstone facies, but also occurs in crystalline rocks (Mabbutt,

1979). The d
structural cor
reflects contr
and well ind
shallow and
hardened zon
are hardened
relief (Mabbu
typically only
honeycombs m
can be disting
typically broad
typically occur
1979).

Mustoe (
occur in textura
shattering and
honeycomb-type
attributed to th
deterioration o
presence of salt

Mustoe
honeycomb w
microscopic alg
together as pro
results from th
chemically resu

1979). The development of honeycomb weathering exhibits a finer scale of structural control (Mabbutt, 1979). Commonly, honeycombing is regular and reflects control by the minor bedding and joint planes that are well cemented and well indurated (Mabbutt, 1979). Honeycomb weathering is generally shallow and exploits the softened subsurface layer beneath a thin case-hardened zone (Mabbutt, 1979). The walls separating the honeycomb cavities are hardened and become increasingly indurated as they are decreased in relief (Mabbutt, 1979). The hollows formed by honeycomb weathering are typically only a few centimeters in diameter (Mabbutt, 1979). Tafoni and honeycombs may both form on the same size scale and in the same areas but can be distinguished by their morphology (Gill et al., 1979). Tafoni are typically broadly rounded and do not occur in clusters, whereas, honeycombs typically occur in large groups of cells reminiscent of honeycomb (Gill et al., 1979).

Mustoe (1982) points out that most examples of honeycomb weathering occur in texturally homogenous sandstones. Wind erosion, exfoliation, frost shattering and salt weathering have all been proposed as explanations for honeycomb-type weathering features. Weathering of building stone has been attributed to these same weathering processes. One common factor in the deterioration of some building stones and honeycomb weathering is the presence of salt efflorescence on the stone.

Mustoe (1982) proposes four hypotheses as plausible origins of honeycomb weathering: (1) Honeycomb weathering is controlled by microscopic algae which grow on the septa surfaces and help hold them together as protective organic coatings. (2) Erosion of honeycomb cavities results from the disaggregation of mineral grains either physically or chemically resulting from the repeated evaporation of salt saturated solutions

and subsequent
released by wea
causing the hor
face weathers a
composition (i
sandstones). (4
to hydration re
resulting debri
movements.

Gill et al.
Otway Coast, A
was rebuilt in 1
cement and the
Gill et al. (197
short a time sp
often exhibited
increase of hor
recent times su
1960).

Wallis ar
Ledge, Michiga
finer-grained m
well-developed
prominent bed
authors find si
developing hor
slower in Grand

and subsequent crystallization of salts in the honeycomb cavities. Ions released by weathering within the cavity precipitate on surrounding surfaces, causing the honeycomb walls (septa) to become strengthened. (3) The rock face weathers at different rates because of internal variations in structure or composition (i.e. controlled by depositional or diagenetic facies in sandstones). (4) The cavities develop through a process of exfoliation related to hydration reactions of feldspars in moist sites on the rock surface with the resulting debris being removed by the action of wind, rain and animal movements.

Gill et al. (1979) conducted a study of honeycomb weathering along the Otway Coast, Australia. Their study area contains a section of sea wall that was rebuilt in 1943. Honeycomb weathering patterns are present in both the cement and the greywacke building stone of the rebuilt section of sea wall. Gill et al. (1979) show that honeycomb weathering features can form in as short a time span as 30 years. The youthfulness of honeycomb features is often exhibited on older sandstone buildings (Kelletat, 1980). The strong increase of honeycomb weathering and deterioration of building stone in recent times suggests a relationship with increased air pollution (Kelletat, 1980).

Wallis and Velbel (1985) report on honeycomb weathering at Grand Ledge, Michigan. They determine that honeycomb weathering occurs in the finer-grained micaceous sandstone outcrops in massively bedded units with well-developed tabular-planar cross-bedding. The flaggy sandstones with prominent bedding-plane parting do not exhibit honeycomb weathering. The authors find significant quantities of efflorescent salts in the small, newly developing honeycombs. The rate of honeycomb weathering is significantly slower in Grand Ledge than in coastal or arid regions as evidenced by 60+ year

old carvings in
the rate of honey
the outcrop.

The occur
specific weather
conditions (Arn
water migration
moves in one o
Arnold (1989)
relative humidit
relation to relat

Salt wea
weathering in
(Mustoe, 1982).
sites, with the t
within the rocks
the deposition o
1982). Accordi
precipitate from
with crystal gr
disaggregation o

If salt we
rock outcrops b
controls insolati
of weathering in
facing slopes ev
chemical weathe

old carvings in the sandstone still in existence. This supports the idea that the rate of honeycomb degradation is influenced by the rate of input of salts to the outcrop.

The occurrence of salts on building stone and rock outcrops is related to specific weathering phenomena and particular microclimatic and hydrologic conditions (Arnold, 1984). Salts in porous rocks are strongly connected with water migration through the rock, and become concentrated where water moves in one direction and then evaporates (Arnold, 1987). Zehnder and Arnold (1989) relate deterioration of rock material to salt crystallization and relative humidity. Their study shows that different crystal forms grow in relation to relative humidity and thus, time of the year (i.e. seasons).

Salt weathering is the most popular hypothesis for honeycomb weathering in coastal and desert environments where salt is abundant (Mustoe, 1982). The same hypothesis is also quite often invoked for inland sites, with the transport of salts to the sites resulting from migrating fluids within the rocks, from salts contained within the original sediments, or from the deposition of atmospheric pollutants on the sandstone surface (Mustoe, 1982). According to this hypothesis, salt weathering occurs as salt crystals precipitate from evaporating solutions, inducing volume changes associated with crystal growth or hydration/dehydration of the salts, causing the disaggregation of the rock (Mustoe, 1984).

If salt weathering controls honeycomb development, then aspect of the rock outcrops becomes another important variable. Aspect of the rock face controls insolation and evaporation effects which control the local variations of weathering in a particular region (Ollier, 1984). In colder climates, south facing slopes experience more sunshine which allows more biological and chemical weathering to take place (Ollier, 1984). North-facing slopes tend to

have less biologi

weathering (Oll

While s

honeycomb we

been invoked f

suggest that an

resistant sands

behind. The po

exposing grains

McGreev

salt weathering

experiment sho

along fine-grai

the rock conta

portions of the

is inferred from

wetting and dr

the control san

solutions did

weathering ov

coincident with

along the bedd

role the clay m

more work nee

Bryan (1

the weathering

textures are lik

have less biological and chemical reactivity and show more signs of physical weathering (Ollier, 1984).

While salt weathering is the most common explanation for honeycomb weathering in coastal and desert areas, another explanation has been invoked for intracontinental, mid-latitude areas. Harris et al. (1977) suggest that an iron oxide crust or "case-hardening" is breached, exposing less resistant sandstone, weathering out "little pockets" and leaving thin walls behind. The pockets are places where groundwater has removed the cement, exposing grains that are loosely cemented, which easily erode away.

McGreevy and Smith (1984) discuss the possible role of clay minerals in salt weathering. These workers find that test specimens in a laboratory experiment show preferential flaking of specimens exposed to salt solutions along fine-grained laminations in sandstones. The finer-grained portions of the rock contain more clay in the pore spaces than in the coarser-grained portions of the rock. The clay is smectite (determined by x-ray diffraction). It is inferred from the control specimens that were subjected to the same cyclic wetting and drying that the clays aided in the breakdown of the rock because the control samples did not weather, whereas the samples subjected to salt solutions did weather. The thin smectite-rich layers showed preferential weathering over the coarser-grained areas. These fine-grained areas were coincident with bedding planes; thus the sandstone weathers preferentially along the bedding planes. However, McGreevy and Smith point out that the role the clay minerals play in aiding salt weathering is inconclusive and that more work needs to be done.

Bryan (1925, 1926) suggests that honeycomb weathering results where the weathering is influenced by local variations in permeability. Honeycomb textures are likely to develop on outcrops where cross-bedding features in

sandstones caused
et al. (1979) noted
of the same material
they recognize
suggesting that
matrix of the rock
existence of the

Infiltration

environment is
well as the extent
Astor, 1987).

Antarctica. The
reduce both the
The coating affects
the cavernous
upward through
underlying a coating
the uncoated, e.g.
the surface, causing
intermittent weathering

Mustoe

weathering (i.e.
microscope and
however, finds
aids in silica dissolution
Young (1987) and
wide) along cracks

sandstones cause many small variations in permeability (Mustoe, 1984). Gill et al. (1979) notice that honeycomb weathering is different for different blocks of the same material, indicating a possible lithologic control. Additionally, they recognize that honeycomb cells are often aligned with joint planes, suggesting that honeycombs develop along preferential orientations in the matrix of the rock. However, honeycomb formation does not require the existence of these features (Mustoe, 1982).

Infiltration and subsequent flow of water through rock in a weathering environment is affected by changes in the physical properties of the rock as well as the external conditions to which the rock is subjected (Conca and Astor, 1987). Conca and Astor (1987) investigate the Ferrar dolerite in Antarctica. The dolerite contains coatings of both hematite and quartz, which reduce both the permeability and chemical reactivity of the rock at the surface. The coating affects moisture flow through the rock, which in turn controls the cavernous weathering of the rock. Flow paths of moisture migrating upward through the rock by capillary action are deflected around areas underlying a coated, impermeable surface. Moisture loss is primarily through the uncoated, exposed sides. The sides weather preferentially as compared to the surface, causing cavernous weathering. Gill et al. (1979) state that intermittent wetting occurs at all honeycomb weathering sites.

Mustoe (1982) claims that grains only show signs of physical weathering (i.e. no solution of grains is apparent as observed in a binocular microscope and scanning electron microscope (SEM) (1984)). Young (1987), however, finds that NaCl associated with cavernous weathering in Australia aids in silica dissolution (viewed by SEM), resulting in cavernous weathering. Young (1987) also observes large wedges of salt (up to 20 cm thick and 1 m wide) along cross-bedding and bedding planes in the back of caverns in areas

of Australia w
show the appre
play a role in th
silica dissolutio
enhance quart
involving hydr
cations takes
temperatures (I

Quartz-r

showing differ
minor mineral
may increase t
joints/incisions
the surface, c
evaporates an
Williams, 1994
water into the
strength of the
of honeycomb
Britain and Eu

Williams, 1994

Mustoe

mechanism by
workers large
Mottershead, 1
at least in part

of Australia where cavernous weathering is prevalent. These salt wedges show the appreciable flow of water along the planes of weakness, which may play a role in the cavernous weathering. In support of Young's (1987) view of silica dissolution, Dove and Rimstidt (1994) find that alkali cations indirectly enhance quartz dissolution by promoting a faster dissolution reaction involving hydroxyl ion. The enhancement of quartz dissolution by alkali cations takes place in near neutral pH conditions and at ambient temperatures (Dove, 1994)

Quartz-rich sandstones vary considerably in texture and composition, showing differences in grain size, density, strength, porosity, cement, and minor mineralogy (Robinson and Williams, 1994). Once developed, cliffs may increase their resistance to weathering and erosion because as more joints/incisions form, the rock tends to become drier, drawing moisture to the surface, causing a case-hardening of the surface as the moisture evaporates and minerals precipitate on the rock surface (Robinson and Williams, 1994). These hardened rock surfaces prevent the infiltration of water into the rock from the hardened surface and increase the surface strength of the rock. Gypsum and halite are often found within the hollows of honeycombs along coastal areas; however, in many inland locations in Britain and Europe, little or no salt efflorescence can be found (Robinson and Williams, 1994).

Mustoe (1982) proposed that salt weathering was the dominant mechanism by which honeycomb weathering was developing. Several workers largely accept or support that inference (Takahashi et al., 1994; Mottershead, 1994; Robinson and Williams, 1994). This study was undertaken at least in part to test that hypothesis.

Salt Weathering

Salt wea

(efflorescence)

together loose

from the weath

solution has i

growth of the

solution ensues

precipitation, g

as anthropogen

The process is

removes the pr

to form. It is t

weathering (Mu

The proc

disrupt the roc

1984). Salts in

from solution,

Halite and gY

common salts

mirabilite (N

($MgSO_4 \cdot 6H_2O$)

they are not fo

(Cooke, 1994; s

crystallization

Salt Weathering

Salt weathering is the process by which a thin layer of salt (efflorescence) grows from the rock surface. The salt efflorescence binds together loose grains of the weathered material which the salt has prized from the weathering surface (Wellman and Wilson, 1968). After a salt solution has impregnated the interstices of the weathering surface, the growth of the grains slowly pushes the grains apart as evaporation of the solution ensues (Ollier, 1984). Salts may be provided by air-borne salt particles, precipitation, groundwater, chemical degradation of the rocks themselves or as anthropogenic inputs such as deicing salts (Wellman and Wilson, 1968). The process is renewed again when an erosional agent such as wind or water removes the present salt crust and layer of prized grains, allowing a new crust to form. It is thought that these same processes work to create honeycomb weathering (Mustoe, 1982, 1984).

The processes of crystal growth from solution produce pressures which disrupt the rock, causing it to disaggregate (Winkler and Singer, 1972; Ollier, 1984). Salts in a confined space may cause stress on the rock through growth from solution, thermal expansion, or hydration/dehydration (Ollier, 1984). Halite and gypsum are the most effective salt weathering agents of the common salts (Ollier, 1984). Salts that hydrate and dehydrate easily such as mirabilite ($\text{Na}_2\text{SO}_4 \cdot 10\text{H}_2\text{O}$), epsomite ($\text{MgSO}_4 \cdot 7\text{H}_2\text{O}$) and hexahydrate ($\text{MgSO}_4 \cdot 6\text{H}_2\text{O}$) are the most effective salts involved in salt weathering, but they are not found in salt weathering studies as often as gypsum and halite (Cooke, 1994; Smith and McGreevy, 1983; McGreevy and Smith, 1982). The crystallization pressure of the salts is often of the same order of magnitude as

the tensile strength
and widen microcracks

The chemical weathering
surface area increases
grow at the expense of
Furthermore, vugs
continue to grow
expanding the pore space

Salt weathering
salts in the ground
weathering on
capillary fringe
evidenced by
efflorescence of
between the contact
air temperature
allowing evaporation
(Cooke, 1994).

able to hydrate
which further cements

Smith et al.
sandstone building
hardened layers
hardened layers
accumulation
surface. Common
mechanism by

the tensile strength of the rocks, thus allowing the salts to prize grains apart and widen micro-fractures (Ollier, 1984).

The chemical free energy of a given mass of solid increases as its surface area increases (Wellman and Wilson, 1965). Thus, larger crystals will grow at the expense of the smaller crystals in a saturated solution. Furthermore, when larger crystals completely fill a pore space, they will continue to grow against the constraint imposed by pore walls, thus expanding the pore and fragmenting the rock (Wellman and Wilson, 1965).

Salt weathering appears to be related to capillary rise and availability of salts in the groundwater (Cooke, 1994). Cooke (1994) finds that salt weathering on buildings in Uzbekistan occurs at the ground level where the capillary fringe above the water table meets the building stones and is evidenced by dampness and salt efflorescence on the bricks and mortar. Salt efflorescence on the outside of building walls occurs because of differences between the cooler internal temperature of the brick and the warmer external air temperature, causing moisture movement to the outside wall and allowing evaporation of saline solutions on the outer surface of the wall (Cooke, 1994). Further disruption of the walls may arise from salts which are able to hydrate and dehydrate, causing volume changes in the efflorescence which further disaggregates the wall (Cooke, 1994).

Smith et al. (1994) find that a case hardening of iron oxides on sandstone building blocks may aid in salt weathering. When the case hardened layer is breached, rapid breakdown of the rock beneath the hardened layer occurs due to loss of iron oxide cement or the long-term accumulation of salts by inward migration through a still-porous outer surface. Commonly, once the case hardened layer is breached, flaking is the mechanism by which the newly exposed rock is eroded (Smith et al., 1994).

Liesegang Bands

Liesegang

present at most

mobility under

iron is available

describe the se

banding features

of these iron fe

such as iron cr

phenomena, al

Kinetics

interesting pat

1984a). The

oxyhydroxides

bands are know

or self-pattern

Ortoleva et al.,

non-equilibriu

other words, t

1986).

Merino

propagation of

goethite bands

oxygenated v

sandstone. T

precipitate-rich

Liesegang Banding

Liesegang banding and groundwater ferricretes are relict features present at most of the outcrops studied. These features imply substantial iron mobility under the proper conditions. The features also imply that plenty of iron is available for subsequent redistribution. The following paragraphs describe the self-organization phenomena thought to result in the Liesegang banding features. Self-organization is only brought up to elucidate the origins of these iron features and is not meant to imply that later formed features such as iron crusts or honeycomb weathering result from self-organization phenomena, although this may eventually be proven to be the case.

Kinetics of precipitation coupled with transport can lead to an interesting pattern-forming process known as Liesegang bands (Ortoleva, 1984a). These parallel-banded precipitates often consist of ferric oxyhydroxides and frequently occur in sandstones (Merino, 1984). These bands are known as Liesegang bands and are often described as self-organizing or self-patterning phenomena (Merino, 1984, 1986, Ortoleva, 1984a, 1984b, Ortoleva et al., 1987a, 1987b). Self-organization is the generation of patterns in non-equilibrium systems without the intervention of external causes; in other words, the patterns can not be accounted for by inheritance (Merino, 1986).

Merino (1984) predicts, through quantitative kinetic modeling, that the propagation of redox fronts through a sandstone may induce the formation of goethite bands through instabilities arising from the interaction of flow of oxygenated water and dissolution/precipitation reactions within the sandstone. Typically, the goethite bands form a pattern of alternating precipitate-rich and precipitate-poor bands (Ortoleva, 1984a). In additions to

banded pattern
discovered (Ort
are actually se
stratification, th

Surficial Geology

The out
(Pennsylvanian
Ohio, western
The sandstone
Michigan; Pen
Springs Sands
Pennsylvanian
Sandstone an
Conglomerate,
outcrop areas s
sandstones are
provided in Ap

Environ
porosity, and
exist between
degree of sor
literature. Mi
from point co
weathered ha
weathering. V

banded patterns, concentric ring and spiral banded patterns have also been discovered (Ortoleva, 1984a). Determining whether iron bands in sandstone are actually self-patterning is difficult; however, if the bands cut across stratification, the bands must be true cases of self-patterning (Merino, 1984).

Surficial Geology

The outcrop areas studied in this thesis consist of Carboniferous (Pennsylvanian and Mississippian) sandstones outcropping in Michigan, Ohio, western Indiana, western Kentucky and southern Illinois (Figure 2). The sandstones studied are as follows: Pennsylvanian Eaton Sandstone, Michigan; Pennsylvanian Mansfield Sandstone, Indiana; Mississippian Tar Springs Sandstone and Pennsylvanian Caseyville Sandstone, Kentucky; Pennsylvanian Pounds (Caseyville) Sandstone, Illinois; Mississippian Berea Sandstone and Black Hand Sandstone and Pennsylvanian Sharon Conglomerate, Ohio. An overview and comparison of the surficial geology at outcrop areas studied is provided in this section. Detailed descriptions of the sandstones are provided in Appendix A. Site locations for the study areas are provided in Appendix B.

Environment of deposition, mineralogy, grain size, degree of sorting, porosity, and amount of iron cement are all compared to see if correlations exist between the different sandstone units. Depositional environments, degree of sorting and grain size determinations are obtained from the literature. Mineralogy, porosity and degree of iron cement are determined from point counting of thin sections. The thin sections were made from weathered hand samples obtained from outcrops containing honeycomb weathering. Weathered samples are difficult to point count because of their

friability and in

not fresh expos

The sand

Late Paleozoic.

large portions of

East and the C

the Canadian

clastics laid d

studied lack ab

pollen spores,

Coogan et al,

sedimentologic

sediments. De

deltaic to stric

create characte

Some w

believe that be

honeycomb w

porosity and

depositional e

bedding cha

weathering.

Average

controlling

permeability

to coarse-gra

portions of t

friability and induration. However, honeycombs form in the indurated rock, not fresh exposures.

The sandstones were deposited during the Carboniferous period of the Late Paleozoic. During this time, shallow seas with shifting margins covered large portions of North America, bounded by the Appalachian positive to the East and the Canadian Shield to the North. The Appalachian positive and the Canadian Shield provide the source materials for the Carboniferous clastics laid down at this time (Potter and Siever, 1956). The sandstones studied lack abundant fossils. The fossils that are found in the rocks consist of pollen spores, plant fossils and brachiopods (Barclay, 1968; Bohm, 1981; Coogan et al, 1981; Gault, 1938; Kelly, 1936). The lack of fossils and other sedimentological data suggest a range of depositional environments for the sediments. Depositional environments range from strictly fluvial to fluvio-deltaic to strictly deltaic. These environments provide enough energy to create characteristic bedding patterns in the rock record.

Some workers (Mustoe, 1982, Gill et al., 1979, Conca and Astor, 1987) believe that bedding and lithologic changes associated with bedding influence honeycomb weathering through differences associated with changes in porosity and permeability along the bedding planes. Thus, although depositional environments differ slightly for the sandstones, they all contain bedding characteristics that could control the formation of honeycomb weathering.

Average grain size and degree of sorting could also play a role in controlling honeycomb formation due to differences in porosity and permeability. Average grain sizes in the sandstones range from fine-grained to coarse-grained sand. In some cases, pebbly sandstones and conglomeratic portions of the sandstones also contain honeycomb weathering. Honeycomb

weathering has

Australia (Gill et

Mineralog

development.

minerals may

disaggregation

sections of sev

mineralogy, po

diagram show

data for the th

sandstones plo

(1994) has sho

Michigan, wer

arenites by sel

other sandston

Wallis

preferentially

Sandstone in

point counts.

Carboniferous

samples.

Porosity

Porosity and

exposures of

exposures of

porosity in su

Figure 5 show

weathering has also been reported in greywackes on the Otway Coast, Australia (Gill et al., 1979).

Mineralogy of the sandstones may also play a role in honeycomb development. Mustoe (1982) suggests that the weathering of feldspars to clay minerals may provide volumetric changes which could cause the disaggregation of sand grains, forming honeycomb cells. Petrographic thin sections of several different sandstones were made for point counting of mineralogy, porosity, and degree of iron cementation. Figure 3 is a ternary diagram showing bulk mineralogy of the different sandstones. Point count data for the thin sections are included as Table 4 in Appendix C. The sandstones plot in the quartz arenite region of the diagram. However, Price (1994) has shown that the Pennsylvanian Eaton Sandstone in Grand Ledge, Michigan, were probably originally lithic arenites, but were altered to quartz arenites by selective destruction of micaceous lithic fragments. Thus, the other sandstones studied may have undergone similar alteration.

Wallis and Velbel (1985) find that honeycomb weathering preferentially occurs in the flaggier (more micaceous) outcrops of the Eaton Sandstone in Grand Ledge, Michigan. Mica was also counted during the point counts. Figure 4 shows the percent mica present in the samples of Carboniferous studied. Percent mica ranges from 0 to less than 5% in all samples.

Porosity and relative abundance of iron were also point counted. Porosity and iron cement values correlate with well-indurated, surface exposures of each of the sandstones and do not represent the porosity of fresh exposures of the sandstones. In many cases, the iron cements occlude porosity in surface exposures that would occur as pores in subsurface sections. Figure 5 shows the relative surface porosities and abundance of iron cement

in the rocks from

the samples with

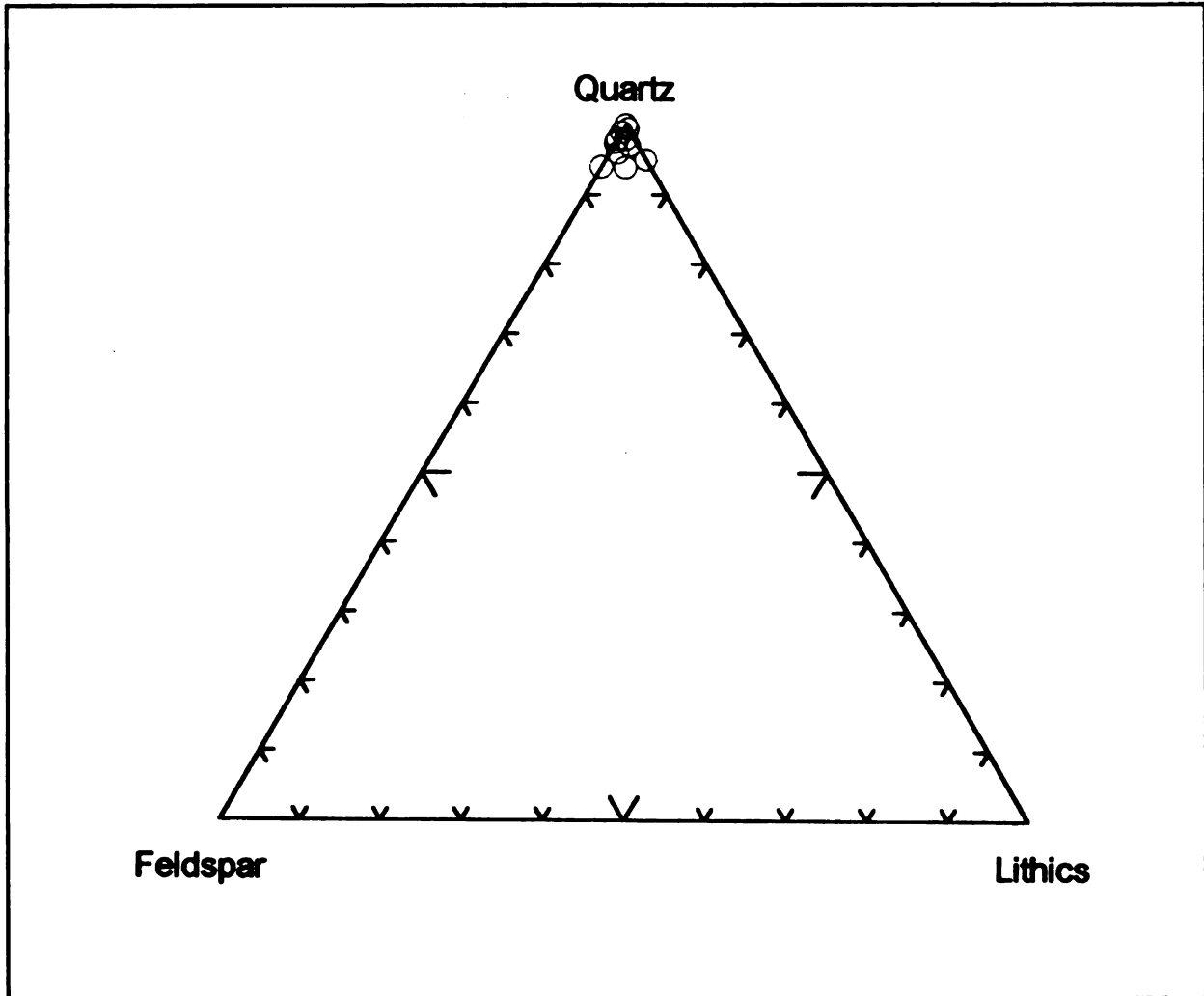
versa.

in the rocks from weathered surface samples of the sandstones. In general, the samples with abundant iron cement have lower porosity values and vice versa.

Felds

Ternary d
sandstones

Figure 3



Ternary diagram showing modal mineralogy of the Carboniferous sandstones.

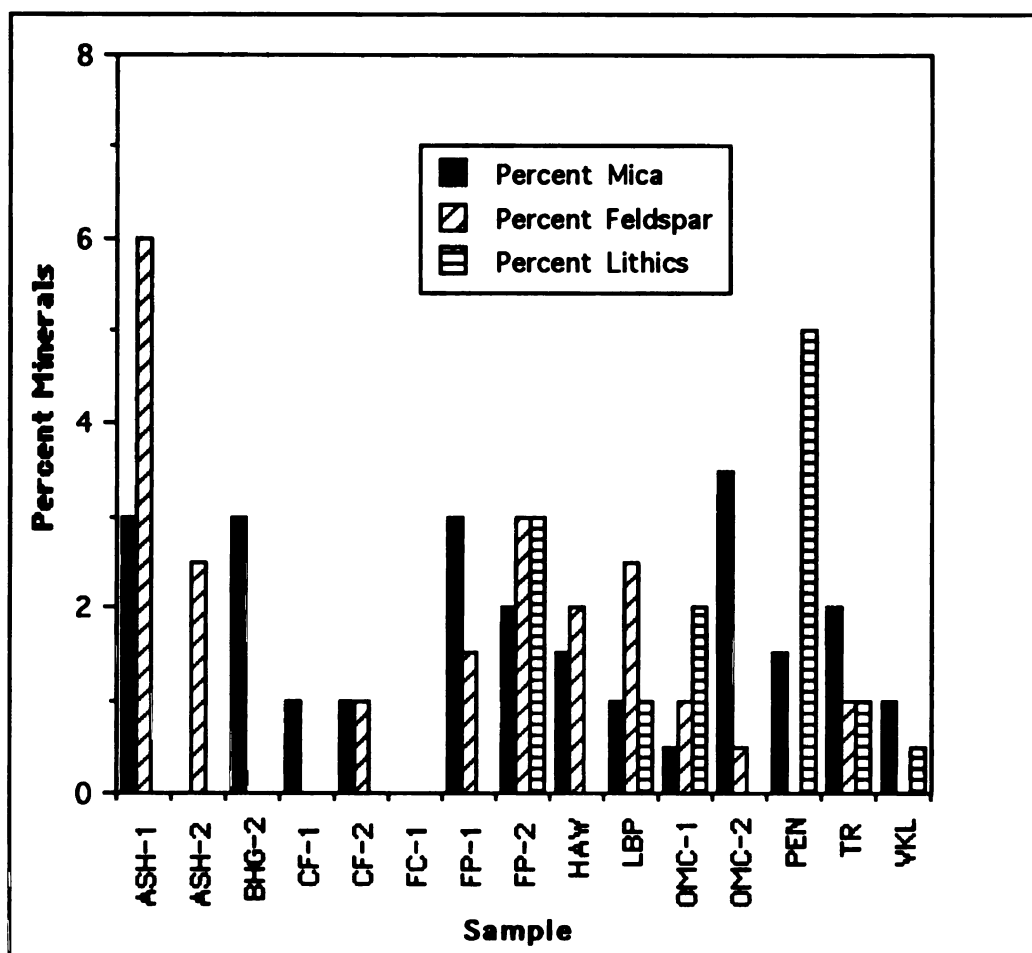


Percent

ASH -
BHG -
CF - B
FC - P
HAW
LBP -
OMC
PEN
VKL

TR -
FP -

Figure 4



Percent minerals present in the sandstones other than quartz.

ASH - Black Hand Sandstone from Ash Cave, Hocking Hills State Park, Ohio.

BHG - Black Hand Sandstone from Black Hand Gorge State Nature Preserve, Ohio.

CF - Black Hand Sandstone from Cedar Falls, Hocking Hills State Park, Ohio.

FC - Pounds Sandstone (Caseyville) from Ferne Clyffe State Park, Illinois.

HAW - Caseyville Sandstone from Indian Lake east of Hawesville, Kentucky.

LBP - Eaton Sandstone from Lincoln Brick Park, Grand Ledge, Michigan.

OMC - Black Hand Sandstone from Old Man's Cave, Hocking Hills State Park, Ohio.

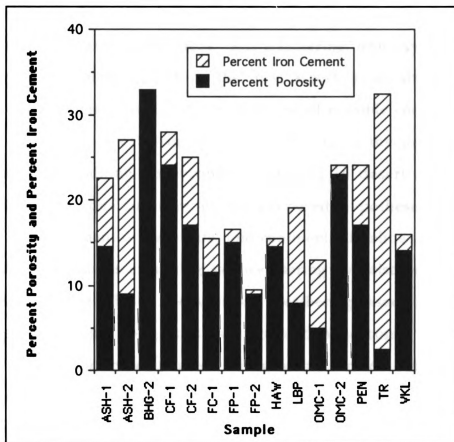
PEN - Caseyville Sandstone from Pennyryle State Resort Park, Kentucky.

VKL - Sharon Conglomerate from Virginia Kendall Ledges Park, Cuyahoga Valley National Recreation Area, Ohio.

TR - Mansfield Sandstone from Turkey Run State Park, Indiana.

FP - Eaton Sandstone from Fitzgerald Park, Grand Ledge, Michigan.

Figure 5



Percent porosity and percent iron cement in the sandstones studied.

- ASH - Black Hand Sandstone from Ash Cave, Hocking Hills State Park, Ohio.
 BHG - Black Hand Sandstone from Black Hand Gorge State Nature Preserve, Ohio.
 CF - Black Hand Sandstone from Cedar Falls, Hocking Hills State Park, Ohio.
 FC - Pounds Sandstone (Caseyville) from Ferne Clyffe State Park, Illinois.
 HAW - Caseyville Sandstone from Indian Lake east of Hawesville, Kentucky.
 LBP - Eaton Sandstone from Lincoln Brick Park, Grand Ledge, Michigan.
 OMC - Black Hand Sandstone from Old Man's Cave, Hocking Hills State Park, Ohio.
 PEN - Caseyville Sandstone from Pennyryle State Resort Park, Kentucky.
 VKL - Sharon Conglomerate from Virginia Kendall Ledges Park, Cuyahoga Valley National Recreation Area, Ohio.
 TR - Mansfield Sandstone from Turkey Run State Park, Indiana.
 FP - Eaton Sandstone from Fitzgerald Park, Grand Ledge, Michigan.

Several
proposed for
mineralogy, li
characteristics
origin of hor
hypothesis fo
locales. How
honeycomb de

Additio
ascertain any
weathering o
Sites display
used in the t
two outcrops

Petro
on the por
mica cont
examining
porosity
feldspar,
under a
weather

HYPOTHESIS

Several hypotheses for the origin of honeycomb weathering have been proposed for desert and coastal areas. Salt weathering, iron oxyhydroxides, mineralogy, lichen/algae growth on the rock, aspect, grain size, bedding characteristics, and clay content of the rocks are all possible controls on the origin of honeycomb weathering. Salt weathering is the most popular hypothesis for explaining honeycomb weathering in desert and coastal locales. However, one or more of the proposed hypotheses influence honeycomb development in temperate, mid-continental localities.

Additionally, areas exhibiting salt weathering will also be studied to ascertain any existing relations between salt weathering associated with the weathering of building stone, rock outcrops and honeycomb weathering. Sites displaying efflorescence (but not honeycombs) include building stone used in the front steps area of Morrill Hall, Michigan State University and two outcrops of the Eaton Sandstone in the Grand Ledge area.

METHODS

Petrographic analysis of the sandstones studied provided information on the porosity, iron oxyhydroxide content, clay content, feldspar content and mica content of the rocks. The petrographic analyses were done by examining petrographic thin sections and point counting mineralogy and porosity to determine percent porosity, iron oxyhydroxide cement, quartz, feldspar, lithic fragments, and mica. Additionally, samples were examined under a SEM to determine the possible role of clay in the origin of salt weathering and/or honeycomb weathering.

Mustoe
their reliance
weathering. H
diffraction (XR
assessing the c
EDS analyzer
rock grains an
viewed with t
relationships.
and orientatio
sandstone. M
minerals, thu
grain to gra
microfracture
sandstone.

Salts
sandstone s
were jelly
mineralogy
themselves
and inconsi

X-ra
efflorescen
powder. 7
The sampl
cover all
study.

Mustoe (1982) indicates that a major limitation of previous studies is their reliance on visual observations to explain the origins of honeycomb weathering. He further states that scanning electron microscopy (SEM), X-ray diffraction (XRD) analysis and energy dispersive spectrometry (EDS) can aid in assessing the origins of honeycomb weathering. A SEM equipped with an EDS analyzer were used to establish the relationship between the constituent rock grains and the mineral efflorescence. Fresh fracture surfaces were also viewed with the SEM and EDS to observe cross sectional (surface-subsurface) relationships. The SEM analysis provided information regarding the habit and orientation of the salts as well as their role in the breakdown of the sandstone. Images from the SEM show the orientation of efflorescent minerals, thus showing if the force of crystallization is physically breaking grain to grain contacts, splitting apart individual grains through microfractures, or not causing any effects which aid in the breakdown of the sandstone.

Salts found within honeycomb structures were removed from the sandstone surface and analyzed on a Rigaku Geigerflex XRD. The samples were jelly mounted on glass slides for XRD analysis. Efflorescence mineralogy was compared from site to site. Internal variation of the rocks themselves was investigated during the site visits to determine consistencies and inconsistencies between the different sandstones studied.

X-ray diffraction is used to establish the mineralogy of the salt efflorescences. Samples were crushed with a mortar and pestle to a fine powder. The sample was then jelly mounted onto a glass slide for analysis. The samples were analyzed from 2° to $60^{\circ} 2\theta$. The range of 2θ is adequate to cover all clays and efflorescent minerals that may be encountered in the study.

Introduction

The wa
Hall, Michiga
Cambrian Jacc

The blocks of
years. White
following pre
weather the
process of w

Salt p

Several year
porch-cover
deteriorated
support the
Science, Mi
are now sto
weathering
caused by
Since its st
sandstone
where the
weathers

CHAPTER 2 - SALT WEATHERING

MORRILL HALL

Introduction

The walls along the stairway leading to the main entrance of Morrill Hall, Michigan State University, are composed of Late Precambrian to Early Cambrian Jacobsville Sandstone ("Lake Superior Sandstone") (Gilchrist, 1947). The blocks of Jacobsville Sandstone have deteriorated over the last several years. White salt crusts (efflorescence) appear on the sandstone blocks following precipitation events. These salt crusts may be acting to physically weather the rock by prizing sand grains apart as the salt crystallizes. This process of weathering is known as salt weathering.

Salt proves to be quite an effective weathering agent at Morrill Hall. Several years ago, the pedestals and bases beneath the pillars supporting the porch-covering entryway had to be replaced. The efflorescent salts had deteriorated the pillar bases to such a degree that the bases could no longer support the porch. Dr. Michael A. Velbel of the Department of Geological Science, Michigan State University, acquired a base and a pedestal. The bases are now stored in a basement laboratory of the Natural Science building. Salt weathering continues to degrade the pillar base. The physical weathering caused by the salt destroys the decorative sculpturing on the pillar bases. Since its storage in the laboratory, efflorescence has continued to grow on the sandstone surface. A fine grit or gres develops on the portions of the block where the efflorescence is most abundant, showing how the salt physically weathers the sandstone. Figure 6 shows the destruction of the sculpturing,

Figure 6



Weathered pillar base from Morrill Hall. The picture shows a) the destruction of the decorative sculpturing, b) the efflorescence build up and c) the grit/loess development.

the efflorescence
during storage

Efflorescence

Generally, sandstone is
very friable, and
beneath the surface
of the sandstone
honeycomb weathering
the blocks are
apparent for
suggests that

Salt weathering

the sandstone
centimeters and
the sandstone
into the rock
maximum depth
with a non-uniform
blocks stick out
Thus, the material
occurred at New York
1947), and is thought
is 7.25 cm.

approximately

A study of
coastal bridge
erosion rate of

the efflorescence build up during storage and the grit/gres development during storage of the base.

Efflorescence attacks the sandstone blocks in several different ways. Generally, sandstone underlying the greatest concentrations of efflorescence is very friable, weak, and crumbles to the touch. In some areas, the sandstone beneath the efflorescence exhibits weathering rinds or contour scaling. Some of the sandstone blocks at Morrill Hall have begun to show signs of honeycomb weathering. The salts have created small indentations in some of the blocks no more than a few centimeters in diameter (Figure 7). The apparent formation of small honeycombs in some of the blocks at least suggests that salt weathering may be a precursor to honeycomb weathering.

Salt weathering at Morrill Hall also creates much larger indentations in the sandstone blocks (Figure 8). The larger indentations span as much as 25 centimeters across a block. These larger indentations probably occur where the sandstone is weakly cemented. The efflorescence weathers deeper cavities into the rock where the large indentations occur. Cavity pockets reach a maximum depth of 4 cm. The sandstone blocks were decoratively fashioned with a non-uniform, convex surface (Figure 8). The convex edges of the blocks stick out approximately 3.25 cm from the "flat" edge of the blocks. Thus, the maximum depth of material removed by salt weathering has occurred at Morrill Hall is 7.25 cm. Morrill Hall was built in 1899 (Gilchrist, 1947), and is thus approximately 100 years old and the maximum cavity depth is 7.25 cm. Thus, the maximum weathering rate at Morrill Hall is approximately 0.0725 cm/yr.

A study of salt weathering erosion rates for a sandstone used in a coastal bridge pier yields interesting data (Takahashi et al., 1994). An average erosion rate of 0.52 cm/yr is determined for the first twenty years after

Figure 7

Small indentations (incipient honeycomb weathering) created by salt efflorescence at Morrill Hall.

Figure 8

a) Large indentation weathered into a sandstone block at Morrill Hall. Note the depth of the indentation. b) Example of the non-uniform, convex fashioning of the sandstone blocks.

construction
yields an ave
weathering d
by Takahash
calculated fo
zone which
Morrill Hall
the year whe
Hall are spo
material that

Several
monuments f
1965; Meier
derived for t
phyllite and
0.0012 cm/y
(Meierding,
(Winkler, 19
rates determ
weathering

Efflo
stone becom
increases, t
larger area
first rains
precipitatio
the season

construction of the bridge (Takahashi et al., 1994). The subsequent 18 years yields an average erosion rate of 0.22 cm/yr, showing that erosion due to salt weathering decreases with time. The rates determined in the study conducted by Takahashi et al. (1994) are significantly greater than the maximum rate calculated for Morrill Hall. The sandstone bridge is located in a coastal spray zone which receives a constant input of water and salts in the sea spray. Morrill Hall on the other hand receives salt inputs for a limited time during the year when the walkways are salted. Additionally, water inputs at Morrill Hall are sporadic. Thus, Morrill Hall does not receive the constant input of material that the sandstone bridge does, resulting in a lower erosion rate.

Several studies have also been undertaken on tombstones and monuments to retrieve erosion rates due to acid rain and pollution (Winkler, 1965; Meierding, 1984; Carey, 1995). Much smaller weathering rates are derived for the effects of acid rain on building stone: 0.00020 cm/yr for slate, phyllite and schist, 0.00021 cm/yr for granite, 0.00045 cm/yr for sandstone, 0.0012 cm/yr for marble (Carey, 1995); 0.0020 cm/yr to 0.0002 cm/yr for marble (Meierding, 1984); and 0.00076 cm/yr, 0.00085 cm/yr, 0.00050 cm/yr for granite (Winkler, 1965). These reported weathering rates are much lower than the rates determined for salt weathering of sandstone, suggesting that perhaps salt weathering degrades stone at a faster rate than does acid rain and pollution.

Efflorescence on Morrill Hall forms after precipitation events when the stone becomes saturated with water. As time between precipitation events increases, the efflorescence crust becomes thicker and the efflorescence covers larger areas of the sandstone. During the spring, as the snows melt and the first rains occur, efflorescence appears on the stone within one day of a precipitation event and thick efflorescence crusts grow within a few days. As the seasons progress into summer and autumn, it takes longer for the first

appearance of
crusts usually
efflorescence
seasonal decr

X-ray

efflorescence
present in the
results for
orthoclase and
Hamblin, 19
some of the
calcite is pre
EDS peaks t
intensities ar
found in the
intensities ar

Halite

Halite

to de-ice the
Campus Arc
from the ste
The melt-wa
and the san
After the w
draws the w
temperature

appearance of efflorescence on the stone after a precipitation event and thick crusts usually do not develop. Thus, the supply of salt contributing to efflorescence formation decreases from spring to fall. The implication of the seasonal decrease in efflorescence is that the salt contributions are seasonal.

X-ray diffraction and energy dispersive spectroscopy analyses of efflorescence samples obtained from Morrill Hall reveal a suite of minerals present in the efflorescence. Table 5 in Appendix D lists the XRD and EDS results for efflorescent salts associated with salt weathering. Quartz, orthoclase and plagioclase constitute the actual sandstone (Kalliokoski, 1982; Hamblin, 1958) and represent the small amounts of sand that contaminate some of the efflorescence samples. The sandstone is calcite cemented, thus calcite is present in minor amounts in the XRD analyses. The major XRD and EDS peaks typically indicated halite. Table 6 of Appendix E lists the peak intensities and d-spacings for halite. Alunite, $(\text{Na,K})\text{Al}_3(\text{SO}_4)_2(\text{OH})_6$, is also found in the XRD and EDS analyses. Table 7 of Appendix F lists the peak intensities and d-spacings for alunite.

Halite

Halite is used in the vicinity of the main entranceway to Morrill Hall to de-ice the steps during the winter months (pers. comm. Donald Freed, Campus Architect, Michigan State University). As halite melts snow and ice from the steps the melt-water dissolves the halite and it goes into solution. The melt-water containing dissolved halite then infiltrates into the pillars and the sandstone blocks used to construct the walls alongside the steps. After the water has infiltrated into the sandstone blocks, capillary action draws the water up into the blocks (Conca and Astor, 1987; Cooke, 1994). As temperatures rise, the water inside the blocks is drawn to the surface where

temperatures
dissolved hal
water evapor
solution can
Figure 10 sho
be seen.

Halite
damage to c
erosive facto
sand grains,
as they are e
1994). Cryst
are prized f
ground below
efflorescence
southeast. I
amount of s
creates a co
interior (Wi
towards the
Repeating th
blocks use in
the same bu
degree that t

Soluti
non-harmful
on the steps

temperatures are slightly higher than inside the blocks (Figure 9). The dissolved halite-water solution is drawn to the surface of the block where the water evaporates and the halite precipitates. The maximum height the salt solution can achieve depends upon the infiltration capacity of the sandstone. Figure 10 shows a pillar in which the maximum height of salt infiltration can be seen.

Halite is a very effective weathering agent; it has generally done more damage to concrete and building stone near ground level than any other erosive factor (Winkler, 1994). Halite can exert considerable pressure on the sand grains, forcing them to be prized from the surface of the rock (Figure 11) as they are entrained in the efflorescence to be washed away later (Winkler, 1994). Crystallization pressures can become so great that pieces of sandstone are prized from the surface of the blocks and can be found lying on the ground below the broken blocks. The broken pieces of sandstone also display efflorescence on the former fracture surfaces. The entranceway faces the southeast. It is this portion of the building which experiences the greatest amount of salt weathering, due to exposure to the sun. The sun exposure creates a contrast between physical environments of the stone surface and interior (Winkler, 1994). As moisture from within the stone migrates towards the surface, the moisture evaporates, leaving behind efflorescence. Repeating this process many times over creates depressions in the sandstone blocks use in the entranceway. Other portions of Morrill Hall constructed of the same building stone also experience mild salt weathering, but not to the degree that the main entranceway does.

Solutions to the salt weathering problem at Morrill Hall do exist. A non-harmful deicer such as sand or other commercial products could be used on the steps leading to Morrill Hall. Alternatively, the sandstone blocks

could be impi

of the buildin

causing furth

controlling sa

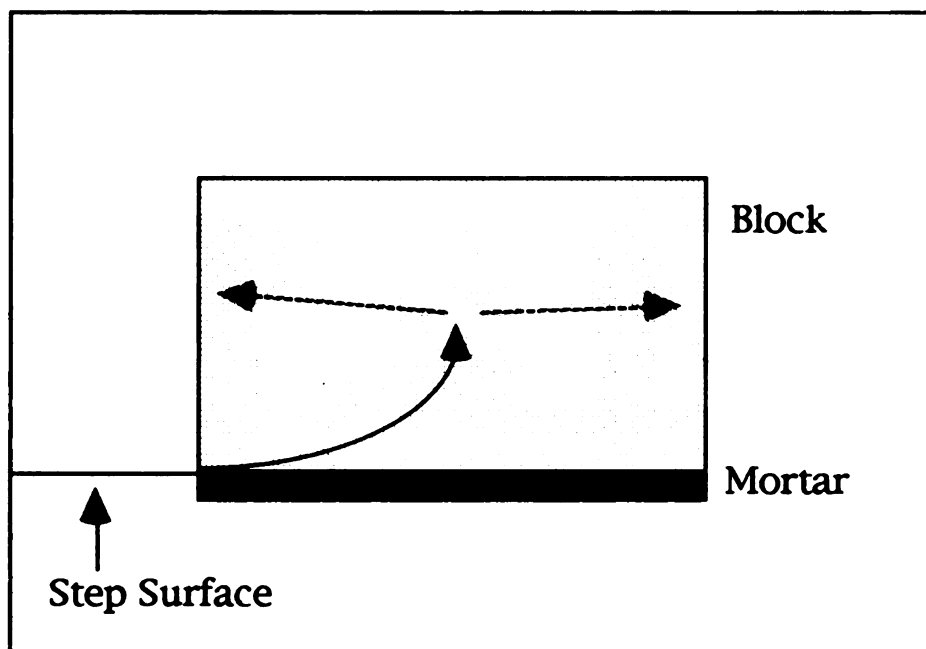
place of halit

could be impregnated with an epoxy or other binder to maintain the integrity of the building stone. However, sealers often trap salts inside the stone, causing further damage to the stone (Winkler, 1994). The best method of controlling salt weathering at Morrill Hall is to use a non-harmful deicer in place of halite.



Halite infiltr
indicates th
solution. T
solution as

Figure 9



Halite infiltration and movement inside a sandstone block. The solid arrow indicates the infiltration and subsequent capillary rise of the water-halite solution. The striped arrow indicates the movement of the water-halite solution as temperatures begin to rise.

Figure 10



Eroded pillar showing the maximum height of capillary rise in the sandstone at Morrill Hall. The black line on the pillar marks the maximum height (approximately 8 inches).



SEM photo
grains (b) at

Figure 11

SEM photograph showing halite efflorescence (a) growing between sand grains (b) at Morrill Hall. The halite is pushing the grains apart.

Alunite

Alunite

XRD, EDS and

alunite). A

(Hendricks,

minerals in

(Stoffregen

conditions s

of acidity fo

sulfide, such

inputs of ac

weathering

alunite (Lon

The fo

the destruct

minerals an

sulfate in so

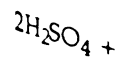
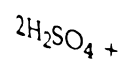
thus it is usu

alunite show

aluminum s

represent r

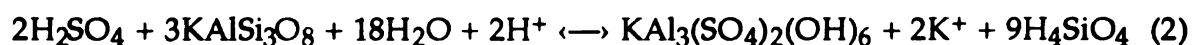
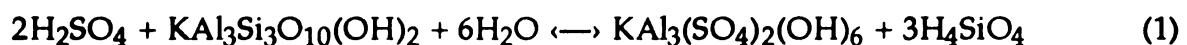
respectively



Alunite

Alunite is also present in Morrill Hall efflorescence as indicated by XRD, EDS and SEM analyses (Table 7 of Appendix F lists the XRD data for alunite). Alunite has a rhombohedral structure similar to that of calcite (Hendricks, 1937). Alunite forms as an alteration product of Al-bearing minerals in oxidizing, sulfur-rich environments between 15 and 400 °C (Stoffregen and Alpers, 1992). The formation of alunite requires acidic conditions so that Al^{3+} can be mobilized (McArthur et al., 1991). The source of acidity for alunite-precipitating solutions may come from the oxidation of sulfide, such as pyrite, precipitation of iron oxyhydroxides, and possibly large inputs of acid rain into poorly buffered systems (Long et al., 1992). Acid weathering of aluminosilicates mobilizes Al and K, both constituents of alunite (Long et al., 1992).

The formation of alunite can be looked upon as a two step process: (1) the destruction of an aluminum and/or potassium bearing mineral or minerals and (2) the combination of the aluminum and potassium with sulfate in solution (Knight, 1977). Aluminum has a relatively low solubility, thus it is usually conserved in the solid phase (Knight, 1977). Observations of alunite show that it replaces feldspar and muscovite grains, supporting a local aluminum source for the aluminum (Knight, 1977). Equations 1 and 2 represent replacement reactions for muscovite and potassium feldspar, respectively.



The presence

the likely so

of formation

and/or po

atmospheric

potassium fe

Many

including: Fe

K⁺ (Stoffre

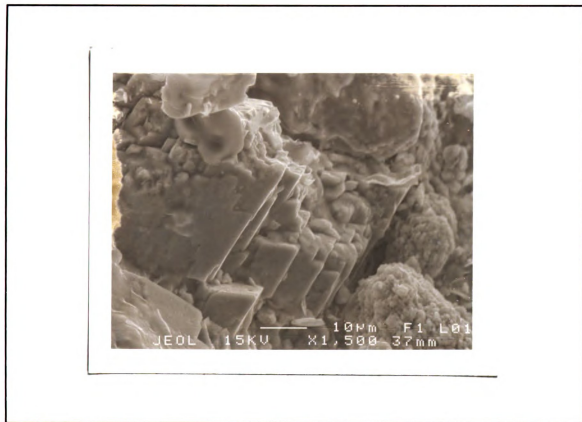
substitution

The presence of these two minerals in the Jacobsville Sandstone make them the likely sources for potassium and aluminum. The most likely mechanism of formation for alunite at Morrill Hall is the acid dissolution of muscovite and/or potassium feldspar during a precipitation event rich in atmospherically derived sulfuric acid. Alunite is only found replacing potassium feldspar in the SEM photographs (Figure 12).

Many chemical substitutions are possible in the alunite structure, including: Fe^{3+} for Al^{3+} , PO_4^{3-} or AsO_4^{3-} for SO_4^{2-} and Na^+ , H_3O^+ , Ca^+ , or $+$ for K^+ (Stoffregen and Alpers, 1992). The EDS analyses corroborate these substitutions with the presence of Na, Fe, and Ca in the alunite.



Alunite (A) repl.
the rhombohedr

Figure 12

Alunitic (A) replacing a potassium feldspar sand grain at Morrill Hall. Note the rhombohedral habit of alunitic.

Introduction

The study of
Grand Ledge, Mich
sandstone and sh
efflorescence gro
(Figure 13). Effl
seams in Fitzgera

Two types
contain a well d
layers and pryin
efflorescence, bu
them. Effloresc
sandstone efflore
the outcrop. Sev
and coal seams i
Eaton Sandston
efflorescence mi
Brick Park and
sulfates grow in
efflorescent min

LINCOLN BRICK PARK AND FITZGERALD PARK

Introduction

The study areas in Lincoln Brick Park and Fitzgerald Park are located in Grand Ledge, Michigan (Figure 38, Appendix B) above former shale pits. Both sandstone and shale crop out around the shale pits. In Lincoln Brick Park, the efflorescence grows on the shale beds and coal seams located above the pit (Figure 13). Efflorescence grows on the sandstone units, shale beds and coal seams in Fitzgerald Park (Figure 14). Both sites are geologically similar.

Two types of efflorescence appear in each park. The shale layers contain a well developed white efflorescence growing between the shale layers and prying them apart. The coal seams contain the same white efflorescence, but also have a yellow, botryoidal efflorescence growing on them. Efflorescence is also present on the sandstone units, however, the sandstone efflorescence in Lincoln Brick Park grows in unreachable areas of the outcrop. Several samples of efflorescence were taken from the shale beds and coal seams in each park. Efflorescence samples were also taken from the Eaton Sandstone bed in Fitzgerald Park. Table 5 in Appendix D lists the efflorescence minerals found in association with salt weathering in Lincoln Brick Park and Fitzgerald Park. Although several different hydrous iron sulfates grow in the two parks, halotrichite ($\text{FeAl}_2(\text{SO}_4)_4 \cdot 22\text{H}_2\text{O}$) is the major efflorescent mineral in the area.

Figure 13

Efflorescence on the shale bed in Lincoln Brick Park. The lower portion of the picture contains the shale bed which is coated with a white crust or efflorescence.

Figure 14



Outcrop area in Fitzgerald Park containing salt weathering.

Hydrous Iron S

Halotric

amarantite (Fe

minerals in the

Lincoln Brick

found in Table

rozenite and Ta

occur in very s

growing in the

habit (Figure 15

Ehlers a

halotrichite as

Kittanning Co

involves the in

al., 1987). Th

sulfides is imp

Wiese et al. (19

rich portion o

minerals (usin

written as (Wie

$\text{Al}_2\text{Si}_2\text{O}_5(\text{OH}$

$2\text{SiO}_2 + \text{Fe}^{2+}$

Hydrous Iron Sulfate Efflorescence

Halotrichite ($\text{FeAl}_2(\text{SO}_4)_4 \cdot 22\text{H}_2\text{O}$), rozenite ($\text{FeSO}_4 \cdot 4\text{H}_2\text{O}$), and amarantite ($\text{FeSO}_4 \cdot 3\text{H}_2\text{O}$) make up the hydrous iron sulfate efflorescence minerals in the shale beds and coal seams exposed in Fitzgerald Park and Lincoln Brick Park. Peak intensities and d-spacings of each mineral can be found in Table 8 of Appendix G for halotrichite, Table 9 of Appendix H for rozenite and Table 10 of Appendix I for amarantite. Rozenite and amarantite occur in very small amounts. Halotrichite is the major hydrous iron sulfate growing in the parks. Halotrichite exhibits a fibrous or needle-like crystal habit (Figure 15) (Wiese et al., 1987).

Ehlers and Stiles (1965) find melanterite ($\text{FeSO}_4 \cdot 7\text{H}_2\text{O}$), rozenite and halotrichite as alteration products on pyrite crystals from the Pennsylvanian Kittanning Coal in Vinton County, Ohio. The formation of halotrichite involves the interaction of iron sulfides and the breakdown of clays (Wiese et al., 1987). Thus, the occurrence of clay minerals in association with iron sulfides is important to the oxidation of the sulfides (Wiese et al., 1987). Wiese et al. (1987) find that halotrichite is dominant in shales and in the clay-rich portion of coals. A reaction involving both iron sulfides and clay minerals (using kaolinite as a representative clay) to form halotrichite can be written as (Wiese et al., 1987):

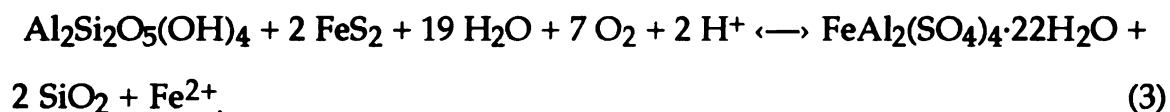


Figure 15



Fibrous crystal habit of halotrichite as seen under the SEM.

Introduction

The ledge
Recreation Area
honeycomb wall
Cave, a seep is
Very small holes
rock face. A
water issues from
honeycombs.
evaporation of
"washed" appearance
Table 5 of Appendix
Kendall Ledge
mineral associations
phosphate. Phosphorus
11 of Appendix

Taranakite

Taranakite
discovery of
taranakite in
(Murray and
clay-like nodules

VIRGINIA KENDALL LEDGES PARK

Introduction

The ledges in Virginia Kendall Park, Cuyahoga Valley National Recreation Area (see Figure 49, Appendix B) contain excellent examples of honeycomb weathering. However, in one area of the ledges near Ice Box Cave, a seep issues from a fracture in the Sharon Conglomerate (Figure 16). Very small honeycombs exist below the seep where the water runs down the rock face. A buildup of efflorescence occurs below the point at which the water issues from the rock, but the efflorescence is not associated with the honeycombs. The efflorescence buildup appears to result from the evaporation of the water issuing from the seep. The efflorescence takes on a "washed" appearance as if the efflorescence flowed down the rock surface. Table 5 of Appendix K contains the efflorescence mineralogy for Virginia Kendall Ledges. X-ray diffraction, EDS and SEM data reveal the efflorescence mineral associated with the seep to be taranakite, a potassium aluminum phosphate. Peak intensity and d-spacing data for taranakite is located in Table 11 of Appendix J.

Taranakite

Taranakite is a rare potassium aluminum phosphate mineral. This discovery of taranakite is probably only the second reported occurrence of taranakite in the United States, with the first being in Pig Hole Cave, Virginia (Murray and Dietrich, 1956). Taranakite usually appears as yellowish white, clay-like nodular masses (Fiore and Laviano, 1991). Several different

chemical formula
18H₂O and K
formulas (Fior
unknown, how
17) (Fiore and
further state th
Because there
suffice. Very l
can occur with
corroborated w

Taranak
guano is prese
and Dietrich, 1
with clay min
limestone. T
taranakite is
solution deriv
1956; Sakae a
highly acidic
(pH<=3) can
for uptake by
potassium ph
taranakite can

McCon
structure ana
McConnell ne
is not an ort

chemical formulas have been proposed for taranakite, but $\text{H}_6\text{K}_3\text{Al}_5(\text{PO}_4)_8 \cdot 18\text{H}_2\text{O}$ and $\text{KAl}_3(\text{PO}_4)_3(\text{OH}) \cdot 9\text{H}_2\text{O}$ are the two most commonly used formulas (Fiore and Laviano, 1991). The taranakite structure is still unknown, however it occurs as small, flat, clay-like hexagonal sheets (Figure 17) (Fiore and Laviano, 1991; Smith and Brown, 1959). Smith and Brown further state that the phosphate sheets are separated by water molecules. Because there is not a well accepted mineral structure, either formula will suffice. Very limited substitutions of Ca and Na for K, Fe for Al, and S for P can occur within the taranakite structure (Fiore and Laviano, 1991) which is corroborated with the EDS data from this research.

Taranakite usually forms in karstified limestone where appreciable bat guano is present as the phosphate source (Fiore and Laviano, 1991; Murray and Dietrich, 1956; Sakae and Sudo, 1975). The taranakite is usually associated with clay minerals found in stylolites and other terrigenous portions of the limestone. Thus, the only proposed hypothesis for the formation of taranakite is the chemical reaction between clay minerals and a phosphatic solution derived from guano (Fiore and Laviano, 1991; Murray and Dietrich, 1956; Sakae and Sudo, 1975). Taranakite precipitates and is stable under highly acidic pH (Fiore and Laviano, 1991). The highly acid conditions ($\text{pH} \leq 3$) can dissolve clay minerals, mobilizing the aluminum and potassium for uptake by the phosphate. A study involving the acid attack of illite in a potassium phosphate solution at pH 3 over a two week period shows that taranakite can form in this manner (McConnell, 1976).

McConnell (1976) proposes that taranakite is a phyllophosphate with a structure analogous to illite, from which it can be synthesized. Additionally, McConnell notes that taranakite has a hexagonal unit cell. Thus, if taranakite is not an orthophosphate, that is if taranakite does not contain PO_4 groups,

then the phyllo

$K_x[Al_{2-y}(H_3)_y](C)$

kaolinite only e

1 mm of the ta

McConnell's (19

Previous

Fiore and Lavia

clay minerals.

taranakite gro

mechanisms of

origin of the s

quantities of b

clay soils. (2)

and phosphati

water issues a

groundwater s

Summary

Salt we

may be prov

chemical deg

such as deici

both sandsto

salts act on t

include halit

salt types rar

the most eff

then the phyllophosphate structure requires a different chemical formula: $K_x[Al_{2-y}(H_3)_y](OH)_2[Al_xP_{4-x-z}(H_3)_zO_{10}]$. Murray and Dietrich (1956) show that kaolinite only exists where the taranakite is not present and that illites within 1 mm of the taranakite appear to be altered to vermiculite, supporting McConnell's (1976) idea that taranakite replaces illite.

Previous workers (Murray and Dietrich, 1956; Sakae and Sudo, 1975; Fiore and Laviano, 1991) find taranakite in close proximity or in contact with clay minerals. In contrast, field observations at Virginia Kendall Ledges show taranakite growing as a precipitate on a quartz arenite. Three possible mechanisms of taranakite formation exist at Virginia Kendall Ledges. (1) The origin of the seep is at the upper surface of the ledges where significant quantities of bird droppings have accumulated where they react with acidic clay soils. (2) Fluids from beneath the outcrop are mixing with clay minerals and phosphatic minerals or fish bones within a Carboniferous shale and the water issues at the ledges. (3) Fertilizers rich in phosphate have entered the groundwater system and are discharging at the seep.

Summary

Salt weathering occurs on building stone and on outcrop surfaces. Salts may be provided by air-born salt particles, precipitation, groundwater, chemical degradation of the rocks themselves or as anthropogenic inputs such as deicing salts (Wellman and Wilson, 1968). Salt weathering acts on both sandstone and shale to physically erode the rock. Several efflorescent salts act on the rocks examined in this study to break them down. The salts include halite, alunite, halotrichite, rozenite, amarantite and taranakite. The salt types range from halides to sulfates to phosphates. Halite and gypsum are the most effective salt weathering agents of the common salts (Ollier, 1984),

however it can

erode outcrop s

mirabilite (Na

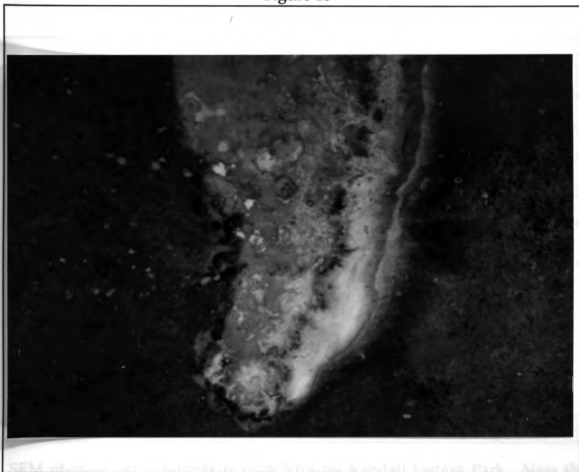
($\text{MgSO}_4 \cdot 6\text{H}_2\text{O}$)

gypsum and ha

1994; Smith and

however it can be seen that other salts will also damage building stone and erode outcrop surfaces. Other salts that hydrate and dehydrate easily such as mirabilite ($\text{Na}_2\text{SO}_4 \cdot 10\text{H}_2\text{O}$), epsomite ($\text{MgSO}_4 \cdot 7\text{H}_2\text{O}$) and hexahydrate ($\text{MgSO}_4 \cdot 6\text{H}_2\text{O}$) are the most effective salts involved in salt weathering, but gypsum and halite are more commonly involved in salt weathering (Cooke, 1994; Smith and McGreevy, 1983; McGreevy and Smith, 1982).

Figure 16



Outcrop photograph of area below the seep at Virginia Kendall Ledges. Note honeycomb cells in the picture. The buff colored area in the photograph is the area where the seep water washes over the rock face. The white substance on the stone is the efflorescence. The band of taranakite is approximately one inch wide.

Figure 17



SEM photograph of taranakite from Virginia Kendall Ledges Park. Note the clay-like hexagonal sheet structure.

Ten dif
Carboniferous
study area are
characteristics,
hypotheses ha
Salt weatherin
rock, aspect, g
are all possibl
in Chapter 1).

Salt we
formation of h
1984, 1982; G
Robinson (199
containing ho
mechanisms
hypotheses pr
the likely cau
temperate, m

Motter
Weston-supe
coping stone
The walls we
onset of ho

CHAPTER 3 - HONEYCOMB WEATHERING

INTRODUCTION

Ten different outcrops of honeycomb weathering occurring in Carboniferous quartz arenites were studied. Detailed site descriptions for each study area are provided in Appendix M. Comparisons between the outcrop characteristics, efflorescence salts and iron abundances can be made. Several hypotheses have been proposed for the origins of honeycomb weathering. Salt weathering, iron oxyhydroxides, mineralogy, lichen/algae growth on the rock, aspect, grain size, bedding characteristics, and clay content of the rocks are all possible controls on the origin of honeycomb weathering (see review in Chapter 1).

Salt weathering is the most common hypothesis invoked for the formation of honeycomb weathering in desert and coastal regions (Mustoe, 1984, 1982; Gill et al., 1979; McGreevy, 1984). However, Williams and Robinson (1994) note that salts are not nearly as abundant in inland sites containing honeycomb weathering. Mustoe (1982) also suggests that different mechanisms of formation may exist at different sites. Thus, all of the hypotheses proposed by different workers (Table 1) will be tested to see what the likely cause of honeycomb weathering is in Carboniferous sandstones in temperate, mid-continental areas.

Mottershead (1994) studied honeycomb weathering on the seawalls of Weston-super-Mare in the United Kingdom. The walls are capped with coping stones which exhibit honeycomb weathering of varying intensities. The walls were constructed at a known time and thus create a baseline for the onset of honeycomb weathering, allowing the determination of the

weathering rate

seawalls are ap

length. Motter

variable intens

increase, so do

the progress of

Eventually the

which repres

honeycomb br

(1994) classifi

present in the

refers to emer

cells similar to

refers to the p

by walls only

scale). The l

honeycombs i

- 8 on Motter

weathering rate due to honeycomb weathering. The coping stones along the seawalls are approximately 0.4 m wide, 0.2 m deep and 1.4 m to 2.0 m in length. Mottershead (1994) used a numerical scale from 0 to 9 to classify the variable intensity of the honeycombing (Table 2). As the numerical index increase, so does the degree of honeycomb formation (Table 2), representing the progress of honeycombing through a sequence of development and decay. Eventually the honeycomb walls are reduced to vestigial rounded humps which represent the only relief remaining after advanced stages of honeycomb breakdown. This study invokes terms similar to Mottershead's (1994) classifications to represent the degree of honeycomb development present in the study areas. The term infant or newly formed honeycombs refers to emerging honeycombs which generally occur as isolated honeycomb cells similar to numbers 1 and 2 on Mottershead's scale. Mature honeycombs refers to the presence of small to large clusters of honeycomb cells separated by walls only millimeters in thickness (numbers 3 and 4 on Mottershead's scale). The last term used in this study is old honeycombs, referring to honeycombs in which the walls are beginning to erode back to a flat surface (5 - 8 on Mottershead's scale).

Hypotheses

Salt weathering

Salt weathering

Algae/lichen h
together

Exfoliation resu
feldspars

Infiltration and

Breach of case-

Hydration reac

Local variation

Previous hypo

Table 1

Hypotheses	Reference
Salt weathering	Mustoe (1982)
Salt weathering and subsequent ion diffusion	Mustoe (1982)
Algae/lichen holding honeycomb walls together	Mustoe (1982)
Exfoliation resulting from hydration of feldspars	Mustoe (1982)
Infiltration and waterflow through the rock	Conca and Astor (1987)
Breach of case-hardened crust	Harris et al. (1977)
Hydration reactions of clay minerals	McGreevy and Smith (1984)
Local variations in permeability	Bryan (1925, 1926)

Previous hypotheses for the origin of honeycomb weathering.

0
1
2
3
4
5
6
7
8
9

Classification
(1994).

Table 2

0	No visible weathering forms
1	Isolated circular pits
2	Pitting >50% of area
3	Honeycomb present
4	Honeycomb >50% of area
5	Honeycomb with some wall breakdown
6	Honeycomb partially stripped
7	Honeycomb stripping >50% of area
8	Only reduced walls remain
9	Surface completely stripped

Classification of honeycomb weathering intensities used by Mottershead (1994).

Salt Weathering**Efflorescence**

recent heavy
occurrences are
honeycomb can
more recently
older honeycomb
surface. Quite
photographs (Fig.
on the honeycomb
efflorescence, s
of each other.

Table 12

associated with
the efflorescence
13 of Appendix
honeycomb with
precipitation of
Geochemistry

COMPARISON OF HONEYCOMB WEATHERING

Salt Weathering

Efflorescence is found at most honeycomb weathering sites unless a recent heavy rain occurred, washing away the salt. The efflorescence occurrences are similar in each of the study areas. Salts precipitate in the honeycomb cavities of newly forming honeycombs or honeycombs that are more recently formed (Figure 18). Efflorescence precipitates on the walls of older honeycombs in which the honeycomb walls are eroding back to a flat surface. Quite often, the older honeycomb walls are black (Figure 19). Both photographs (Figures 18 and 19) also show that efflorescence is not ubiquitous on the honeycomb weathered outcrops. Quite often, small amounts of efflorescence, such as in the photographs only occur within 75 to 200 meters of each other.

Table 12 of Appendix K lists the XRD and EDS data for efflorescence associated with honeycomb weathering. Peak intensities and d-spacings for the efflorescence associated with honeycomb weathering are located in Table 13 of Appendix L. Gypsum is the only salt growing in association with honeycomb weathering in all of the study areas. The significance of the precipitation of gypsum in all of the weathering sites is discussed later in the Geochemistry of Honeycomb Formation section of this chapter.

Figure 18

Efflorescence growing inside recently formed honeycomb cavities at Black Hand Gorge State Nature Preserve, Ohio.

Figure 19

Efflorescence growing on the walls of older honeycomb cavities in which the honeycomb walls are retreating at Old Man's Cave in Hocking Hills State Park. Note the black color of the honeycomb walls as compared to the honeycomb cavities.

Iron Oxyhydroxide

Salt we

honeycomb we

to other phen

al., 1977). In

weathering si

like color. TH

manifestation

Ground

phenomena s

outcrops. Gr

the sandston

formed when

20 and 21).

cemented by

the outcrop

tubes. The th

Similar to L

bedding, how

several repea

Lieseg

banding is de

that occur in

bedding. Lie

In some area

present on th

exists behind

Iron Oxyhydroxides

Salt weathering is the most popular hypothesis for the formation of honeycomb weathering, but others have attributed honeycomb development to other phenomena, such as the diffusion of iron in the sandstone (Harris et al., 1977). Iron oxides and hydroxides are ubiquitous at the honeycomb weathering sites studied. The sandstones studied maintain an orange, rust-like color. The sandstones in the study areas share several characteristic iron manifestations that, at least in part, influence honeycomb development.

Groundwater ferricretes, Liesegang banding and other self-organization phenomena similar to Liesegang banding are present in many of the rock outcrops. Groundwater ferricretes may record paleo-groundwater levels in the sandstones before their erosion to their present level. Ironstones have formed where the groundwater ferricretes are prevalent in the rock (Figures 20 and 21). The ironstones consist of a sandstone framework completely cemented by iron oxyhydroxides. The ironstones form thick bands traversing the outcrop and thick rinds surrounding the original sandstone creating tubes. The thickness of the ironstones is usually about 2.5 to 3.0 centimeters. Similar to Liesegang banding, the groundwater ferricretes do not follow bedding, however the ferricretes are usually a single discrete band rather than several repeating bands.

Liesegang bands are also present in many of the study areas. Liesegang banding is defined as sub-parallel sets of iron-rich bands or bands of ironstone that occur in a sandstone and do not follow bedding but rather cut across bedding. Liesegang banding takes on several different forms from site to site. In some areas, the Liesegang bands consist of sub-linear, sub-parallel bands present on the outcrop surface (Figure 22). Liesegang banding at other sites exists behind the case-hardened, honeycomb weathered outcrop surface.

(These bands
from the surf
outcrops (Fig
also present in
most rare of
iron-saturated
rose above the
the outcrop s
entities rather
and the sand
Liesegang cir
formation (F
contain honey

In some
fractures. T
groundwater
precipitates a
from the fra
the sandston
oxyhydroxid
occur in th
honeycomb

One I
At every ou
ridges due t
arises becau
oxyhydroxid

(These bands could only be revealed by breaking some of the honeycombs from the surface.) Liesegang bands also occur in concentric rings in some outcrops (Figure 23). Ironstone structures similar to Liesegang banding are also present in the rock outcrops. "Flame"- type structures (Figure 24) are the most rare of the phenomena. The "flame" structures most likely represent iron-saturated water at the vadose zone boundary where the iron-rich water rose above the saturated zone in the capillary fringe. Iron rings also occur on the outcrop surfaces (Figure 25). These rings or circles occur as separate entities rather than concentric bands. Sometimes the rings or circles coalesce and the sandstone inside the rings weathers out (Figure 26). Where the Liesegang circles coalesce and weather, they exhibit a control on honeycomb formation (Figure 26). The areas where these rings are prevalent do not contain honeycomb weathering except within the ring structures (Figure 26).

In some of the study areas, iron oxyhydroxides precipitated in vertical fractures. The precipitates do not consist of sandy ironstones as with the groundwater ferricretes, but exist solely as iron oxyhydroxides. The iron precipitates appear as if they extruded from the fracture and splay out away from the fracture. The solid iron oxyhydroxides form a thick layer on top of the sandstone surface. Honeycomb weathering has formed in the solid iron oxyhydroxide precipitates (Figure 27). Thus, honeycomb weathering can also occur in the iron precipitates, suggesting that iron may play a role in honeycomb development.

One last iron oxyhydroxide precipitation feature deserves discussion. At every outcrop studied, the bedding planes of the sandstones form resistant ridges due to differential weathering of the rock. The differential weathering arises because the bedding planes in the rock contain larger quantities of iron oxyhydroxides than the sandstone between the bedding planes. The bedding

planes become
than the rest
planes and pre
honeycomb ce
bedding plane
honeycomb d
form resistant
cells occurring
older, they m
honeycomb c

Honey

oxyhydroxic
honeycomb v
shows a repr
honeycomb
sections thro
Hawesville,
the eight th
assess the d
honeycomb
transport or
the thin sec
the same de
counted sec
cement wa
honeycomb

planes become iron enriched because the bedding planes are more permeable than the rest of the rock and allow iron enriched waters to infiltrate the planes and precipitate the cement. The ridges act as bounding surfaces for the honeycomb cells. The increased iron content of the sandstone cements the bedding planes and because they are more resistant to weathering they control honeycomb development. In the areas of the rock where the bedding planes form resistant ridges, honeycomb cells parallel the bedding surface with the cells occurring between two resistant ridges (Figure 28). If the honeycombs are older, they may breach the bedding plane ridge forming large coalescing honeycomb cells.

Honeycomb walls are often more darkly stained with iron oxyhydroxides than are the honeycomb cavities. This suggests that honeycomb walls contain more iron cement than do the cavities. Figure 29 shows a representative cross section through a honeycomb cell, defining the honeycomb wall and the honeycomb cavity. Eight thin sections of cross sections through honeycomb cells were made from samples collected from Hawesville, Kentucky, Cloverport, Kentucky and Black Hand Gorge, Ohio. Of the eight thin sections, three thin sections were point counted (Table 3) to assess the degree of iron cementation in the honeycomb cavities versus the honeycomb walls. The remaining five thin sections either damaged during transport or so plucked that point counts could not be performed. However, the thin sections could be observed under the microscope and they showed the same degrees of iron cementation in the walls and cavities as the point counted sections. In all of the honeycomb cell cross sections studied, iron cement was more concentrated in the honeycomb walls than in the honeycomb cavities.

Figure 20

Groundwater ferricrete in Ferne Clyffe State Park in southern Illinois. The ferricrete is the dark band above the ground surface and below the red key ring in the picture.

Figure 21

Piece of a ferricrete tube taken from the same outcrop in Ferne Clyffe State Park. Note the ironstone rim and the "clean" sandstone inside the tube.

Figure 22

Sub-linear, sub-parallel Liesegang banding in Giant City State Park, southern Illinois.



Concen

Figure 23**Concentric Liesegang banding in Giant City State Park.**



Figure 24



"Flame-type" Liesegang structures in Giant City State Park. The structures are most likely the result of iron-rich waters being drawn up in the capillary fringe in an ancient aquifer.

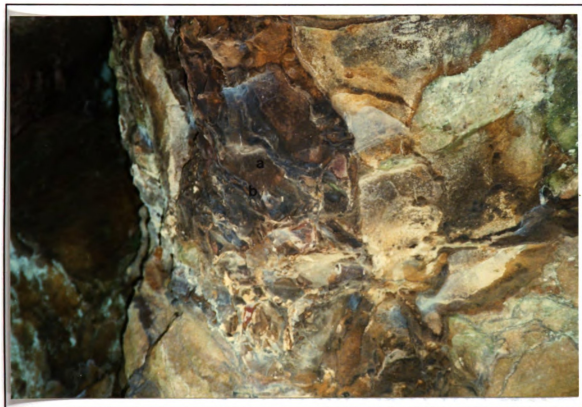
Figure 25



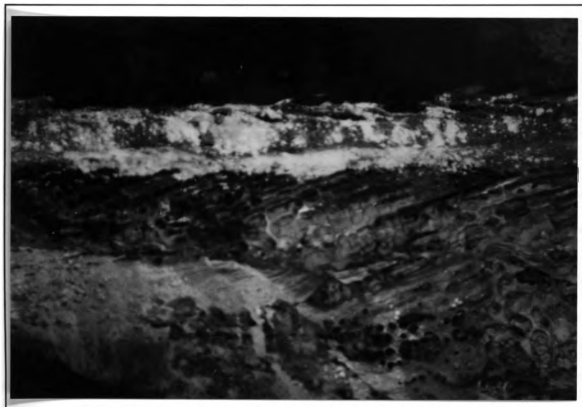
Individual iron cemented circles in a sandstone in Giant City State Park.

Figure 26

Coalescing iron-cemented rings that have weathered to create honeycomb-like cells in the rock face at Ferne Clyffe State Park.

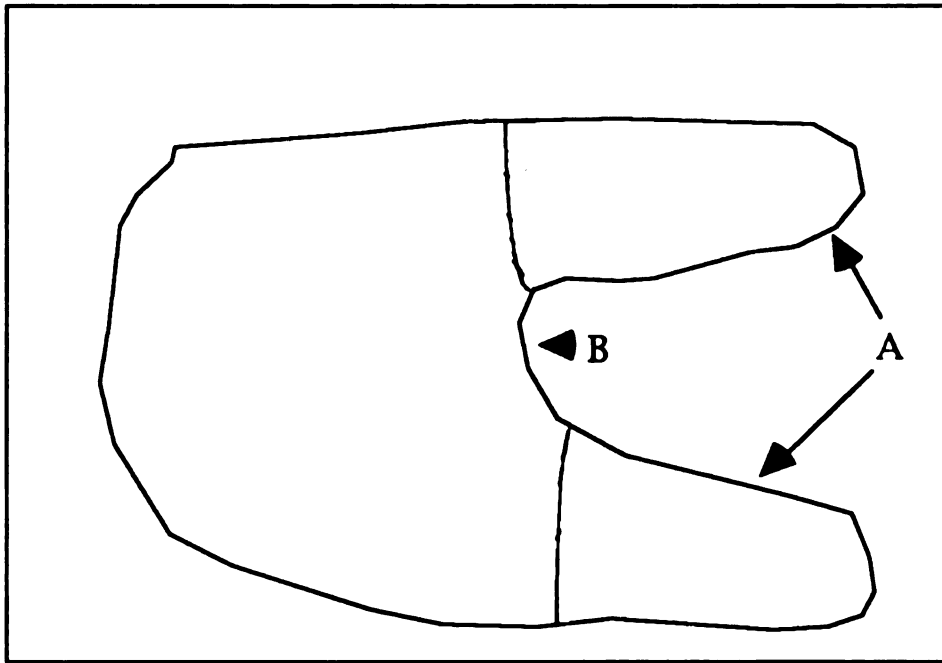
Figure 27

Honeycomb weathering occurring in iron oxyhydroxide precipitates at Turkey Run State Park, Indiana. Honeycomb cavity (a), honeycomb wall (b) and fracture (c).

Figure 28

Honeycomb development along resistant bedding plane ridges in Black Hand Gorge State Nature Preserve, Ohio.

Schematic
honeycom

Figure 29

Schematic cross section of a honeycomb cell, A) honeycomb walls, B) honeycomb cavity.

Location

Hawesville

Hawesville

Cloverport

Point count
cement is

Table 3

Location	Cavity Grains	Cavity Pores	Cavity Iron Cement	Wall Grains	Wall Pores	Wall Iron Cement
Hawesville	64 (68%)	18 (19%)	12 (13%)	50 (47%)	16 (15%)	38 (37%)
Hawesville	69 (70%)	15 (15%)	15 (15%)	58 (48%)	22 (18%)	40 (34%)
Cloverport	59 (61%)	20 (21%)	17 (18%)	55 (49%)	13 (12%)	45 (40%)

Point count data for honeycomb walls versus honeyocmb cavities. Iron cement is almost doubled in the walls relative to the cavities.

Mineral

A

Mississi

and lith

point c

greywa

granites

both te

develop

So

in salt w

1982) pr

honeyco

associati

Figure 4

studied d

enough q

developm

and clay c

in the stud

Aspect

The

related to

Outcrop a

occur at th

northern

Mineralogy and Clay Content

All of the sandstones studied are Carboniferous (Pennsylvanian and Mississippian) quartz arenites (Figure 3). Modal abundances of feldspar, mica and lithics do not exceed 5% (Figure 4). (Refer to Appendix C, Table 1 for point count data.) Other workers report on honeycomb weathering in greywackes in Australia (Gill et al., 1977) and on honeycomb weathering in granites in the desert southwest (Blackwelder, 1929), supporting the idea that both texture and composition probably do not affect honeycomb development.

Some workers (McGreevy and Smith, 1984) find that clay minerals aid in salt weathering and honeycomb development in the rock. Others (Mustoe, 1982) propose that feldspars in the sandstone weather to clays and cause honeycomb weathering. SEM work does not reveal clay minerals in association with salt weathering or honeycomb development in this work. Figure 4 shows that the abundance of feldspar and mica in the sandstones studied does not exceed 5%. Feldspar and mica may not be present in high enough quantities for their alteration to clay minerals to be significant in the development of honeycomb weathering. Thus, mineralogy of the sandstone and clay content of the rock do not appear to control honeycomb weathering in the study areas.

Aspect

The importance of aspect of the honeycomb-weathered outcrop is related to the salt weathering hypothesis for honeycomb development. Outcrop aspect relates to the degree of insolation and evaporation that can occur at the outcrop. South-facing outcrops receive direct sunlight in the northern hemisphere due to the sun's position, thus insolation and

evaporati

facing out

part of th

Sev

honeycom

outcrops

(2) All of

The shadi

insolation

of azimuth

of directio

As can be

entire 360°

which ma

honeycom

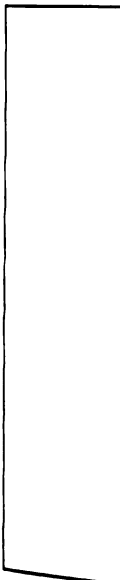
suggest th

weathering

developme

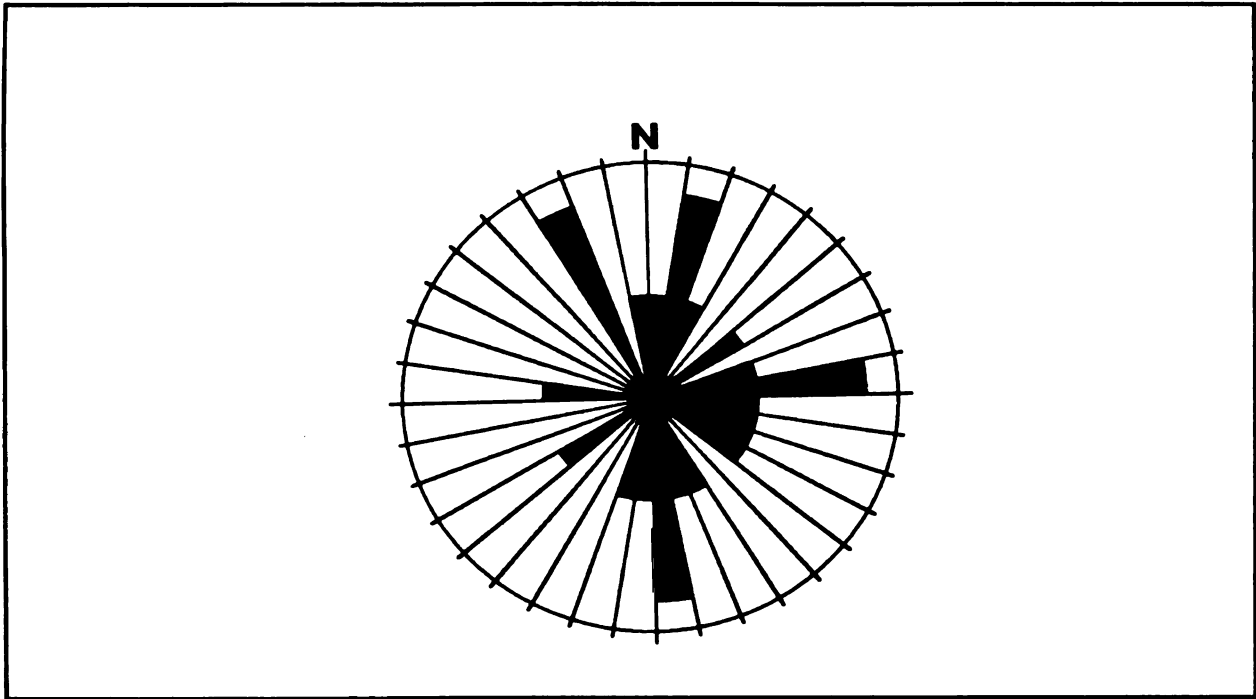
evaporation effects should be greater on south-facing outcrops than on north-facing outcrops. East- and west-facing outcrops also receive direct sunlight for part of the day, also more than north-facing outcrops.

Several factors discredit the hypothesis that aspect plays a role in honeycomb weathering. (1) Some of the largest honeycombs seen in the outcrops exist in the roofs of overhangs which do not receive any sunlight. (2) All of the outcrops are well shaded by trees growing on top of the ledges. The shading allows very little sunlight to directly hit the outcrop, nullifying insolation effects. (3) Aspect measured at the outcrops has a very wide range of azimuthal values. Azimuthal values of outcrop aspect cover a wide range of directions. Figure 30 shows the range of outcrop aspects as a rose diagram. As can be seen, the aspect of honeycomb weathered outcrops ranges over the entire 360° of azimuth. These findings agree with those of Gill et al. (1977) in which many different outcrop aspects exhibit honeycomb weathering and honeycombs are also present on horizontal bedding surfaces. These factors suggest that aspect does not influence honeycomb development and that salt weathering, a consequence of evaporation, may not play a role in honeycomb development.



Rose diag

Figure 30



Rose diagram showing the range aspects of honeycomb weathered outcrops.

Grain Si

G

pebbles.

rocks (M

not impo

also occu

homogener

report ho

and sort

weatherin

Bedding C

Bed

lithologies

may cont

bedding p

developme

ridges and

bedding in

contradict

was quite

honeycomb

in the sand

the bedding

overhangs

depths of

Grain Size and Sorting

Grain size of the sandstones studied ranges from fine-grained sand to pebbles. Honeycomb weathering also occurs in granite and other crystalline rocks (Mustoe, 1982; Conca and Astor, 1987), suggesting that grain size does not impose a control on honeycomb weathering. Honeycomb weathering also occurs in texturally inhomogenous pebbly sandstones and in texturally homogenous well-sorted sandstones. As noted previously, Gill et al. (1977) report honeycomb weathering in a greywacke in Australia. Thus, grain size and sorting do not appear to control the development of honeycomb weathering.

Bedding Characteristics

Bedding surfaces have different porosities, permeabilities and lithologies than the sandstone between the bedding surfaces. Thus, bedding may control honeycomb development. As discussed previously, where bedding planes form resistant ridges (Figure 31), bedding confines honeycomb development between two resistant bedding planes. Seeing the resistant ridges and the control on honeycomb weathering leads to the conclusion that bedding influences honeycomb development. However, several observations contradict this inference. In all of the study areas, honeycomb development was quite common below overhangs. Many of the overhangs also contain honeycomb weathering on their down-facing side. These honeycombs form in the sandstone parallel to the bedding planes rather than perpendicular to the bedding planes. Additionally, most of the honeycombs formed in the overhangs have diameters on the order of 50 to 75 centimeters and cavity depths of the same order. Smaller honeycombs have also developed inside

the large
large flo
large bo
oriented
planes o
either pe

the larger honeycombs (Figure 32). Honeycomb weathering also develops on large float boulders that have broken away from the outcrop. Often these large boulders are oriented in the ground such that the bedding planes are oriented vertically. Honeycombs weathering develops parallel to the bedding planes on these pieces of float (Figure 32). Thus, honeycombs can develop either perpendicularly to bedding or parallel to bedding.

Figure 31

Honeycomb weathering in the roof of an overhang in west of Cloverport, Kentucky. Note the smaller honeycomb development within the larger honeycomb cavities. Also note the Liesegang banding in the sandstone.



Figure 32

Honeycomb weathering development parallel to bedding in a piece of float in Ferne Clyffe State Park, Illinois.

Preser

honey

honey

lichen

the ob

presen

the fac

lichen

growth

and alg

rocks.

contain

present

lichen a

L

honeyco

honeyco

and wet

the rock

honeyco

honeyco

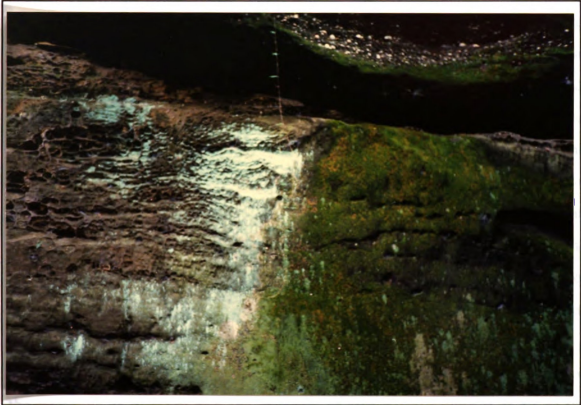
the rock.

Presence of Lichen/Algae

Mustoe (1982) alluded to the presence of lichen and/or algae in many honeycomb weathered rocks. The lichens and algae generally appeared in the honeycomb cavities but not on the honeycomb walls. He proposed that the lichens and algae may secrete organic acids which break down the rock into the observed honeycomb cavities. However, he also suggested that the presence of lichen and algae in the honeycomb cavities may have been due to the fact that the cavities provide shade and a place on the rock where the lichen or algae prefer to grow.

The association between honeycomb weathering and lichen/algae growth was observed at all of the honeycomb weathering study areas. Lichen and algae are not ubiquitous in the honeycomb weathered portions of the rocks. Some outcrops did not contain any visible lichen or algae while others contained plentiful lichen and algae. The lichen and algae are sometimes present where honeycomb weathering is not prevalent and sometimes the lichen and algae appear to influence honeycomb development.

Lichens and algae were most often observed in areas where the honeycomb walls are eroding back to flat surface or where only a few honeycomb cells exist. The rock in the vicinity of the lichen is usually colder and wetter to the touch and only relicts of honeycomb walls can be seen on the rock (Figure 33). It often appears that the lichen and algae destroy the honeycomb weathering. Lichen and algae growth do not appear to enhance honeycomb development but rather appear to erode the honeycombs from the rock surface, destroying the honeycomb weathered surface of the outcrop.

Figure 33

Lichen/algae growth in association with honeycomb weathering on Little Mountain in Holden Arboretum. The left hand portion of the photo (a) contains excellent honeycomb weathering. The right hand portion of the photo (b) contains lichen/algae growth that appears to be destroying honeycomb cells. Rounded humps outlining degraded honeycomb walls are prevalent on the lichen covered side of the picture.

Discussion

Several hypotheses for the origin of honeycomb development were investigated in this study. The only two hypothesized controls on honeycomb weathering that are consistent with the observations of this study are the presence of iron oxyhydroxides and the presence of salts in the honeycombs. However, the salts are not very abundant and the fact that gypsum is the only efflorescent salt present is peculiar. Mustoe (1982) proposes that ion diffusion (such as iron within the sandstone) from the honeycomb cavities to the honeycomb walls may play a role in honeycomb development, however Mustoe rejects this hypothesis. Mustoe rejects ion diffusion based on chemical studies done on the oxide content of honeycomb walls versus honeycomb cavities. The chemical analyses showed that the honeycomb walls did not contain significantly greater concentrations of oxides than did the cavities (Mustoe, 1982). Iron appears to be the only factor that could control honeycomb development in the areas studied. Thus, a geochemical model for honeycomb development is proposed to account for the presence of gypsum and the ubiquity of iron oxyhydroxides at all of the outcrops. Additionally, iron oxyhydroxides are more concentrated in honeycomb walls than in honeycomb cavities, suggesting that ion diffusion (as iron ions) plays a much larger role in honeycomb development than previously expected.

Two possibilities for the presence of honeycomb weathering in temperate, mid-continental sites exist. The first possibility is that salt weathering is not the sole mechanism of honeycomb formation and that iron oxyhydroxides account for the honeycomb development. Studies by Gill et al. (1979) and Takahashi et al. (1994) show that the salt weathering and incipient

honeycomb formation on rocks along the coast occurs in a few tens of years. Honeycomb weathering occurring in temperate, mid-continental sites occurs at a much slower rate, as evidenced from graffiti on outcrop surfaces from the turn of the century that have not yet been compromised. This suggests that honeycomb formation in these sites is a slower process than in coastal sites, or another possibility for the presence of honeycomb exists. The second possibility is that honeycombs in temperate, mid-continental sites are relict geomorphological features left behind from a time when the outcrop areas experienced desert-like conditions. As the glaciers retreated from the Midwest, a cold desert climate prevailed in the area. Honeycombs could have formed in the desert climate and still be preserved in the rocks as relict geomorphological features. The presence of honeycomb features on buildings constructed within the last 200 years in temperate mid-continental regions (this study; Kelletat, 1980; Livingston, 1992) and their similarity to rapidly formed honeycomb features on newly built seawalls (Gill et al., 1977; Mottershead, 1994) suggest that honeycombs are forming in the modern environment and that they are ephemeral features.

CHAPTER 4 - GEOCHEMICAL MODEL FOR HONEYCOMB FORMATION

INTRODUCTION

Most widely accepted models for honeycomb formation invoke salt weathering to prize apart sand grains (Mustoe, 1982; Mottershead, 1994). In those instances where a well-indurated case-hardened crust exists at the surface, with less-well indurated sandstone behind the crust, it is explicitly acknowledged by most researchers that the crust must be breached in order for honeycomb weathering to develop (Winkler, 1994). However, the mechanism by which the crust is breached is seldom explicitly stated; the existing literature conveys the sense that physical prizing apart of the grains in the crust also occurs by salt weathering (Winkler, 1994).

This thesis proposes a geochemical, rather than physical, mechanism for the destruction of the well-indurated surficial iron crust common on outcrops and artificial exposures of sandstone. The hypothesis is that the iron crust is destroyed because of organically mediated chelation, reduction, mobilization, and redeposition of the iron in the crust. Once the crust is breached, disaggregation of the more friable sandstone behind the crust proceeds by salt-wedging as postulated by previous workers. However, this thesis proposes that geometry of the honeycombs is strongly influenced by the pattern of iron mobilization during the dismantling of the iron crust.

Several outcrop characteristics lead to the idea that iron diffusion may control honeycomb development. (1) Iron oxyhydroxide cements are more concentrated in honeycomb walls than in honeycomb cavities. (2) All of the outcrops studied contain an iron oxyhydroxide case-hardening on unhoneycombed outcrop surface. (3) The outcrops all contain prevalent iron banding that suggests a large supply of iron oxyhydroxides for honeycomb

development. (4) Little or not salt is found in association with the honeycomb weathering. (5) The observation of honeycomb weathering forming in iron oxyhydroxide precipitates.

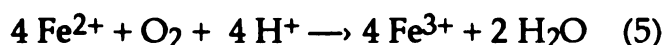
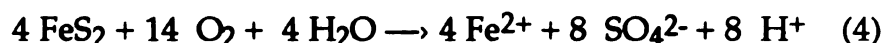
DISCUSSION

Ion Sources for Iron Oxyhydroxides and Gypsum

A source of iron is needed to account for the abundance of iron oxyhydroxides occurring as case-hardening on the sandstone surface, in the honeycomb walls and in the Liesegang banding and ground water ferricretes. Gypsum efflorescence in the honeycomb cavities also requires a source of calcium and sulfate. The simplest source for the ions required to form iron oxyhydroxides and gypsum are pyrite and calcite. Pyrite is documented in subsurface cores from several of the sandstones studied (Price, 1994; Gault, 1938; Holt, 1957). Calcite is also present in many of the sandstones as a minor cement (Price, 1994; Kalliokoski, 1982; Gault, 1938; Holt, 1957). Pyrite-derived iron may also come from shales underlying and overlying the sandstones. Price (1994) demonstrates that the dissolution of small amounts of pyrite and siderite present in the subsurface can account for the iron oxyhydroxide case-hardening in the Eaton Sandstone.

Pyrite is generally stable in subsurface environments where conditions remain reducing. Percolation of oxygen-rich rain water in pyritic sediments or exposure of pyrite bearing sediments to oxic environments causes pyrite to oxidize and dissolve. Pyrite oxidizes to form ferric hydroxide and dissolved sulfate by the reactions (Stumm and Morgan, 1981):





The overall reaction shows that the ultimate driving force for, and limiting factor in the oxidation of pyrite is the reactivity and availability of atmospherically derived O_2 (Williams, 1990).

The primary result of the oxidation of pyrite is the production of SO_4^{2-} , ferric oxyhydroxides and H^+ (Williams, 1990). The resultant decrease in pH allows for the dissolution of matrix minerals and cements in the sandstone, especially carbonates (i.e. calcite). The dissolution of calcite by acid appears as:



Thus, Ca^{2+} is produced by reaction 8. As can be seen from the above reactions, the ions needed to form gypsum and iron oxyhydroxides are produced from the oxidation of pyrite and the dissolution of calcite, two common constituents in sandstones.

Liesegang Banding and Self-Organization

Banded concentrations of ferric oxyhydroxides are common in sandstones, and are caused by a combination of water flow and reaction (Merino, 1984). These bands are known as Liesegang bands and are often described as self-organizing or self-patterning phenomena (Merino, 1984, 1986, Ortoleva, 1984a, 1984b, Ortoleva et al., 1987a, 1987b). Self-organization is the generation of patterns in non-equilibrium systems without the

intervention of external causes, in other words, the patterns can not be accounted for by inheritance (Merino, 1986).

Merino (1984) predicts, through kinetic and quantitative modeling, that the propagation of redox fronts through a sandstone may induce the formation of goethite bands through instabilities arising from the interaction of flow of oxygenated water and dissolution/precipitation reactions within the sandstone. Ortoleva (1984b) presents schematic reactions for the effect of oxygenated waters moving through a sandstone aquifer containing pyrite.



Where P and G represent the minerals pyrite and goethite, respectively, while X, F, and T represent mobile oxygen, Fe²⁺ and thiosulfate species in solution, respectively. Initially, the goethite concentration in the aquifer is zero. Once the oxygenated waters reach the pyrite, Fe²⁺ will be mobilized and oxidized to Fe³⁺, until a supersaturation with respect to goethite occurs. Goethite then nucleates and precipitates as a band along the back edge of the advancing redox front. As reactive waters are forced to flow through the rock, chemical transformation zones move through the medium along the flow path (Ortoleva, 1984a).

Ortoleva points out that the interesting aspect of these reactions is that the goethite content behind the advancing redox front may be oscillatory. In other words, as the redox front moves through the rock, goethite will periodically become saturated in the solution and precipitate, forming Liesegang bands. Ostwald (1925) postulated that the mechanism of band formation in rocks involved a sequence of saturation, nucleation and depletion events in the zone where coprecipitate concentration profiles meet. This sequence repeats itself if one coprecipitate has a higher concentration or

is more mobile than the other such that its profile invades that of the other. When the coprecipitate concentration profile overlap region moves far enough away from the first band, the first band becomes a sink for the coprecipitate and supersaturation can build up again to form a second band (Sultan et al., 1990).

Ground Water Ferricretes

Two types of ferricretes exist, pedogenic ferricretes, forming in the soil horizon and ground water ferricretes, forming in porous, lithified rocks. The focus of this paper is on non-pedogenic ferricretes which are interpreted as being produced by the mobilization and segregation of iron by ground waters (Wright et al., 1992). The ground waters involved are reducing, and during high stands the reduced water causes ferric oxyhydroxides to be reduced to the mobile ferrous ion (Wright et al., 1992). Upon water table lowering or infiltration of oxygenated waters after heavy rainfalls, the mobilized ferrous iron is re-oxidized by the water and deposited as ferric oxyhydroxide nodules or bands (Wright et al., 1992). The formation of iron oxide nodules is the most common expression of ground water ferricretes (Wright et al., 1992). However, if a self-organizing phenomenon occurs, Liesegang banding may form (Merino, 1984; Ortoleva, 1984a).

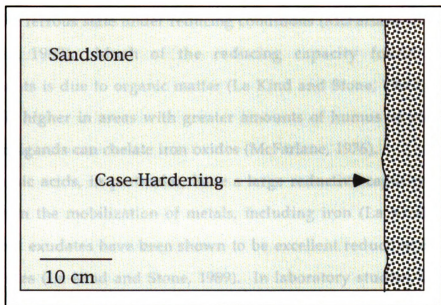
Bourman et al. (1987) find the mineralogy within the sandstones containing ferricretes is not consistent with intense weathering, rather, the micas and feldspars remain fairly unaltered. Thus, ferricretes are linked to the mobilization and redistribution of iron with the rock by the flow of ground water.

Precipitation of Iron on the Rock Surface: Ferruginization/Case-Hardening

Weathering processes in the surface and sub-surface environments can act on the sandstone to either weaken and/or disintegrate the rock or lead to a toughening or hardening of the outer surface of the rock (Robinson and Williams, 1994). Iron oxyhydroxides are often found as case-hardened "skins" several millimeters thick on exposed outcrop surfaces. Exposure to sunlight and drying winds provide a contrast in physical environments from the surface of the stone inward (Winkler, 1994). Case-hardening results as moisture moves toward the stone surface and evaporation of the water redeposits an iron oxyhydroxide cement on the rock surface (Williams and Robinson, 1989; Winkler, 1994). The case-hardened "skin" left behind after evaporation may be evenly distributed, forming a uniformly thick iron-enriched zone, or unevenly distributed, forming an undulatory iron-enriched zone (Figure 34).

In addition to the evaporative precipitation of iron oxyhydroxides at the surface, gypsum can also be precipitated at the surface. As mentioned previously, pyrite dissolution creates free sulfate ion and the low pH created by free hydronium ions can dissolve calcite, generating free calcium in solution. If these two ions become enriched in solution, they can form gypsum efflorescence on the outcrop wall, or within the honeycomb structures.

Figure 34



A uniformly thick case-hardened skin forming at the outcrop surface. The skin may also have a more undulatory expression. The dark stippled area represents the case-hardened zone.

Dissolution of Iron Oxides from the Rock Surface

Goethite and hematite are sparingly soluble minerals under oxidizing conditions found at the earth's surface, rendering iron essentially immobile in surface environments (La Kind and Stone, 1989, McFarlane, 1976). However, ferric iron may move on a limited basis as a colloid or as an organic complex (McFarlane, 1976). Long distance transport of iron appears to take place in the ferrous state under reducing conditions (McFarlane, 1976, La Kind and Stone, 1989). Much of the reducing capacity found in aquatic environments is due to organic matter (La Kind and Stone, 1989). Thus, iron mobility is higher in areas with greater amounts of humus as solutions rich in organic ligands can chelate iron oxides (McFarlane, 1976).

Humic acids, in particular, have a large reductive capacity and play a large role in the mobilization of metals, including iron (La Kind and Stone, 1989). Root exudates have been shown to be excellent reductive dissolvers of Fe(III) oxides (La Kind and Stone, 1989). In laboratory studies, Luther et al. (1992) have shown that ferrous iron complexed with carboxylic acids further enhances hematite reduction and dissolution. The dissolution of iron oxyhydroxides reintroduces iron into pore waters and enables the migration and/or diffusion of iron through the sandstone (La Kind and Stone, 1989). Phenolic substituents have been identified in humic and fulvic acids and are also important sources of reductant capacity in aquatic environments (La Kind and Stone, 1989).

After precipitation events, organic acids are washed out of the overlying soil into the outcropping sandstone. The organic acids slowly dissolve and chelate the iron in the case-hardening. Thus, the organic acids dissolve the iron cement present at the outcrop surface. The acids preferentially chelate iron where an instability exists. The instability could

result from a local porosity or permeability high or a local low concentration of iron cement. Thus, the organic acids will dissolve and breach the case-hardening where the acids can most easily chelate and remove the iron (Figure 35).

A simplified reaction mechanism between the iron oxides and phenolic compounds involves the transport of the reductants to the iron oxide surface, a surface chemical reaction, diffusion of the ions away from the newly forming cavity, and finally, re-oxidation of the reduced iron a specified distance away from the newly forming cavity (La Kind and Stone, 1989). The distance of diffusion from the center of the forming cavity is the radius of the honeycombs, or on the average, approximately 2.5 to 6 cm. La Kind and Stone (1989) find that pH plays a role in the reductive dissolution of iron oxides and oxyhydroxides by phenolic compounds where lower pH's cause faster rates of dissolution of the iron compounds. Thus, naturally occurring phenolic compounds may enhance the mobilization of iron in aquifer environments. Once the reduced and complexed Fe comes into contact with an oxygenated environment, the iron can re-oxidized and precipitate as an iron oxide or oxyhydroxide (Luther et al., 1992).

As the organic acids breach the case-hardening, pockets or cavities develop where the acidic ground water has removed the cement, exposing grains that are otherwise loosely cemented, which easily erode away (Figure 36). As the diffused iron reprecipitates, it forms the honeycomb walls as ferric oxyhydroxides, strengthening the walls and making them more resistant to weathering. The average honeycomb cell ranges in diameter from 5 to 12 centimeters. Diffusion of the iron-organic acid complex across the 2.5 to 6 cm radius from the center of the forming cavity to the honeycomb wall is related

to the characteristic length-scale for diffusion (Lerman, 1979):

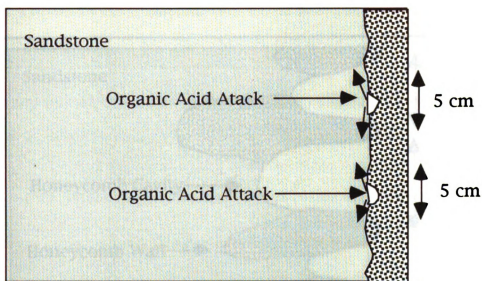
$$L^2 = Dt \quad (11),$$

where L is length of diffusion (i.e. radius of the honeycomb cell), D is the diffusion coefficient for organic acid or case-hardening material and t is the time of diffusion. The diffusion coefficient for the organic acid involved in the case-hardening break down may substituted for the organic complex because organic acids are very large molecules and their diffusion constants are not significantly changed by the chelation of a metal ion (Lerman, 1979). Using citric acid may as a representative organic acid, the diffusion constant of citric acid in water is $6.61 \times 10^{-6} \text{ cm}^2/\text{sec}$ (Weast, 1979) and two values of L , 2.5 and 6 cm, one can determine the time required for the diffusion of iron from the honeycomb cavities to the honeycomb walls. The time values range from 10.9 days for a radius of 2.5 cm to 63 days for a radius of 6 cm. Accounting for porosity and tortuosity effects in the sedimentary environment may reduce the diffusion constants by as much as 10% which does not significantly change the charactersitic lenght and time scales for diffusion (Lerman, 1979).

The average radius of honeycomb cells in this thesis correlate well with studies of honeycomb weathering in other rock types, such as greywackes and granite (Gill et al., 1979; Blackwelder, 1929). The time of diffusion may correlate well with the time it takes the rock to "dry out" after a precipitation event. That is, the organic acids are introduced to the sandstone during a precipitation event and as the rock dries out, the reduced and chelated iron can become oxidized at the newly forming wall, reprecipitating as an iron oxyhydroxide. Diffusion coefficients for other organic acids and case-hardening materials yield similar D values: amino-benzoic acid, $7.74 \times 10^{-6} \text{ cm}^2/\text{sec}$ (Weast, 1979); silica, $3.3 \times 10^{-6} \text{ cm}^2/\text{sec}$ (Lerman, 1979); Mg^{2+} , $7.05 \times 10^{-6} \text{ cm}^2/\text{sec}$; Ca^{2+} , $7.93 \times 10^{-6} \text{ cm}^2/\text{sec}$; Fe^{2+} , $7.19 \times 10^{-6} \text{ cm}^2/\text{sec}$; Fe^{3+} , 6.07×10^{-6}

cm^2/sec (Li and Gregory, 1974). Thus, the diffusion of different case-hardening materials or organic acids that break down case-hardening materials should yield similar characteristic times for diffusion, which may account for the similarity of honeycomb cell sizes.

Figure 35



Representation of preferential organic acid attack on iron oxyhydroxide case-hardened sandstone. The larger stipples represent the iron enriched zone. Honeycomb cavities form where instabilities are present at the iron-enriched zone. The arrows leading away from the newly forming cavities represent the diffusion of chelated iron from the forming cavities.

Figure 36

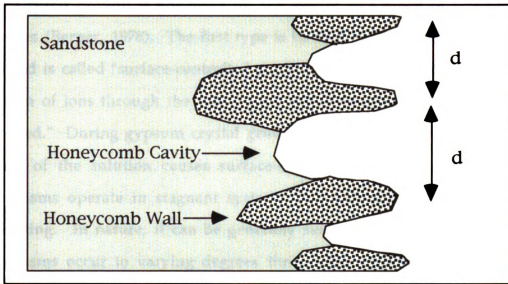


Diagram showing iron concentrations after case-hardening is breached and honeycomb formation. The dark stipples represent the ferruginous honeycomb walls. The width of the honeycomb cavities is indicated by "d," which ranges in diameter from 5 to 12 cm. This width is representative of honeycomb cavity diameters.

Gypsum Efflorescence and Acid Environments

As mentioned previously, every sample of efflorescence found within honeycombs consists of gypsum. Two different crystal habits of gypsum grow in the different study areas. Several authors have done work on different "poisons" that determine which gypsum habit will grow in specific chemical environments. The different gypsum habits are controlled by the presence of different types of acid during the growth of the gypsum crystals.

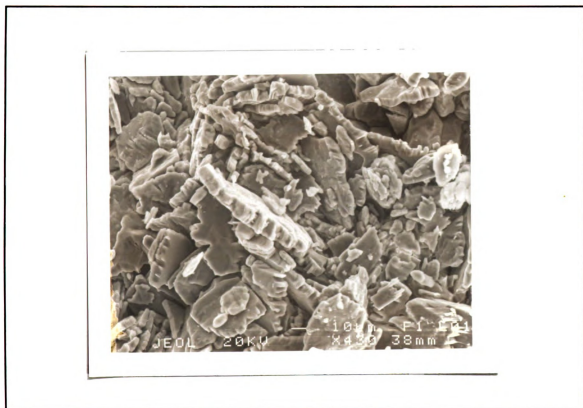
Crystal growth is governed by any one of two types of rate-limiting processes (Berner, 1978). The first type is limited by reactions at the crystal faces and is called "surface-controlled growth." The second is controlled by diffusion of ions through the bulk liquid and is known as "bulk diffusion-controlled." During gypsum crystal growth under experimental conditions, stirring of the solution causes surface-controlled growth, whereas both mechanisms operate in stagnant systems, but with bulk diffusion-control dominating. In nature, it can be generally seen that both growth limiting mechanisms occur to varying degrees throughout gypsum growth (Cody, 1979).

Cody (1979) finds that in all experimental solutions without the input of organic material and with or without the addition of inorganic salts, elongate prismatic crystals form. Lenticular gypsum crystals result from slow growth in the presence of decomposing plant material, while other factors such as temperature of solution, presence of inorganic salts, and sediment type do not affect growth. The lenticular crystals viewed parallel to the c axis appear as small, flat, tabular crystals (Figure 37). The presence of organic material in solution with the gypsum significantly decreases the rate of c axis growth (Cody, 1979). Several organic constituents have been found that cause the lenticular gypsum crystals to grow: sodium citrate, certain posphonates,

glycolic acid, citric acid, tannic acid, carbon-numbered fatty acids, and sodium acetate (Cody, 1979). Cody (1990) states that the effectiveness of even small concentrations of organic substances on the inhibition of crystal growth is usually attributed to the fixation of the organic inhibitors to the growth surfaces of the crystal. The same adsorption poisoning also inhibits growth rates of the crystals (Cody, 1990).

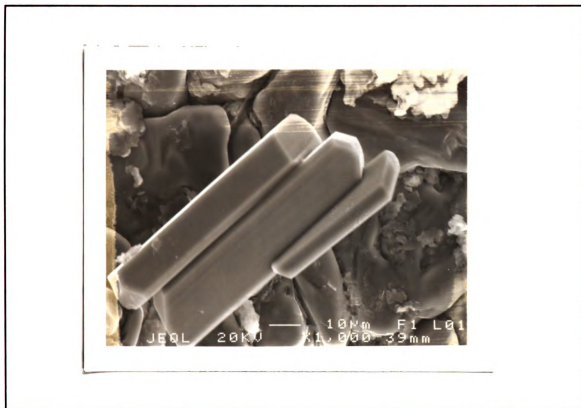
Elongate, prismatic crystals (Figure 38) grow in acid solutions containing organic material, thus, elongate crystals indicate acidic environments, whereas lenticular crystals indicate alkaline conditions (Cody, 1979). Several extrinsic factors exist which can destroy organic inhibitor effectiveness (Cody, 1990). The most effective of these is low pH because the low pH is below the pK values for the functional groups attached to the organic substances, thus deprotonating the organic substance and rendering it as ineffective in inhibiting gypsum growth (Cody, 1990). Oxidative, thermal and biologic degradation of inhibitor molecules will also greatly reduce their effectiveness. Inhibitor molecules can also be adsorbed by strongly adsorbing particulate substances in solution (Cody, 1990).

The two gypsum crystal morphologies found in the different study areas support the inferred rule of organic acids in breaching case-hardened sandstone. The tabular crystals suggest the presence of organic "poisons" inhibiting the growth along the c-axis of gypsum. The elongate, prismatic crystals support the hypothesized acid conditions that arise when reduced iron is oxidized. Thus, both crystal morphologies are consistent with the hypothesis proposed here for the case-hardening breaching of sandstone.

Figure 37

Lenticular or tabular gypsum crystal habit resulting from organic substances acting as c-axis growth inhibitors at Virginia Kendall Ledges Park.

Figure 38



Elongate, prismatic gypsum crystal habit resulting from acid conditions at Stebbins Gulch in Holden Arboretum.

CONCLUSIONS

The minerals pyrite and calcite are common constituents in sandstones. Dissolution of these two minerals provides the ions needed to match the observations made in the study areas. Certainly, other minerals could give rise to the same ionic constituents, however, quartz arenites contain very few minerals other than quartz.

When iron-rich solutions reach the sandstone surface, evaporation of the iron-rich water causes a case-hardening to precipitate. The subsequent introduction of organic matter in the study areas provides a mechanism for breaching the case-hardening and the diffusion of ions from the honeycomb cavity to the wall, supporting the case-hardening breach portion of the model. Once the case-hardening is breached, the honeycomb walls become strengthened and the cavities become weakened. The enrichment of iron in the honeycomb walls and depletion of iron in the honeycomb cavities supports the ion diffusion portion of the model. The case-hardening breach also changes the permeability of the surface at the point of breach. The permeability increases, causing a local area of high permeability. At this point, waters with calcium and sulfate ions can reach the honeycomb cavities. Thus, gypsum will precipitate inside the cavities. Liesegang banding and other iron sources such as pyrite or siderite provide an ample iron supply, such that the outcrop surface will never be completely depleted in iron available for case-hardening. The high iron supply allows honeycombs to completely erode from the rock surface and regenerate as a new Liesegang band is reached as the rock surface erodes or iron is transported to the surface as secondary case-hardening.

CHAPTER 5 - SUMMARY AND CONCLUSIONS

SUMMARY

This study compares honeycomb weathering in Carboniferous quartz arenites cropping out in the temperate, mid-continental American Midwest. By comparing different honeycomb weathering characteristics at the outcrop level, a new geochemical model of honeycomb weathering is developed. This investigation suggests that perhaps more than one mechanism exists for the origin of honeycomb weathering.

The hypothesis that salt weathering is the sole cause for honeycomb weathering is questionable. Breaching the iron oxyhydroxide case-hardening on the outcrop surface is the best hypothesis proposed for honeycomb weathering in the type of area studied. Salt weathering, however, may still be the best explanation in coastal and desert regimes.

Certain outcrop characteristics do influence honeycomb weathering. The presence of Liesegang rings in the rock confines honeycomb development to within the rings. Resistant ridges formed by iron oxyhydroxide precipitation along bedding planes also influences the distribution of honeycomb weathering. Honeycomb development is confined between two resistant ridges which act as bounding surfaces for the honeycomb cells. None of the other outcrop characteristics exert a control on the development of honeycomb weathering.

A model for the development of honeycomb weathering is proposed involving geochemistry as the mechanism of formation rather than physical weathering. Two new ideas are proposed in the model. (1) It is widely accepted that where a case-hardened crust exists, it must be broken down in

order for honeycomb weathering to develop, but no chemical mechanism has previously been proposed (Conca and Astoe, 1987; Harris et al., 1977; Mustoe, 1982, 1984). A specific chemical mechanism for the breaching or breakdown of the ferruginous crust is proposed in this study. (2) The mobilization of iron by a specific process gives rise to a characteristic length/time scale of diffusion, which may be appropriate to and help explain the commonly observed size of honeycomb cells. Additionally, the proposed process draws upon the well known abundance and reactivity of common sandstone materials. The model is supported by physical observations at the outcrop, laboratory observations and previous work reported in the literature.

CONCLUSIONS

- (1) Salt weathering does not cause honeycomb weathering in Carboniferous sandstones in temperate, mid-continental areas in the Midwest.
- (2) Iron oxyhydroxides are ubiquitous in all of the sandstones studied. Their presence appears to exert several influences on honeycomb development in the form of bedding plane ridges and Liesegang Circles.
- (3) Honeycomb weathering can also develop in solid iron oxyhydroxides, suggesting that iron oxyhydroxides play a role in honeycomb development.
- (4) Lichen and other plant growth on the outcrop appear to destroy honeycomb weathering rather than cause it.

(5) The formation of honeycombs in well-indurated, case-hardened sandstone may not develop by the action of salt weathering. When the case hardened layer is composed of iron oxyhydroxides, organic acids may breach the case-hardened layer by reductive dissolution. Once the case-hardened layer is breached, less-well indurated sandstone is exposed, allowing physical erosion processes to occur.

(6) Gypsum morphologies suggest that organic acids are present at the time of their formation, further bolstering the idea of case-hardening breach by organic acids.

(7) Different gypsum morphologies support the case-hardening breach hypothesis proposed in this paper.

SUGGESTIONS FOR FUTURE WORK

Ranges of honeycomb cell sizes for different localities appear to be similar. Measurement of the diameter of hundreds of honeycomb cells at several different localities and in several different rock types may provide some insight into honeycomb formation (i.e. similar cell sizes regardless of rock type, case-hardening material, etc.). Frequency histograms of the honeycomb cell sizes may help to elucidate these questions.

The relative age of honeycomb development also needs to be resolved. This would answer the question as to whether honeycomb weathering are ephemeral weathering features forming at present or if the honeycombs are relict features of past weathering conditions. Age dating using ^{10}Be could

resolve the answer to these questions by revealing the age of exposure of the honeycombs.

Materials other than iron oxyhydroxides, such as quartz, make up the case-hardened crusts on other areas exhibiting honeycomb weathering. Determination of the mechanisms of honeycomb development may reveal interesting insights into the origin of honeycomb weathering. Further work can also be done to test the proposed geochemical model in this study to determine the presence or absence of organic acids and the potential for self-organization phenomena to play a role in honeycomb development.

APPENDICES

APPENDIX A

APPENDIX A**SANDSTONE DESCRIPTIONS****Michigan****Eaton Sandstone, Fitzgerald Park and Lincoln Brick Park, Grand Ledge**

The Pennsylvanian Eaton Sandstone Member of the Grand River Group crops out as the ledges along Grand River and its tributary, Sandstone Creek, in Grand Ledge, Michigan. The outcrop areas studied can be found on the 7.5 minute Eagle, Michigan topographic quadrangle (Appendix B, Figure 37). The Eaton Sandstone in this area makes up the most extensive natural exposure of Pennsylvanian rocks in the Michigan Basin and provides an excellent resource for investigations of Pennsylvanian geology.

The Grand River group consists of the Woodville, Ionia and Eaton sandstones which unconformably overly the Saginaw Formation (Dorr and Eschman, 1970). The name Eaton sandstone is proposed by Kelly (1936) for the uppermost sandstones forming the ledges along the Grand River and its tributaries in the area of Grand Ledge, Michigan. The name Ionia Sandstone includes the cross-bedded, coarse grained sandstones exposed in the Grand River valley near Ionia, Michigan (Kelly, 1936). The name Woodville Sandstone is invoked for the sandstones capping the Saginaw Formation in the vicinity of the Woodville mine in Jackson County, Michigan (Kelly, 1936). Lack of stratigraphic marker beds and local absence of Members of the Grand River Group lead to an indeterminable stratigraphic relationship between the individual members of the Grand River Group (Kelly, 1936).

Kelly (1936) describes the Grand River Group as massive, crossbedded, coarse grained sandstones containing little or no mica and frequently iron

APPENDIX A (cont'd)

stained on fresh fracture surfaces. The Eaton Sandstone Member is a porous, thick-bedded, medium-grained, buff-colored quartz arenite to subarkose (Kelly, 1933; Hudson 1957). The maximum outcrop thickness is approximately 18 meters (Price, 1994).

The upper section of the Eaton sandstone is exposed along Sandstone Creek and consists of approximately 15 meters of thickly bedded (up to 1 meter) sandstone with predominantly tabular-planar cross-stratification (Velbel et al., 1994). The predominant grain size in the study area ranges from 0.250 to 0.500 mm (Hudson, 1957). The sandstones consist mainly of quartz with a siliceous or ferruginous cement, however, minor amounts of mica and feldspar are also present (Kelly, 1936). The Eaton sandstone exhibits a "case-hardening" of the faces of joint blocks and bedding planes where iron hydroxides have precipitated and left behind a resistant layer on the outside of the rocks. Sources of the iron have been much debated. Price (1994) proposed that the iron originates from within the Eaton sandstone from dissolving pyrite grains and siderite and ankerite cements. Others believe that the iron comes from pyrite oxidized in the shales underlying the Eaton Sandstone, and still others think that the iron is transported into the sandstones from Jurassic "red-beds" that formerly overlay the Grand River Group prior to their erosion locally (Velbel, 1995, personal communication).

The rocks of the Grand River group thicken and thin rapidly and disappear locally (Dorr and Eschman, 1970). Discontinuous lensing, presence of ripple marks, and abundance of waterworn land plants and tree parts suggest that the Late Pennsylvanian Grand River Group was deposited by meandering rivers and streams (Dorr and Eschman, 1970). Kelly (1933) and Hudson (1957) also suggest a continental fluvial environment for deposition

APPENDIX A (cont'd)

of the Grand River Group. However, sedimentological data from outcrops in the Grand Ledge area suggest a marginal-marine, probably deltaic depositional environment (Velbel and Brandt, 1989). Velbel et al. (1994) further conclude that marine incursions evidenced by the Verne Limestone and *Lingula* brachiopod beds indicate proximity to and/or hydraulic connectivity to open marine environments with occasional onshore-directed flow.

Jacobsville Sandstone - Morrill Hall

The walls of the main entryway to Morrill Hall, located on the Michigan State University campus, are constructed of Jacobsville Sandstone (Gilchrist, 1947). Outcrops of the Jacobsville can be found in the Upper Peninsula of Michigan. The Jacobsville Sandstone also includes the "lower red member" of Houghton's "Lake Superior Sandstone" (Hamblin, 1958). The Jacobsville consists of feldspathic and quartzose sandstones, conglomerates, siltstones, and shales between 2 to 4 km thick (Kalliokoski, 1982). The sandstone was deposited during Late Precambrian and/or Early Cambrian time (Kalliokoski, 1982).

The Jacobsville varies from subarkose to quartz sub-litharenite with some beds of arkose and quartz arenite (Kalliokoski, 1982). The Jacobsville consists of a fine-grained to medium-grained red sandstone deposited as a fluvial sequence during the Late Precambrian to Early Cambrian (Kalliokoski, 1982). The primary mineralogy consist of volcanic and metamorphic quartz grains, relatively unaltered microcline, fresh to altered plagioclase and metamorphic and volcanic lithic fragments (Kalliokoski, 1982). Average grain size is in the 0.25 to 0.5 mm diameter range (Hamblin, 1958).

The basal contact of the Jacobsville encompasses 230 m of relief with

APPENDIX A (cont'd)

soil layers present on the pre-Jacobsville surface (Kalliokoski, 1982). The sandstone is trough-bedded and well laminated on a 3 to 30 mm scale (Kalliokoski, 1982). East of Keweenaw Bay and north of Bete Grise Bay, the sandstone is locally calcite cemented (Kalliokoski, 1982). Other important cementing materials consist of authigenic quartz, calcite, and iron oxides (Hamblin, 1958).

Indiana**Mansfield Sandstone, Turkey Run State Park**

The basal Pennsylvanian Mansfield Formation (Sandstone) forms the bluffs along Sugar Creek and its tributaries in Turkey Run State Park in western Indiana (Appendix B, Figure 38). The Mansfield Formation unconformably overlies Mississippian rocks and is conformably overlain by Pennsylvanian strata (Holt, 1957). The Mansfield is typically characterized by massiveness, cross-bedding, and abundant iron concretions (Wier and Esarey, 1951). Fossils are rare in the Mansfield (Holt, 1957).

The Mansfield Formation ranges in thickness from 100 to 300 feet and consists of coarse-grained, cross-bedded, brown, red, purple, buff, tan or white sandstones with occasional conglomerate, shale and coal phases (Holt, 1957; Wier and Esarey, 1951; Gault, 1938). The color is dependent upon the amount and type of iron oxide present at the outcrop (Gault, 1938). Locally the base of the Mansfield Formation is a coarse conglomerate of quartz and chert pebbles (Wier and Esarey, 1951).

Holt (1957) finds that the Mansfield Sandstone has a grain diameter ranging from 0.126 mm to 0.277 mm and an average diameter of 0.212 mm.

APPENDIX A (cont'd)

Gault (1938) finds the sandstone is medium-grained with grain diameters ranging from 0.15 mm to 0.6 mm, with sub-angular to sub-rounded grains. The light minerals found in the Mansfield sandstone consist of quartz, orthoclase, plagioclase, microcline, and muscovite, with quartz comprising 90 to 100 percent of the light mineral fraction (Holt, 1957). Holt (1957) also finds that muscovite is abundant in the Mansfield sandstone with values approaching 5 percent in many samples. The primary cementing materials are silica and iron oxide with sparse calcium carbonate and pyrite cements also present (Gault, 1938). The iron oxide cements (limonite and hematite) are present as authigenic cementing material and as coatings on the mineral grains (Holt, 1957).

The Mansfield Formation was deposited by episodes of deltaic progradations (Huff, 1985). Orbiculoid brachiopods, and several types of fluvial sedimentation, including cut and fill by lateral migration, channel fill by vertical accretion and crevasse splay deposition all provide evidence for deltaic deposition (Huff, 1985). Clay chip conglomerates, quartz pebbles, *lepidodendron* fossils and local shale, limestone and coal beds constitute additional evidence for a fluvio-deltaic depositional environment.

Illinois**Pounds Sandstone, Ferne Clyffe State Park**

The Pounds Sandstone of southern Illinois is the upper member of the Caseyville Formation of Early Pennsylvanian age. The Caseyville unconformably overlies Mississippian Strata and is conformably overlain by the Abbott Formation. The Abbott Formation is lithologically similar to the

APPENDIX A (cont'd)

Caseyville, however, the Abbott has a greater proportion of shale and is rarely conglomeratic (Jacobson, 1987). The Pounds sandstone forms the bluffs in Ferne Clyffe State Park that crop out along Round Bluff Trail within the park in Johnson County, Illinois (Appendix B, Figure 39). The maximum exposure of rock along Round Bluffs Trail ranges from 3.5 m to 15 m.

The Pounds Sandstone consists of a medium-grained sandstone with minor amounts of clay chip conglomerate, average bed thicknesses of 5 feet, ripple marks, ripple scours and a few shaly beds up to 1 inch thick making up the lower unit (Simon and Hopkins, 1966). The upper unit of the Pounds sandstone, the unit in the main exposures in Ferne Clyffe State Park, is a medium-grained sandstone with beds averaging 6" thick, festoon cross-bedding and quartz pebbles up to 3/4" in diameter near the base of the bluff (Simon and Hopkins, 1966). Quartz is the dominant mineral with minor clay chips in the sandstone, locally. The lower part of the unit appears structureless due to good sorting of constituent grains, while the upper part contains planar and trough cross-beds.

River-dominated or high-constructive deltaic sediments comprise the Caseyville Formation. The Caseyville contains three main facies: active channel facies, interdistributary facies, and overbank facies (Jacobson, 1987). Bohm (1981) recognizes that fluvial channel facies in the Caseyville are characterized by conglomeratic coarse- to fine-grained sandstones with associated sedimentary structures including large to small scale trough and planar cross-stratification, erosional truncation, overturned and horizontal bedding, and basal scours with an overlying lag deposit. The lag deposits consist mainly of shale or clay chip and quartz pebble conglomerates and

APPENDIX A (cont'd)

conglomeratic sandstones with abundant plant molds and casts. The exposures in Ferne Clyffe contain many of the aforementioned features, suggesting that the Pounds Sandstone in the Ferne Clyffe area was deposited as fluvial channel facies.

Kentucky**Caseyville Sandstone, Pennyrile State Park and Hawesville, Kentucky**

The Pennsylvanian (Upper Pottsville) Caseyville Sandstone (Formation) forms the bluffs in Pennyrile State Park (Appendix A, Figure 40) and outcrops in roadcuts east of Hawesville, Kentucky on U.S. Route 60 in the vicinity of Indian Lake (Appendix B, Figure 41). Although the Caseyville contains limestone, shale and coal beds, they are not laterally extensive, thus the Caseyville in Kentucky is mapped as one unit. The base of the Caseyville in Kentucky is conglomeratic with varying thicknesses of conglomerate, averaging one third of the total thickness. The upper lithologies of the Caseyville are exposed in Pennyrile (Whaley et al., 1979), whereas the basal lithologies are exposed east of Hawesville.

The Caseyville consists of a medium-grained quartz sand with sparse zones of quartz pebbles (Whaley et al., 1979). Pebbles in the Caseyville are usually less than one half inch in diameter (Glenn, 1922). The limonitic iron also forms streaks, plates or masses of sandy-ironstone (Glenn, 1922). The sand contains little or no silt or clay, however sorting is poor and grain shape varies from angular to well rounded (Whaley et al., 1979). Bedding features within Pennyrile are very large (up to 15 m long and 3 m high) (Whaley et al., 1979). Large-scale bedding is discontinuous and the lithologic character of the

APPENDIX A (cont'd)

rocks is quite uniform (i.e. no coarsening or fining upward) (Whaley et al., 1979). Cross-bedding is often accentuated by differential weathering where limonitic iron is concentrated in the rock (Glenn, 1922).

Whaley et al. (1979) note that the Caseyville sandstones appear to be composed of coalescing dendroids of channels commonly forming belts that focus into channels incising the Mississippian paleosurface. Between the sandstone-filled channels, the Caseyville consists of dark-gray shales, thin tabular to festoon bedded sandstones, thin coals and limestone beds. The coarser-grained beds (conglomerates and sandstones) tend to be the focus of studies because they tend to crop out more frequently than the limestones, shales and coals. Although no lithologic changes occur in the Caseyville Formation within Pennyryle, observations of truncation of bedding and discontinuous bedding suggest channel fill facies (Whaley et al., 1979). Support for fluvial depositional environments lies in the fact that no fossils have been found in the Pennyryle outcrops (Whaley et al., 1979). However, some trace fossils do exist in sands higher in the section several miles north of Pennyryle; thus, the sands may have been deposited as channel fill facies or a delta/barrier bar complex (Whaley et al., 1979; Davis et al., 1974).

Greb (1989) reports on the Caseyville Sandstone in the Indian Lake area east of Hawesville, Kentucky. The basal Pennsylvanian strata in the Indian Lake area range in thickness from 59 to 152 meters with the thickest portions lying in the paleovalleys (Greb, 1989). In the Indian Lake area, the Caseyville overlies Chesterian marine carbonates, sandstones and shales which are exposed further east along U.S. 60. A sub-Pennsylvanian paleodrainage system exists at the base of the Caseyville Formation termed the Indian Lake

APPENDIX A (cont'd)

paleovalley system after exposures near Indian Lake, Hancock County (a few miles east of Hawesville, Kentucky) (Greb, 1989).

The paleovalley follows fault lines along horsts and grabens, forming a sub-rectangular paleovalley system. In the area of Indian Lake, the basal Pennsylvanian consists of conglomeratic sandstones unconformably overlying the Chesterian Series (Greb, 1989). The principal valley-fill section in the Indian Lake area consists of buff to yellow, poorly sorted, fine- to coarse-grained, quartz litharenites. The sandstone commonly contains quartz pebbles, and is thus informally known as the Indian Lake pebbly-sandstone facies (Greb, 1989). Planar cross-bedding and small-scale trough cross-bedding dominate the section studied in this investigation (Greb, 1989). The Indian Lake pebbly-sandstone generally fines upward with grain sizes ranging from fine sand to coarse-pebble gravel and average grain size ranging from medium- to coarse-grained sand (0.25 to 0.50 mm) (Greb, 1989). Quartz pebbles commonly occur above and beneath bedding-plane surfaces and along foresets (Greb, 1989). Pebbles most commonly occur in layers a single pebble in thickness (Greb, 1989). Pebbles are most abundant in the lower five meters of the section (Greb, 1989). The conglomeratic nature and the poor sorting of the Indian Lake pebbly-sandstone, point towards a fluvial depositional environment (Greb, 1989).

Tar Springs Sandstone, Cloverport, Kentucky

The Tar Springs Sandstone crops out in roadcuts along U.S. Route 60 west of Cloverport, Kentucky. Excellent outcrops exhibiting honeycomb weathering occur at the southwest corner of the intersection of U.S. 60 and

APPENDIX A (cont'd)

Kentucky Route 144 west of Cloverport, Kentucky (Appendix B, Figure 42). The Tar Springs Formation is the first member of the Mississippian Upper Chesterian Series.

The Chesterian Series consists of cyclically alternating shallow marine carbonates and siliciclastic rocks, and deltaic siliciclastic rocks deposited as deltaic progradations from the Canadian Shield area (Treworgy and Norby, 1989). Some of the Chesterian transgressive-regressive cycles have been correlated with eustatic sea-level changes as defined by fossils collected in the Mississippi River Valley region (Treworgy and Norby, 1989). Chesterian sandstones generally occur as lenticular tidal bars, fluvial-deltaic bodies or submarine channel-fill bodies, all commonly reworked, even though in regional cross-sections they may appear as blanket sandstones (Treworgy and Norby, 1989).

The Tar Springs Formation consists mainly of quartz arenites and sublitharenites, however, in some areas it is almost entirely siltstone and shale (Treworgy and Norby, 1989, Wescott, 1982). In most outcrops, the Tar Springs is a fine-grained, yellow to yellow-brown sandstone with variable bedding character ranging from thinly bedded to massively bedded and even cross bedded in some areas; however, most of the Tar Springs is thinly bedded or flaggy in character (Weller, 1921). As a typical Chester sandstone, the Tar Springs is iron-stained and can only be distinguished from other Chesterian sandstones from its stratigraphic position (Tisza, 1956).

Glenn Dean Limestone underlies the Tar Springs Sandstone and the Vienna Limestone overlies the Tar Springs Sandstone. As mentioned previously, the Chesterian Series consist of alternating sequences of

APPENDIX A (cont'd)

sandstone grading upwards into limestone/shale with the lower units of the Chester Series representing the transgression and the upper units of the Chester Series representing the regression (Weller, 1921). Unconformities exist at the upper surface of some of the cycles, suggesting regression and transgression of an epeiric sea (Weller, 1921). The subsurface thickness of the Tar Springs is highly variable and it is locally absent, due to either differential compaction or the presence of an erosional unconformity at the top of the Glenn Dean Limestone (Weller, 1921). Like most other Chesterian sandstones, few fossil remains exist in the Tar Springs sandstone. The only fossils found in the Tar Springs consist of small, indeterminable, fragmentary plant remains (Weller, 1921).

Fossils within the Tar Springs are rare and those present do not lead to the conclusion of a strictly marine depositional environment (Weller, 1921). Thus, the Tar Springs may have been deposited under marine or non-marine conditions or a combination of the two. The best evidence for the transgression of the sea is the thick shale bed separating the two sand bodies of the Tar Springs. Herringbone cross bedding and ripple laminations suggest the Tar Springs Sandstone was deposited in fluvio-deltaic and associated coastal environments with four major facies being distinguished: cross-stratified sandstone, horizontally bedded sandstone, flaser and lenticular bedded sandstone, and interbedded sandstone and shale (Treworgy and Norby, 1989).

APPENDIX A (cont'd)**Ohio****Berea Sandstone, Holden Arboretum, Ohio**

The Berea Sandstone crops out in Holden Arboretum, east of Kirtland, Ohio (Appendix B, Figure 43). The Berea Sandstone comprises a portion of the Lower Waverly group of Early Mississippian age in northern and central Ohio. The Waverly Group composes the sediment packages overlying the Devonian Ohio Shales and underlying the Pennsylvanian Pottsville Group (Coogan et al., 1981). Mississippian sediments in Ohio were derived from the Appalachian positive area to the east and the Canadian Shield to the north (Coogan et al., 1981). The Lower Waverly (Bedford Shale and Berea Sandstone) in eastern Ohio represent open marine, marginal marine and deltaic deposits (Coogan et al., 1981).

The Berea Sandstone is a fine- to medium-grained, moderately sorted, often calcareous, lithic sandstone (Lewis, 1988). In the Cleveland area, the upper portion of the Berea has a blanket geometry and the lower portion shows channel-form features (Lewis, 1988). Bedforms within the upper blanket portion of the sandstone consist of large scale cross-beds alternating with horizontal, symmetrical rippled beds ranging from 0.7 to 4.0 m thick (Lewis, 1988). Thin mud laminations and thin bioturbated mudstones are scattered throughout the sandstone (Lewis, 1988). Similar to Price's (1994) subsurface investigation in the Michigan Basin, Jackson (1985) finds pyrite and siderite in significant quantities in the subsurface of the Berea Sandstone in Northeastern Ohio.

The clastic sediments of the Berea Formation were derived from southeastern, northeastern and eastern sources, and prograded westward into

APPENDIX A (cont'd)

a shallow basin (Lewis, 1988). Marine clastic wedges provided a northwest paleoslope and a distal, gentle-shelf margin that controlled the emplacement of coarse clastics (Lewis, 1988). Occasionally, coal fragments and rip-up clasts occur as scattered fragments or as thin lenses in cross-bed sets (Lewis, 1988). However, erosional contacts are rare (some evidence of mudcracks has been found) and more often than not, soft sediment deformation is seen between the underlying Bedford Shale and the Berea Formation (Lewis, 1988). Although paleochannels exist in the Bedford, the soft sediment deformation and apparent association with blanket sands suggests a marine distributary system of sands constructively deposited in areas containing thick muds of the gentle slope and distal basin (Lewis, 1988; Corbett and Manner, 1988). Brachiopods and rare trilobite resting marks have been noted in the Cleveland region, which suggests a marine environment (Lewis, 1988; Corbett and Manner, 1988).

Black Hand Sandstone, Black Hand State Nature Preserve, Toboso, Ohio

The Black Hand Sandstone crops out in central Ohio in three north-south trending sand bodies or lobes (Barclay, 1968). The three lobes are known as the Toboso Lobe, the Hocking Lobe and the River Styx Lobe. The study areas outcrop in the Toboso Lobe (Black Hand Gorge State Nature Preserve (Appendix B, Figure 44)), and the Hocking Lobe, in Hocking Hills State Park (Old Mans Cave (Appendix B, Figure 45), Cedar Falls (Appendix B, Figure 46) and Ash Cave (Appendix B, Figure 47)). Black Hand Gorge State Nature Preserve is the type locality for the Black Hand Sandstone. The sandstones and pebbly sandstones of the Black Hand Member are the predominant resistant rocks of the Cuyahoga Formation of Mississippian age

APPENDIX A (cont'd)

forming the ridges and ledges in the outcrop areas (Barclay, 1968).

The Black Hand is commonly light brown to yellow-brown in color but may be light buff or red due to iron oxide coatings locally (Barclay, 1968). The sandstones are coarse-grained and cross-bedded with a lobate geometry that grades into finer-grained material containing marine fossils to the south (Coogan et al., 1981). Within the Black Hand Gorge area, the Black Hand is exposed as a cross-bedded conglomeratic sandstone (Malcuit and Bork, 1987). Granules and pebbles within the sandstone are generally concentrated in zones ranging in thickness from one to several feet, but may be randomly scattered locally (Barclay, 1968). Quartz and chert are the primary pebble lithologies (Malcuit and Bork, 1987).

Within the Black Hand, two distinct varieties of sandstone exist, quartz arenite and quartz wackes (Barclay, 1968). The quartz wackes are not encountered in the study areas. The quartz arenites are the most common and contain between 90% and 98% quartz, chert and quartzite in the detrital grains. Most of the quartz arenite beds are medium-grained, well-sorted sandstones to pebbly sandstones (< 25% pebbles) with a few conglomerates (> 25% pebbles) (Barclay, 1968). The sand-sized grains are equant and subrounded and the pebbles and granules are rounded to well-rounded (Barclay, 1968). The arenites contain 0.5% or less muscovite and minor amounts of feldspar are found in thin sections (Barclay, 1968).

Cross-bedding is the predominant structural feature of these sandstones with dip angles between 10° and 20°, common (Coogan et al., 1981). Barclay (1968) finds limonite to be present as a surface coating on sand grains and as an interstitial cement in the arenites. Vargas (1975) reports porosity and permeability values for the Black Hand. The values for porosity

APPENDIX A (cont'd)

and permeability range from 18.2% to 29.1% for porosity and from 0 to 336 millidarcies for permeability.

The Upper Waverly (Mississippian) Cuyahoga Formation was deposited during a marine transgression over Lower Waverly (Mississippian) sediments and conformably overlies the Berea Sandstone (Coogan et al., 1981, Barclay, 1968). The upper surface of the Black Hand is an erosional surface evidenced by the presence of channels and truncation of cross-bed sets (Malcuit and Bork, 1987). The Cuyahoga Formation coarsens upwards and is interpreted as consisting of prodeltaic marine shales; delta-front, fine-grained sandstones and siltstones; and coarser grained distributary mouth bars and marine bars and shoals (Coogan et al., 1981). Malcuit and Bork (1987) determine a deltaic depositional environment which later underwent strong marine influence and some sediments were reworked into a barrier-bar complex. Fossils within the Black Hand Sandstone are rare, however, portions of the sandstone contain brachiopod and pelecypod fossils, suggesting at least a partial marine origin for the sandstone, while other areas contain significant amounts of spores and tree markings, suggesting a brackish to non-marine origin for part of the facies, all of which may indicate a transitional depositional environment between marine and non-marine (Barclay, 1968).

Sharon Conglomerate, Cuyahoga Valley National Recreation Area, Ohio

Virginia Kendall Park (Appendix B, Figure 48) is part of the Cuyahoga Falls National Recreation Area (north of Akron and south of Cleveland, Ohio) and contains excellent outcrops of the Pennsylvanian Sharon Conglomerate. Outcrops of Sharon Conglomerate can also be found in

APPENDIX A (cont'd)

Holden Arboretum on "Little Mountain" (Appendix B, Figure 43). The ledges within Virginia Kendall Park have excellent exposures of honeycomb weathering along the trail leading to Ice Box Cave.

The Sharon Conglomerate consists predominantly of interbedded sandstones, conglomeratic sandstones and conglomerates with abrupt vertical and lithological changes (Norton, 1979). The Sharon Conglomerate consists of a sheet-like deposit infilling the erosional surface of the underlying Mississippian strata leaving behind hills of the older Mississippian rocks that did not get covered during sedimentation, but are covered by later Pennsylvanian strata (Mrakovich and Coogan, 1974).

The Sharon typically consists of medium-grained, clean, friable sands (Hannibal and Feldman, 1987). However, conglomerate layers and lenses are often encountered (Hannibal and Feldman, 1987). The Sharon generally consists of a loosely cemented quartz arenite with the majority of the conglomerate occurring in two north-south trending channels and local shale and siltstone lenses (Mrakovich and Coogan, 1974). Sandstones within the Sharon are predominantly planar cross-bedded with trough cross-bedding common and horizontal bedding uncommon (Mrakovich and Coogan, 1974).

Conglomerates within the Sharon consist of massive, horizontal, planar and trough cross-bedding with horizontal and trough cross-bedding being the most dominant (Mrakovich and Coogan, 1974). Conglomerates of the Sharon are comprised of milky and smoky quartz pebbles, jasper, silicified limestone and in lesser amounts, sandstone, quartzite and quartzite conglomerate pebbles all held together by a loosely cemented matrix of finer sand (Mrakovich and Coogan, 1974). Sandstones of the Sharon consist of clean, white, friable sands with a grain size ranging between 0.25 and 0.5 mm

APPENDIX A (cont'd)

(Mrakovich and Coogan, 1974). Quartz and iron oxides make up the primary cements within the sandstones (Mrakovich and Coogan, 1974). Iron oxides occur principally near the outcrop surfaces and along permeable beds and joints, causing bedding planes to form resistant ridges on the outcrop surface (Mrakovich and Coogan, 1974). No apparent vertical sequence of bedding types exist in the Sharon (Mrakovich and Coogan, 1974). Where conglomerate beds are present, they range in thickness from one or two pebbles thick to several meters thick (Mrakovich and Coogan, 1974). Conglomerates also exist in the form of long belts in which grain size is uniform along the channel and changes as one goes across a channel (Fuller, 1955). The Sharon sandstones are compositionally mature orthoquartzites (Norton, 1979). Detrital grains consist of mono- and polycrystalline quartz with lesser quantities of feldspar, lithic fragments, mica, and opaques (Norton, 1979). The sandstones vary from well to poorly sorted, with sorting increasing from north to south (Norton, 1979). The Sharon Sandstone is a uniformly medium-grained, white to yellow, friable quartz sandstone with a quartz content of over 96% (Pringle, 1982).

Mrakovich and Coogan (1974) interpret that the Sharon Conglomerate as an alluvial plain deposit formed by braided streams, based on lithology, geometry, and abundance of planar cross-stratification. Furthermore, Anderson (1975), in a discussion of Mrakovich and Coogan (1974), points out that easily erodible, non-cohesive stream banks also offer evidence of braided streams. Fine-grained stream banks often correlate to meandering streams, thus, the lack of fine-grained sediments in the Sharon suggests an abundance of soft stream banks and gives direct evidence for braided stream deposition. Fossils are rare in the Sharon; however, two types of fossils have been found,

APPENDIX A (cont'd)

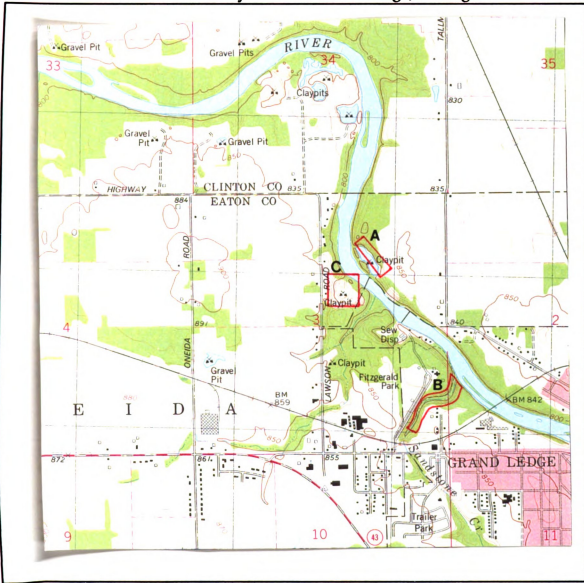
fragments of Pennsylvanian plants and Middle Devonian rugose corals, suggesting possible source areas for the Sharon (Pringle, 1982). Fossils that are typically in poor condition and show evidence of transport (Fuller, 1955). Fuller (1955) suggests that the patterns and alignment of the conglomerate belts suggests a depositional environment consisting of distributary channels on a deltaic or alluvial plain. The axis of the conglomerate belts is sometimes parallel to bedding and sometimes it cuts across bedding, indicating rapidly changing conditions of deposition and erosion (Fuller, 1955).

APPENDIX B

123
APPENDIX B
SITE LOCATIONS

Figure 39

Location of Study Areas in Grand Ledge, Michigan



Location of outcrops in the Grand Ledge study area in Eaton and Clinton Counties on the Eagle, Michigan 7.5 minute topographic quadrangle. A) Lincoln Brick Park, B) Fitzgerald Park - Sandstone Creek, C) Fitzgerald Park - Pond Area . (Study area outlined in red.)

APPENDIX B (cont'd)

Figure 40

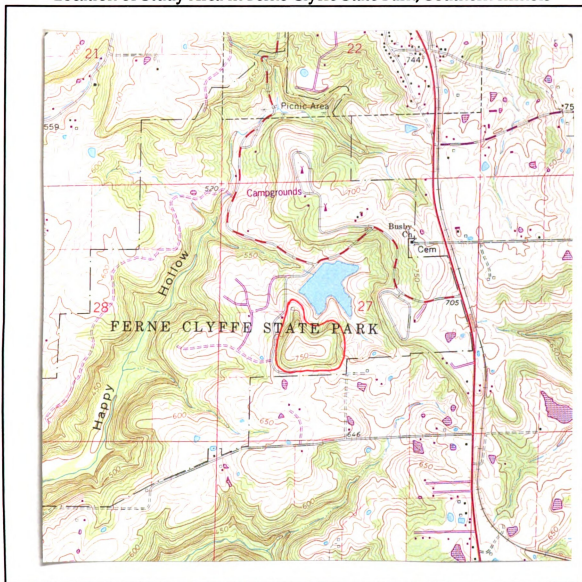
Location of Study Area in Turkey Run State Park, West-Central Indiana



Location of Turkey Run State Park on the Wallace, Indiana 7.5 minute topographic quadrangle. The study area is located along Sugar Creek and its tributaries (Rocky Hollow and unnamed intermittent stream) in sections 27 and 28, R 7 W, T 17 N, Parke County. (Study area outlined in red.)

Figure 41

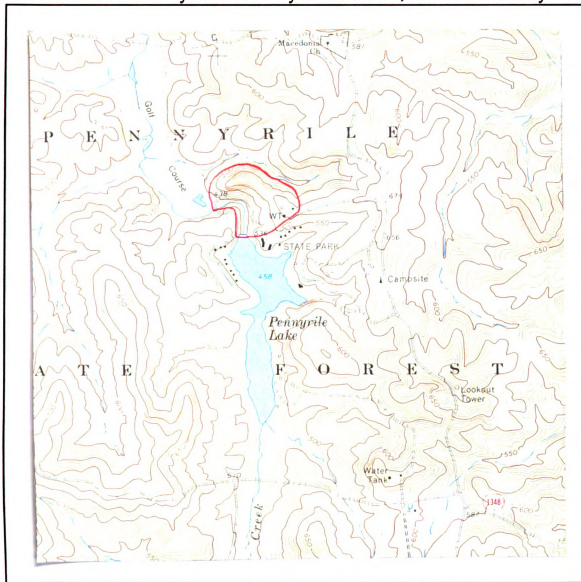
Location of Study Area in Ferne Clyffe State Park, Southern Illinois



Location of Ferne Clyffe State Park on the Goreville, Illinois, 7.5 minute topographic quadrangle. The study area is located in the NE 1/4 of the SW 1/4 of sec. 27, R 2 E, T 11 S, along Round Bluff Trail in Ferne Clyffe State Park, Johnson County, Illinois. (Study area outlined in red.)

Figure 42

Location of Study Area in Pennyriple State Park, Western Kentucky

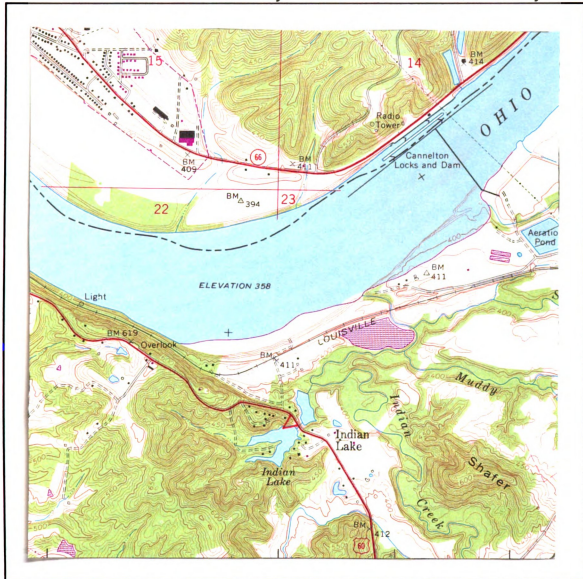


The study area is located along Indian Bluffs Trail in Pennyriple State Forest, Christian County Kentucky, on the Dawson Springs SW 7.5 minute topographic quadrangle. (Study area outlined in red.)

APPENDIX B (cont'd)

Figure 43

Location of Indian Lake Study Area East of Hawesville, Kentucky



The Caseyville Sandstone outcrop containing honeycomb weathering east of Hawesville, Kentucky is located near Indian Lake in figure. (Study area outlined in red.)

APPENDIX B (cont'd)

Figure 45

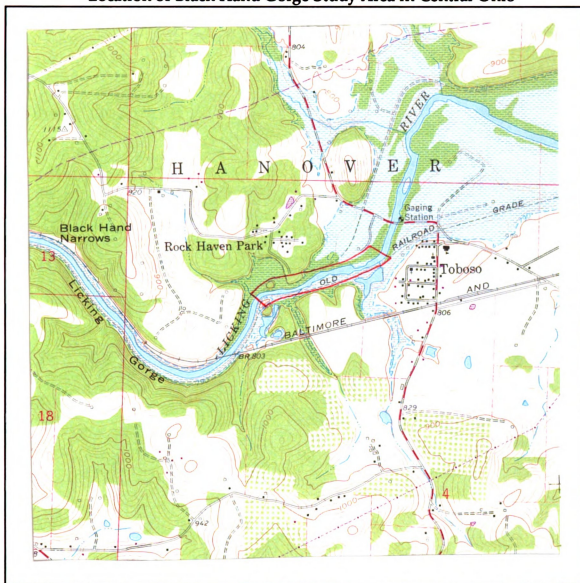
Location of Study Areas in Holden Arboretum, Ohio



Holden Arboretum is located approximately 4 miles east of Kirtland, Ohio. The study areas can be found on the Chesterland, Ohio 7.5 minute topographic Quadrangle, R 9 W, T 9 N, Lake County. A) Little Mountain - Sharon Conglomerate outcrop. B) Stebbins Gulch - Berea Sandstone outcrop. (Study areas outlined in red.)

Figure 46

Location of Black Hand Gorge Study Area in Central Ohio



The area is located on the Toboso, Ohio 7.5 minute topographic quadrangle, T 2 N, R 10 W, Licking County. The most accessible outcrops can be found along the bike trail on the south side of the Licking River in "Rock Haven Park." (Study area outlined in red.)

Figure 47

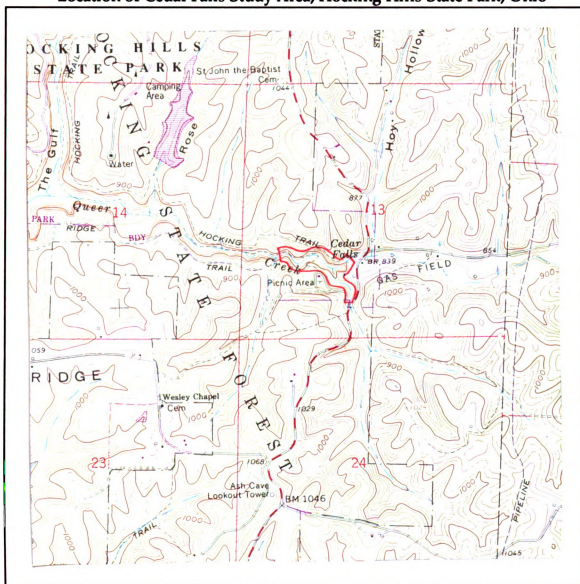
Location of Old Mans Cave Study Area, Hocking Hills State Park, Ohio



Old Mans Cave is located in the South Bloomingville, Ohio 7.5 minute topographic quadrangle, in the SW 1/4 of sec. 11, T 13 N, R 18 W, Hocking County. (Study area outlined in red.)

Figure 48

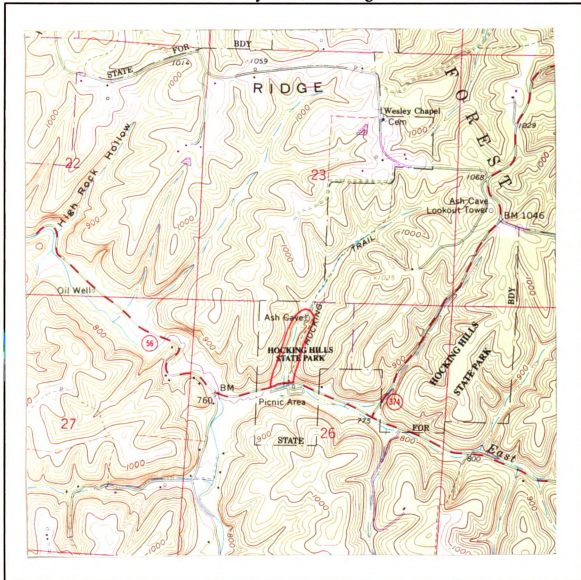
Location of Cedar Falls Study Area, Hocking Hills State Park, Ohio



The study area in the vicinity of Cedar Falls can be found on the South Bloomingville 7.5 minute topographic quadrangle in the SW 1/4 of sec. 13, R 18 W, T 13 N, Hocking County. (Study area is outlined in red.)

Figure 49

Location of Ash Cave Study Area, Hocking Hills State Park, Ohio



Ash Cave is located on the South Bloomingville, Ohio, 7.5 minute topographic quadrangle in the NW 1/4 of sec. 26, R 18 W, T13 N, Hocking County. (Study area is outlined in red.)

134
APPENDIX B (cont'd)

Figure 50
Location of Virginia Kendall Ledges Park Study Area in Cuyahoga Falls
National Recreation Area, Ohio



The study area is located in Virginia Kendall Park along the Ice Box Cave Trail on the Peninsula, Ohio and Hudson, Ohio 7.5 minute topographic quadrangles, R 11 W, T 4 N, Summit County. (Study area outlined in red.)

APPENDIX C

APPENDIX C

POINT COUNT DATA

Table 4

Sample	Quartz	Feldspar	Lithics	Mica	Fe Cement	Porosity
ASH-1	150	10	0	5	14	28
ASH-2	155	4	0	0	34	15
BHG-2	115	0	0	4	0	40
CF-1	160	0	0	1	7	39
CF-2	190	2	0	1	0	40
FC-1	200	0	0	0	9	26
FP-1	190	6	7	4	3	20
FP-2	195	3	0	6	1	37
HAWES	199	4	3	0	2	35
LBP	191	5	2	2	25	17
OMC-1	193	2	1	4	17	10
OMC-2	192	1	7	0	3	59
PENNY	190	0	3	10	16	41
TR	192	2	4	2	87	5
VKL	197	0	2	1	4	32

Point count data for figure 3. Data reported as number of count.

- ASH - Black Hand Sandstone from Ash Cave, Hocking Hills State Park, Ohio.
 BHG - Black Hand Sandstone from Black Hand Gorge State Nature Preserve, Ohio.
 CF - Black Hand Sandstone from Cedar Falls, Hocking Hills State Park, Ohio.
 FC - Pounds Sandstone (Caseyville) from Ferne Clyffe State Park, Illinois.
 HAW - Caseyville Sandstone from Indian Lake east of Hawesville, Kentucky.
 LBP - Eaton Sandstone from Lincoln Brick Park, Grand Ledge, Michigan.
 OMC - Black Hand Sandstone from Old Man's Cave, Hocking Hills State Park, Ohio.
 PEN - Caseyville Sandstone from Pennyryle State Resort Park, Kentucky.
 VKL - Sharon Conglomerate from Virginia Kendall Ledges Park, Cuyahoga Valley
 National Recreation Area, Ohio.
 TR - Mansfield Sandstone from Turkey Run State Park, Indiana.
 FP - Eaton Sandstone from Fitzgerald Park, Grand Ledge, Michigan.

APPENDIX D

APPENDIX D
XRD AND EDS ANALYSIS RESULTS FOR SALT WEATHERING

Table 5

Sample Number	XRD Analysis	EDS Analysis
MH-E-5	Quartz, Orthoclase, Halite, Calcite	-----
MH-E-8	-----	Na, Mg, Al, Si, S, Cl, K, Ca, Fe
MH-E-10	Halite, Orthoclase, Microcline	-----
MH-E-11	Calcite, Halite	Na, Cl, Ca
MH-E-12	Halite, Orthoclase, Microcline	-----
MH-E-16	Halite, Alunite, Microcline, Calcite	Na, Al, Si, S, K, Ca
MH-E-17	Halite, Microcline	Mg, Al, Si, Cl, K, Na
LBP-2	Halotrichite	Mg, Al, S, Mn, Fe
LBP-3	Halotrichite, Melanterite, Rozenite, Ferrohexahydrate	-----
LBP-4	Halotrichite	Mg, Al, Si, P, S, Fe
FP-4	Halotrichite	Mg, Al, Si, S, Mn, Fe
FP-6	Halotrichite	Mg, Si, Al, S, K, Ca, Mn
FP-7	Halotrichite	Mg, Al, Si, S, Mn

X-ray diffraction and energy dispersive spectroscopy analysis results for salts for present in occurrences of salt weathering.

1. MH-E - Samples taken from Morrill Hall, Michigan State University.
2. LBP - Samples taken form Lincoln Brick Park, Grand Ledge, Michigan.
3. FP - Samples taken from Fitzgerald Park, Grand Ledge, Michigan.

----- - indicates that a particular analysis was not run.

APPENDIX E

APPENDIX E

X-RAY DIFFRACTION DATA FOR HALITE AT MORRILL HALL

Table 6

JCPDS	File No	5-628	MHE-5		MHE-10	MHE-11	MHE-12	MHE-13				
d(A)	I/I ₀	(hkl)	d(A)	I/I ₀	d(A)	I/I ₀	d(A)	I/I ₀	d(A)	I/I ₀	d(A)	I/I ₀
3.258	13	111	3.24	22					3.23	16	3.23	15
2.821	100	200	2.81	100	2.8	100	2.79	100	2.79	100	2.80	100
1.994	55	220	1.99	87	1.99	86	1.99	40	1.99	33	1.94	69
1.701	2	311	1.7	4					1.69	2		
1.628	15	222	1.62	13	1.62	14			1.62	12	1.62	21
1.410	6	400	1.40	4					1.40	4	1.40	6

X-ray diffraction data for halite efflorescence at Morrill Hall.

APPENDIX E (cont'd)

Table 6 (cont'd)

JCPDS	File No	5-628	MHE - 16		MHE - 17	
d(A)	I/I _o	(hkl)	d(A)	I/I _o	d(A)	I/I _o
3.258	13	111	3.22	19	3.23	10
2.821	100	200	2.80	100	2.79	100
1.994	55	220	1.98	33	1.98	50
1.701	2	311			1.70	14
1.628	15	222	1.62	7		
1.410	6	400			1.40	5

APPENDIX F

APPENDIX F

X-RAY DIFFRACTION DATA FOR ALUNITE AT MORRILL HALL

Table 7

JCPDS	File No	4-865	MHE-10	
d(A)	I/Io	(hkl)	d(A)	I/Io
5.76	9	101		
4.99	20	012		
3.51	32	110		
3.34	12		3.21	17
3.01	85	015, 113		
2.90	17	006		
2.48	20	024	2.44	13
2.29	73	107		
2.26	28	205, 211	2.27	17
2.21	8	116, 122	2.22	9
2.11			2.11	22
2.04	6	018		
1.90	100	027, 125		
1.75	88	220	1.8	100

X-ray diffraction data for alunite efflorescence at Morrill Hall.

APPENDIX G

APPENDIX G

**X-RAY DIFFRACTION DATA FOR HALOTRICHITE AT LINCOLN BRICK
PARK AND FITZGERALD PARK**

Table 8

JCPDS	File No	11-506	LBP-2		LBP-3		FP-4		FP-6	
d(A)	I/I ₀	(hkl)	d(A)	I/I ₀	d(A)	I/I ₀	d(A)	I/I ₀	d(A)	I/I ₀
10.4	15	200, 120					10.27	5		
9.50	15	210	8.92	26	9.6	36	9.5	23	9.30	13
7.82	10	220	7.43	13	7.55	21	7.82	13	7.68	9
6.02	30	040, 320					5.98	18	5.9	13
5.24	15	240, 121	5.21	33			5.24	13		
4.77	100	150, 420	4.84	20			4.76	100		
4.62	30	231, 321	4.61	100	4.65	43	4.64	8	4.79	39
4.29	55	311, 401	4.24	87	4.34	100	4.27	43	4.34	100
4.09	45	510, 321	4.14	80	4.00	29	4.09	33	4.11	22
3.95	35	160, 350	3.96	53	3.91	79	3.93	20	3.98	30
3.75	40	401, 260	3.85	26			3.75	25	3.74	13
3.48	100	351, 360	3.50	20			3.47	90	3.46	52
3.30	20	620, 261	3.25	80	3.31	79	3.32	15	3.30	22
3.16	15				3.18	37	3.15	13	3.14	13
3.05	15						3.03	10	3.00	17
2.96	20		2.97	13	2.93	93	2.96	13	2.92	17
2.86	30		2.83	33	2.88	21	2.88	15	2.87	30
2.76	20		2.76	13	2.76	21	2.76	10	2.77	17
2.67	25				2.66	21	2.67	18	2.66	30
2.61	20		2.62	40	2.63	7	2.60	8		
2.55	20		2.56	13	2.55	29	2.54	10		
2.47	10				2.45	14				
2.39	5				2.4	14				
2.279	10				2.27	29	2.27	10	2.26	30
2.231	5		2.23	13						
2.009	15						2.01	10		
1.947	5				1.97	29				
1.868	20		1.85	20	1.87	14	1.87	10	1.88	17
1.776	5				1.77	7				
1.663	5									

X-ray diffraction data for halotrichite efflorescence at Lincoln Brick Park and Fitzgerald Park.

APPENDIX G (cont'd)

Table 8 (cont'd)

JCPDS	File No	11-506	FP-7	
d(A)	I/Io	(hkl)	d(A)	I/Io
10.4	15	200, 120		
9.50	15	210	9.21	10
7.82	10	220	7.75	7
6.02	30	040, 320	5.9	12
5.24	15	240, 121	5.3	14
4.77	100	150, 420	4.77	21
4.62	30	231, 321	4.69	43
4.29	55	311, 401	4.31	100
4.09	45	510, 321	4.09	17
3.95	35	160, 350	3.96	17
3.75	40	401, 260	3.70	12
3.48	100	351, 360	3.43	43
3.30	20	620, 261		
3.16	15		3.16	7
3.05	15			
2.96	20		2.93	12
2.86	30		2.86	17
2.76	20		2.76	10
2.67	25		2.66	17
2.61	20			
2.55	20			
2.47	10			
2.39	5			
2.279	10			
2.231	5		2.25	7
2.009	15		2	7
1.947	5			
1.868	20			
1.776	5			
1.663	5			

APPENDIX H

APPENDIX H

**X-RAY DIFFRACTION DATA FOR AMARANTITE AT LINCOLN BRICK
PARK**

Table 9

JCPDS	File No	17-158	LBP-4	
d(A)	I/Io	(hkl)	d(A)	I/Io
11.3	100	010	11.04	100
8.69	100	100	8.65	94
7.34	10	110		
6.50	30	110, 001		
5.88	5	011		
5.61	10	020	5.67	55
5.39	10	011	5.34	30
5.16	40	101		
4.98	40	111	4.98	20
4.46	20	111	4.44	20
4.13	10	121, 121	4.13	35
3.74	10	220		
3.65	20	211, 130		
3.57	80	211, 121	3.56	20
3.41	40	031	3.39	25
3.11	60	102		
3.05	80	112, 102	3.07	20
2.99	30	022		
2.935	10	300, 310	2.91	30
2.818	20	140		
2.742	5	022	2.74	10
2.675	20	301, 202	2.67	20
2.622	40	202, 032		
2.549	20	240, 122	2.57	15
2.476	20			
2.424	10			
2.284	5			
2.239	10			
2.16	5			
2.113	10			
2.062	10			

X-ray diffraction data for amarantite efflorescence at Lincoln Brick Park.

APPENDIX I

APPENDIX I

X-RAY DIFFRACTION DATA FOR ROZENITE AT LINCOLN BRICK PARK

Table 10

JCPDS	File No	16-699	LBP-3	
d(A)	I/I _o	(hkl)	d(A)	I/I _o
6.85	50	011, 020	6.78	43
5.46	90	110	5.36	71
5.17	5	021		
4.73	10	101	4.84	33
4.47	100	111, 120	4.41	100
3.97	70	002	3.91	52
3.61	10	130	3.65	14
3.4	60	040	3.37	38
3.27	10	131	3.31	52
3.22	50	112	3.24	19
2.985	40	032		
2.953	50	140		
2.906	5	210	2.92	62
2.770	10	141	2.76	19
2.722	10	220, 211	2.72	5
2.673	5	132	2.66	14
2.569	40	051, 221	2.55	19
2.470	5	150, 023	2.45	10
2.430	30	103	2.4	19
2.371	20	231, 142	2.35	14
2.360	20	142, 151		
2.335	5	212		
2.286	5	033, 123		
2.266	30	123, 060	2.27	19
2.236	10	052, 240		
2.179	5	061		
2.142	5	241, 133		
2.112	5	160, 232		
2.049	5	161, 161		
1.969	20	143, 062	1.97	19
1.944	10	213, 251		
1.890	20	053, 223		
1.871	10	162, 162	1.87	10
1.819	5	233		
1.798	20	153, 260		
1.755	10	261, 261	1.75	10
1.725	20	063		

X-ray diffraction data for rozenite efflorescence at Lincoln Brick Park.

APPENDIX J

APPENDIX J

**X-RAY DIFFRACTION DATA FOR TARANAKITE AT VIRGINIA
KENDALL LEDGES PARK**

Table 11

JCPDS	File No	8-180	VKL-3	
d(A)	I/Io	(hkl)	d(A)	I/Io
15.5	100	-	16.35	20
7.60	80	-	7.59	96
5.80	60	-		
5.10	20	-	5.12	12
4.40	60	-	4.37	38
3.83	80	-	3.84	100
3.59	60	-	3.63	46
3.35	50	-	3.34	31
3.16	80	-	3.16	69
2.85	80	-	2.84	38
2.74	20	-	2.75	23
2.64	70	-	2.64	35
2.40	60	-	2.40	19
2.26	40	-	2.26	8
2.19	40	-	2.19	8
2.07	70	-	2.07	15
1.97	50	-		
1.91	40	-	1.91	4
1.88	20	-	1.88	4
1.84	50	-	1.83	8
1.77	50	-		
1.73	50	-		
1.68	20	-		
1.65	20	-		
1.61	50	-		
1.572	20	-		
1.545	20	-		
1.505	50	-		
1.469	20	-		
1.430	30	-		
1.399	20	-		

X-ray diffraction data for taranakite efflorescence at Virginia Kendall Ledges Park.

APPENDIX K

APPENDIX K

EDS AND XRD RESULTS FOR HONEYCOMB WEATHERING

Table 12

Sample Number	XRD Analyses	EDS Analyses
FP-2	Gypsum	Ca, S
FP-3	Gypsum	Ca, S
FP-8	Gypsum	Ca, S
FP-9	Gypsum	Ca, S
Penny	Gypsum	Ca, S
OMC-1	Gypsum	Ca, S
VKL-1	Gypsum	Ca, S
VKL-2	Gypsum	Ca, S
VKL-3	Taranakite	Al, Si, P, S, K, Fe
HA-LM-1	Gypsum, Quartz, Microcline	Al, Si, K, Ca, S
HA-SG	Gypsum	Si, Ca, S
BHG-1	Gypsum	Al, Si, Ca, S
BHG-2	Gypsum	Al, Si, K, Ca, S, Fe

X-ray diffraction and energy dispersive spectroscopy analysis results for salts associated with honeycomb weathering.

1. FP - Samples taken from Fitzgerald Park, Grand Ledge, Michigan.
2. Penny - Sample taken from Pennyrite State Park, Western Kentucky.
3. OMC - Sample taken from Old Man's Cave, Hocking Hills State Park, Ohio.
4. VKL - Samples taken from Virginia Kendall Ledges Park, Cuyahoga Valley National Recreation Area, Ohio.
5. HA-LM - Sample taken from "Little Mountain" (Sharon Conglomerate) in Holden Arboretum, Northeastern Ohio.
6. HA-SG - Sample taken from Stebbins Gulch (Berea Sandstone) in Holden Arboretum, Northeastern Ohio.
7. BHG - Samples taken from Black Hand Gorge State Nature Preserve, Ohio.

APPENDIX L

X-RAY DIFFRACTION DATA FOR GYPSUM EFFLORESCENCE

Table 13

JCPDS	File No	6-046	VKL-1		VKL-2		OMC-1		Penny		HA-LM		HA-SG	
d(A)	I/Io	(hkl)	d(A)	I/Io										
7.56	100	020	7.49	100	7.31	100	7.37		7.68	100	7.49	4	7.49	100
4.27	50	121	4.26	36	4.21	100	4.21	100	4.29	25	4.32	19	4.23	50
3.79	20	031, 040	3.78	12			3.56	29	3.81	17			3.79	20
3.163	4	112			3.27	91		21	3.18	<1				
3.059	55	141	3.04	31	3.03	54	3.03	31	3.07	33	3.03	65	3.07	23
2.867	25	002	2.84	5	2.87	54	2.84	12	2.89	7	2.86	27	2.87	6
2.786	6	211	2.76	2	2.75	41	2.76	2			2.79	100	2.79	1
2.679	28	022, 051	2.66	5	2.65	36	2.65	5	2.69	7	2.71	27		
2.591	4	150, 202	2.583	2			2.58	2					2.58	6
2.53	<1	060												
2.495	6	200	2.49	9					2.51	2				
2.45	4	222	2.43	2	2.46	9	2.46	2	2.46	2				
2.40	4	141					2.42	2						
2.216	6	152	2.20	7	2.2	18	2.20	2	2.22	2			2.22	3
2.139	2	242												
2.08	10	123							2.09	2			2.08	3
2.073	8	112, 251			2.07	27	2.06	17						
1.99	4	170	1.98	2										
1.953	2	211			1.97	9								
1.898	16	080, 062	1.89	2					1.9	2			1.89	3
1.879	10	143			1.875	9	1.88	17						
1.864	4	312									1.86	15		
1.843	2	231												
1.812	10	262							1.82	2			1.81	6
1.796	4	321	1.8	9	1.79	9							1.78	5
1.778	10	260												
1.771	2	253					1.76	7						
1.684	2	323												
1.664	4	341					1.67	5						
1.645	2	163					1.66	2	1.63	2				
1.621	6	204, 181, 053	1.62	2			1.61	2	1.61	2			1.62	4
1.599	<1	352, 190			1.6	9								
1.584	2	224												
1.572	2	282												
1.522	2	222, 134									1.52	12		

X-ray diffraction data for gypsum efflorescence associated with honeycomb weathering.

APPENDIX L

APPENDIX L (cont'd)

1. FP - Samples taken from Fitzgerald Park, Grand Ledge, Michigan.
2. Penny - Sample taken from Pennyrile State Park, Western Kentucky.
3. OMC - Sample taken from Old Man's Cave, Hocking Hills State Park, Ohio.
4. VKL - Samples taken from Virginia Kendall Ledges Park, Cuyahoga Valley National Recreation Area, Ohio.
5. HA-LM - Sample taken from "Little Mountain" (Sharon Conglomerate) in Holden Arboretum, Northeastern Ohio.
6. HA-SG - Sample taken from Stebbins Gulch (Berea Sandstone) in Holden Arboretum, Northeastern Ohio.
7. BHG - Samples taken from Black Hand Gorge State Nature Preserve, Ohio.

APPENDIX M

APPENDIX M**SITE DESCRIPTIONS OF HONEYCOMB WEATHERING****Fitzgerald Park**

Honeycomb Weathering at Fitzgerald Park in Grand Ledge, Michigan occurs along Sandstone Creek (See Appendix B for site location). The ledges containing honeycomb weathering along Sandstone Creek range from 6 to 18 meters high. The ledges along the north side of Sandstone Creek from the confluence of Sandstone Creek and Grand River to approximately 300 meters upstream have the best occurrences of honeycomb weathering. Honeycombs along these exposures range in size from 1 cm to approximately 11 cm.

On the north side of Sandstone Creek, aspect of the outcrop containing honeycomb weathering ranges from 104° to 172° to 190°, southeast to just slightly west of south. According to Wallis (1986) these are the only orientations exhibiting honeycomb weathering. However, honeycomb weathering is also present on the ledges of the south side of the creek. The honeycombs on the south side of Sandstone Creek are not visible from the north side of the creek for several reasons. The honeycombs are very tiny, perhaps due to the fact that evaporation and insolation effects on the rock are greatly reduced on the north-facing cliffs. Additionally, the ledges on the south side of the creek are much higher than the north side of the creek, and because of their aspect, the ledges cast shadows, further inhibiting insolation and evaporation effects. The honeycombs tend to only appear beneath overhangs with deep recesses (10-15 feet) into the rock, where sunlight is scarce.

Salt efflorescence in the honeycombs on the north side of the creek is ephemeral and present in very small amounts. Efflorescence tends only to

APPENDIX M (cont'd)

occur in honeycomb cavities on newly forming honeycombs. The older honeycombs contain little or no efflorescence. Efflorescence is not present in honeycomb cavities or on the rock face on the south side of the creek. All efflorescence found along Sandstone Creek occurs beneath overhangs rather than on exposed walls. Each of the honeycomb related efflorescence samples in Fitzgerald Park (FP-2, FP-3, FP-8, FP-9) were taken from the cavities of small, newly-formed honeycombs. The only salt present as efflorescence in Fitzgerald Park is gypsum. Mineralogical and elemental analyses for efflorescence associated with honeycomb weathering are given in Table 3 of Appendix E.

Observation of the sandstone shows that iron oxyhydroxide case-hardening exists over the entire outcrop area. The greatest concentrations of iron occur along bedding planes where permeability and porosity are greatest. The iron concentrations along bedding planes create resistant ridges on the rock surface. The resistant ridges form bounding surfaces for the honeycomb cells and determine the maximum size a honeycomb can achieve. Generally, the honeycombs follow the bedding plane angles and the resistant ridges often comprise two of the honeycomb walls. Honeycombs do sometimes cross the iron-impregnated bedding planes, however. Bedding-plane control suggests that iron-cemented beds and surfaces, at least in part, influences honeycomb weathering .

Several springs exist in Fitzgerald Park. The springs issue from shale layers underlying the Eaton Sandstone. The springs are so rich in iron that a rust colored gel occurs in the bottom of the small stream. The iron gels are probably amorphous iron oxyhydroxides, but no XRD work has been done to verify this assumption.

APPENDIX M (cont'd)

Lichens and algae are prevalent on the rock face in the study area. They occur as white and green growths on the sandstone surface. Lichens growing on the outcrop are not solely concentrated in honeycomb cavities or around honeycomb cavities. Newly forming cavities are found where lichens are not present.

Turkey Run State Park

Turkey Run State Park is located in west-central Indiana (see Appendix B for site location). Honeycomb weathering is concentrated along ledges bordering Sugar Creek and its tributaries. Honeycombs form primarily beneath overhangs with thick vegetative cover on top of the overhang and little exposure to the sun. Honeycombs range in size from less than one centimeter to greater than 12 centimeters in diameter. Efflorescence within the park is very poorly developed, and no samples could be retrieved.

Aspects of the honeycomb outcrops span a wide range of azimuthal directions: 332°, 99°, 50°, 237°, 339°, 152°, 170°, 123°, 83° and 270°. Such a wide range of aspects precludes exposure to sunlight, insolation, or evaporation as causes for honeycomb weathering. Lichens are present on the sandstone outcrops in Turkey Run. The lichens do not appear to either aid in honeycomb development by aiding in eroding the case-hardened walls or to inhibit honeycomb formation by destroying honeycomb cells.

Iron oxyhydroxide case-hardening is prevalent throughout the entire outcrop area. The iron concentrations are greatest along bedding planes. The bedding planes form resistant ridges on the sandstone surface that act as bounding surfaces for the honeycomb cells. The honeycombs strictly follow the bedding planes as they did in Fitzgerald Park. Honeycombs can also be

APPENDIX M (cont'd)

seen growing on flat, horizontal surfaces of float. These pieces of float were oriented such that the bedding planes were exposed on the vertical faces of the boulders. The honeycombs actually formed on the top of the bedding plane surface and not between bedding planes.

In Boulder Canyon, fractures and joints are so iron impregnated, that the iron oxyhydroxide cemented zones protrude from the joint and fracture planes up to about five centimeters. Honeycomb cells actually form within the iron oxyhydroxides protruding from the joint and fracture planes. Irregularly shaped concentrations of iron are also present in Boulder Canyon. These irregular shapes and lines are interpreted as groundwater ferricretes, showing paleo-water-table elevations.

Hawesville and Cloverport, Kentucky

Two outcrops of Mississippian and Pennsylvanian sandstone between Hawesville and Cloverport, Kentucky exhibit honeycomb weathering (see Appendix B for site locations). The first outcrop studied is a roadcut of Mississippian Tar Springs Sandstone at the intersection of U.S. Route 60 and Kentucky Route 144, west of Cloverport, Kentucky. The honeycomb weathering occurs on north facing and east facing sides of the road cut. Honeycombs are well developed and cover a very large area of the roadcut. The largest honeycombs are approximately 120 centimeters across and 60 centimeters deep. New, smaller honeycombs form within larger honeycomb cavities in the roofs of the overhangs. Lichen and algae growth are not significant at this location.

The Tar Springs Sandstone is iron cemented at the surface. Increased iron concentrations along bedding planes form resistant ridges on the rock

APPENDIX M (cont'd)

face. The ridges act as bounding surfaces for the maximum development of honeycomb cells.

The second outcrop area lies east of Hawesville at Indian Lake . A road cut has exposed some weakly cemented basal Pennsylvanian Caseyville conglomeratic sandstone. The weak cementing allowed several samples of honeycombs to be removed for thin sectioning through a honeycomb cell. These thin sections will help determine the role iron plays in honeycomb development. Lichens and algae are not present on the Caseyville in the Indian Lake area.

Iron oxyhydroxide case-hardening is prevalent at both sites. The iron oxyhydroxides are concentrated along the bedding planes forming resistant ridges that act as bounding surfaces for the honeycomb cells. Efflorescence, however, is poorly developed at both sites, and no samples could be retrieved.

Pennyrile State Park

Honeycomb weathering is fairly well developed at certain outcrops in Pennyrile. The best outcrops are located along Indian Bluffs Trail and the Lake Trail west of the beach and boat dock area on Pennyrile Lake. Minor occurrences of honeycomb weathering are also present along Clifty Creek and on the Clifty Creek Trail. Outcrops in Pennyrile consist of the upper Pennsylvanian Caseyville Sandstone. Honeycombs are present on both the cliff faces and the roofs of overhangs.

Green and white lichens/algae grow on the surfaces of the rock. The lichens do not appear to be associated with the honeycomb formation, as they are present on both honeycombed and non-honeycombed portions of the rock.

APPENDIX M (cont'd)

One efflorescence sample was retrieved from honeycomb walls associated with very mature honeycombs in which the walls were beginning to erode back to a flat surface. In most of the outcrops, the honeycomb walls are eroding down to flat surfaces. X-ray diffraction, EDS and SEM analyses reveal gypsum to be the only salt growing on honeycombs in Pennyrile State Park. Table 3 of Appendix E lists the salts associated with honeycomb weathering at Pennyrile State Park and the other study areas.

The sandstones in Pennyrile contain iron staining and are case-hardened. Iron is quite abundant in the rocks. The Caseyville in Pennyrile contains extensive iron concentrations forming rings and lines of sandy ironstones. The iron bands and rings are continuous and are not present solely at the rock surface, but extend into the rock in the third dimension. These ironstones are interpreted as groundwater ferricretes which record ancient aquifer high stands in the Pennyrile area.

Differential weathering of the sandstone along bedding planes due to high iron concentrations exerts bedding plane control on honeycomb development. Honeycomb cavities also develop in layers devoid of bedding planes. Honeycombs in Pennyrile cut across iron impregnated bedding planes more often than in many other study areas. Another control on honeycomb development is noted in Pennyrile: the iron rings or Liesegang circles also control honeycomb development. The iron circles can also act as the bounding surfaces for the honeycombs. In most cases where honeycombs cut across bedding planes, the honeycomb cell boundaries are defined by a Liesegang circle.

APPENDIX M (cont'd)**Ferne Clyffe State Park**

Honeycomb weathering is well developed along portions of Round Bluff Trail in Ferne Clyffe State Park in Southern Illinois (see Appendix B for site location). Honeycomb weathering is present along the trail in small quantities. However, towards the end of the trail, honeycomb weathering is well developed in cliffs from 18 to 35 meters in height. These excellent exposures occur in north, east and west facing outcrops. Honeycomb sizes range from small holes less than 1 centimeter to cavities as large as 270 centimeters. Honeycombs are very well developed parallel to bedding planes and on the roofs of overhangs.

Little efflorescence is present in the rocks. Very minuscule amounts of efflorescence can be found near the bases of the bluff, but not in analyzable quantities.

In the best outcrops of honeycomb weathering, resistant ridges formed by differential weathering of the sandstone due to iron impregnation of the bedding planes are prevalent. Bedding-plane control of honeycomb development is evident in these areas. Honeycomb weathering also develops on very large boulders of float. The float is oriented in the soil such that the bedding planes are perpendicular to the ground surface, rather than parallel to the surface. Honeycombs still develop on the vertical rock surface. However, the honeycomb development occurs on top of a bedding plane instead of between two bedding planes. Thus iron concentration along bedding planes is not the only control on honeycomb weathering in Ferne Clyffe State Park.

Ferne Clyffe also contains brightly colored iron oxide bands, Liesegang circles and iron tubes. Again, these bands and tubes are interpreted as

APPENDIX M (cont'd)

groundwater ferricretes. Where these ironstones are present, they partially control honeycomb formation. The sandy ironstone forming the tubes is approximately one centimeter thick. The tube is so well-cemented by the abundant iron, that striking the tube with a hammer emits a loud metallic ring. The iron tubes contain quantities of specular hematite visible to the naked eye.

Hocking Hills State Park

Hocking Hills State Park is located about 50 miles southeast of Columbus, Ohio. Several different scenic interests divide the park, these include Old Man's Cave, Cedar Falls, and Ash Cave (see Appendix B for site locations).

Honeycomb weathering occurs inside Old Man's Cave over nearly the entire cave surface. The honeycombs are very well developed and very mature, that is, most of the honeycomb walls are eroding back to a flat surface. Old Man's Cave is a recess cave, that is a cave that has formed as the rock has weathered into a cliff face. Smaller recess caves near Old Man's Cave also contain honeycomb weathering. Size of the honeycombs ranges from less than one centimeter to greater than 12 centimeters. Honeycombing also occurs on the large boulder-size float on the cave floor. Efflorescence (OMC-1) is found in the cave roof and on the walls of Old Man's Cave on walls of very mature honeycombs. X-ray diffraction reveals the efflorescence to be gypsum. Table 3 of Appendix E lists all of the XRD and EDS analyses for efflorescence associated with honeycomb weathering.

Iron staining in the area of Old Man's Cave maintains an orange to brown color. Bedding planes form resistant ridges due to increased iron

APPENDIX M (cont'd)

concentrations and differential weathering. Honeycomb cells follow the bedding planes which act as bounding surfaces for the cells. Liesegang circles and other evidence of groundwater ferricretes are present in the vicinity of Old Man's Cave. Some iron oxyhydroxide precipitates are so built up that the oxyhydroxides contain honeycombs, analogous to similar phenomena found in Turkey Run State Park, Indiana.

Honeycomb weathering is prevalent at the top of Cedar Falls and along the trail leaving Cedar Falls. Honeycomb weathering is not as well developed at Cedar Falls as at Old Man's Cave. The best honeycomb weathering occurs beneath overhangs on the trail leaving Cedar Falls. Efflorescence is present at Cedar Falls, but not in analyzable quantities.

Resistant ridges along iron-cemented bedding planes exist at Cedar Falls also. The honeycombs that are present follow the resistant ridges formed by the bedding planes. Liesegang banding is present in fresh exposures of sandstone. Areas in which fresh sandstone is exposed show Liesegang banding while areas of rock in which the honeycombs have been removed from the surface for a longer period of time show dark orange staining on the exposed surface, which covers the Liesegang banding.

Honeycomb weathering also occurs in Ash Cave over the entire cave surface. Ash Cave is another recess cave formed in the Black Hand Sandstone in the Hocking Hills area. Honeycombs from 1 cm to greater than 20 cm form beneath the overhangs of the cliffs and inside the cave. Honeycombs in Ash Cave are small and very mature, that is, the honeycomb walls are eroding back to a flat surface. Honeycomb walls are very short and are eroding back to a flat surface. Efflorescence in the cave and on the trails leading to the cave is

APPENDIX M (cont'd)

very poor. Liesegang circles, Liesegang banding and resistant bedding plane ridges are well developed in the area. Honeycomb development is controlled by the iron phenomena and bedding planes throughout the cave.

Virginia Kendall Ledges Park

Virginia Kendall Ledges Park is located in the Cuyahoga Valley National Recreation Area (see Appendix B for site location). The park contains outcrops of the Pennsylvanian Sharon Conglomerate. Virginia Kendall Park has extensive honeycomb weathering on the ledges along the trail leading to Ice Box Cave. Honeycomb types range from infant/newly forming honeycombs to very mature honeycombs in which the honeycomb walls are eroding back to a flat surface. The best honeycomb development occurs beneath overhangs, however, honeycombs also form on vertical rock faces where overhangs are not present. Honeycombs range in size from less than one centimeter to greater than 12 centimeters. In some areas, several honeycombs have grown together to form linear pockets or recesses in the rock face both parallel and perpendicular to bedding. Honeycombs form equally well in the sandstone and conglomerate facies throughout the ledges area. Aspect of honeycomb weathering exposures consist of 10°, 110°, 150°, and 160°.

Iron oxyhydroxide staining is prevalent on the rock faces. Iron is concentrated along the bedding planes in the outcrop, forming resistant ridges on the rock surface. Honeycombs preferentially develop along bedding planes which act as bounding surfaces for the honeycomb cells.

APPENDIX M (cont'd)

Efflorescence is not ubiquitous on the honeycomb exposures. Salts appear about every 150 to 200 feet along the outcrop. Samples VKL-1 and VKL-2 were taken from the cavities of younger honeycombs. Table 3 of Appendix E lists the efflorescent salts associated with honeycomb weathering in Virginia Kendall Ledges Park and the other areas studied. Gypsum is the major efflorescent salt associated with honeycomb weathering in Virginia Kendall Park. Gypsum precipitates inside younger honeycomb cavities and on the walls of older honeycombs in which the wall of the honeycomb is eroding back to a flat surface. One area of the outcrop contains a nearly solid efflorescence layer beneath which is a thin layer of green material which is likely algae or lichens.

A second salt (sample VKL-3), taranakite (aluminum iron phosphate), is found associated with a water seep issuing from the ledges. Very small honeycombs exist in the vicinity of the seep. The build up of efflorescence below the seep appears to result from the evaporation of the water issuing from the seep. The taranakite takes on a "washed" appearance as if the efflorescence flowed down the rock surface.

Holden Arboretum

Holden Arboretum in Kirtland, Ohio, contains outcrops of Sharon Conglomerate and Berea Sandstone. Honeycomb weathering occurs in the Sharon Conglomerate on "Little Mountain" and in the Berea Sandstone in Stebbins Gulch (See Appendix B for site locations). The best outcrops of honeycomb weathering are found on Little Mountain in the Sharon Conglomerate. The Stebbins Gulch honeycombing contains areas where the

APPENDIX M (cont'd)

honeycombs coalesce to form linear pockets in the rock similar to pockets honeycombs coalesce to form linear pockets in the rock similar to pockets formed in Virginia Kendall Ledges Park.

One area of interest on Little Mountain is an area of considerable lichen coverage on the rock. The portion of the rock covered by lichen is wet to the touch and contains very few honeycomb cells. The area of the outcrop not covered by lichen contains a large quantity of honeycomb cells and is dry to the touch.

Efflorescence occurs in mature honeycomb cavities, mainly beneath overhangs. Samples HA-SG and HA-LM were both taken from within honeycomb cavities in Stebbins Gulch and on Little Mountain. Table 3 of Appendix E lists the salts present with honeycomb weathering. Both study areas in Holden Arboretum contain gypsum as the only efflorescent salt.

Bedding planes with high iron concentrations form resistant ridges in the rock surface. The honeycombs follow bedding planes which act as bounding surfaces for the honeycomb cells. Liesegang circles are also evident in the Sharon Conglomerate in this area.

Black Hand Gorge

Black Hand Gorge State Nature Preserve contains outcrops of the Mississippian Black Hand Sandstone (see Appendix B for site locations). Honeycomb weathering is present on the ledges on both sides of the Licking River. Honeycombs range from infant stages to very well developed, very mature stages. Honeycombs are quite prevalent over the entire outcrop area, however, the best occurrences are beneath overhangs. Honeycombs range in

APPENDIX M (cont'd)

size from less than 1 cm to greater than 12 cm. Aspect of honeycomb development in the ledges consists of S, E, N and W outcrop exposures.

Most of the efflorescence occurs beneath overhangs of rock. Samples BHG-1 and BHG-2 were taken from very mature honeycomb walls, where the honeycomb walls were eroding back to a flat surface. Table 2 of Appendix D lists the efflorescent salts identified in Black Hand Gorge State Nature preserve and the other localities studied. Gypsum is the only salt present at Black Hand Gorge.

Iron staining in the rock is quite prevalent and ranges from brown-orange to reddish black. Most honeycomb development occurs in the darker stained areas of the outcrop. Differential weathering is also prevalent over the entire outcrop area as evidenced by resistant ridges (iron impregnated bedding planes) sticking out from the surface of the rock. Honeycombs tend to follow bedding planes which act as the bounding surfaces for the honeycomb cells. Liesegang banding appears behind the honeycomb surface on fresh surfaces of the rock (i.e. when honeycombs are removed from the weathering surface, Liesegang banding is present on the fresh surface).

BIBLIOGRAPHY

BIBLIOGRAPHY

- Anderson, T.A. (1975) Depositional environment of the Sharon Conglomerate Member of the Pottsville Formation in northeastern Ohio: Discussion. *Journal of Sedimentary Petrology*, 46, 438.
- Arnold, A. (1984) Determination of mineral salts from monuments. *Studies in Conservation*, 29: 129-138.
- Barclay, C.C. (1968) Sedimentary structures and depositional history of the coarse-clastic rocks of the Cuyahoga Formation in Northern Ohio. Unpublished Masters Thesis, Kent State University, Kent, Ohio.
- Berner, R.A. (1978) Rate control of mineral dissolution under earth surface conditions. *American Journal of Science*, 278, 1235-1252.
- Bohm, S.M. (1981) Regional facies of the Caseyville Formation (Lower Pennsylvanian) in Johnson and Pope Counties, Illinois. Unpublished Masters Thesis, Southern Illinois University, Carbondale, Illinois.
- Bourman, R.P., Milnes, A.R. and Oades, J.M. (1987) Investigation of ferricretes and related surficial ferruginous materials in parts of southern and eastern Australia. *Zeitschrift für Geomorphologie N.F.*, Suppl.-Bd. 64, 1-24.
- Bryan, K. (1925) The Papago Country, Arizona. *U.S. Geological Survey Water Supply Paper* 499, 90-93.
- (1926) Niches and other cavities in sandstone at Chaco Canyon, New Mexico. *Zeitschrift für Geomorphologie* 3, 125-140.
- Carey, P.J. (1995) Tombstones, weathering rates and topography across Massachusetts. *Geological Society of America Abstracts with Programs*: 27, 34.
- Cody, R.D. (1979) Lenticular gypsum: occurrences in nature, and experimental determinations of effects of soluble green plant material on its formation. *Journal of Sedimentary Petrology*, 49: 1015-1028.
- (1990) Crystallization inhibition by soluble organic molecules. *Journal of Sedimentary Petrology*, 61: 704-718.
- and Cody, A.M. (1986) Gypsum nucleation and crystal morphology in analog saline terrestrial environments. *Journal of Sedimentary Petrology*, 58: 247-255.

- Conca, J. L. and Astor, A. M. (1987) Capillary moisture flow and the origin of cavernous weathering in dolerites of Bull Pass, Antarctica. *Geology*, 15: 151-154.
- and Rossman, G.R. (1982) Case hardening of sandstone. *Geology*, 10, 520-523.
- Coogan, A.H., Heimlich, R.A., Malcuit, R.J., Bork, K.B. and Lewis, T.L. (1981) Early Mississippian deltaic sedimentation in central and northeastern Ohio in Roberts, T.G. (ed.) *GSA Cincinnati '81 Fieldtrip Guidebooks, Volume 1: Stratigraphy, Sedimentology*. American Geological Institute.
- Cooke, R.U. (1994) Salt weathering and urban water table in deserts in Robinson and Williams (eds.) *Rock Weathering and Landform Evolution*: 193-205, John Wiley & Sons Ltd., New York.
- Corbett, R.G. and Manner, B.M. (1988) Geology and habitats of the Cuyahoga Valley National Recreation Area, Ohio. *Ohio Journal of Science*, 88: 40-47.
- Davis, R.W., Plebuch, R.O. and Whitman, H.M. (1974) Hydrology and geology of deep sandstone aquifers of Pennsylvanian age in part of the Western Coal Field region, Kentucky. *Kentucky Geological Survey Series 10*, report of investigations 15: 1-26.
- Dorr, J.A., Jr. and Eschman, D.F. (1970) *The Geology of Michigan*. The University of Michigan Press, Ann Arbor, Michigan.
- Dove, P.M. (1995) Kinetic and thermodynamic controls on silica reactivity in weathering environments in White, A.F. and Brantley, S.L. (eds.) *Chemical Weathering Rates of Silicate Minerals*, Reviews in Mineralogy 31, 235-290.
- and Rimstidt, J.D. (1994) Silica-water interactions in Heaney, P.J., Prewitt, C.T. and Gibbs, G.V. (eds.) *Silica Physical Behavior, Geochemistry and Materials Applications*, Reviews in Mineralogy, 29, 259-308.
- Ehlers, E.G. and Stiles, D.V. (1965) Melanterite-rozenite Equilibrium. *American Mineralogist*, 50: 1457-1461.
- Faure, G. (1991) *Principles and Applications of Inorganic Geochemistry*. Macmillan Publishing Company, New York, N.Y., 626 p.

- Fiore, S. and Laviano, R. (1991) Brushite, hydroxylapatite, and taranakite from Apulian caves (southern Italy): New mineralogical data. *American Mineralogist*, 76: 1722-1727.
- Fuller, J.O. (1955) Source of Sharon Conglomerate of northeastern Ohio. *Bulletin of the Geological Society of America*, 66: 159-175.
- Gault, H.R. (1938) The petrography of the Mansfield sandstone of Indiana. Master's Thesis, University of Missouri, Columbia, Missouri.
- Gilchrist, M. (1947) *Home Economics at M.S.C. (1895 - 1926)*. Michigan State University, M.S.U. Archives, Conrad Hall.
- Gill, E. D., Segnit, E. R. and McNeill, N. H. (1979) Rate of formation of honeycomb weathering features (small scale tafoni) on the Otway Coast, S.E. Australia. C.S.I.R.O. Division of Applied Geomechanics Research Paper No. 377.
- Glenn, L.C. (1922) *The Geology and Coals of Webster County*. The Kentucky Geological Survey: Frankfort, Kentucky.
- Gouda, A.S. (1986) Laboratory simulations of 'the wick effect' in salt weathering of rock. *Earth Surface Processes and Landforms*, 11: 275-285.
- Greb, S.F. (1989) A subrectangular paleovalley system, Caseyville Formation, Eastern Interior Basin, western Kentucky. *Southeastern Geology*, 30: 59-75.
- Hamblin, W.K. (1958) *The Cambrian Sandstones of Northern Michigan*: State of Michigan Department of Conservation Geological Survey Division, Publication 51, 141 p.
- Hannibal, J.T. and Feldman, R.M. (1987) The Cuyahoga Valley National Recreation Area, Ohio: Devonian and Carboniferous clastic rocks in Biggs, D.L. (ed.) *Centennial Field Guide Volume 3*, North-Central Section of the Geological Society of America.
- Harris, S.E., Jr., Horrel, C.W. and Irwin, D. (1977) *Exploring the Land and Rocks of Southern Illinois*. Southern Illinois University Press, Carbondale, Illinois.
- Hendricks, S.B. (1937) The crystal structure of alunite and the jarosites. *American Mineralogist*, 22, 773-784.

- Holt, O.R. (1957) A petrologic study of the Cypress, Tar Springs, and Mansfield sandstones. Master's Thesis, Indiana University, Bloomington, Indiana.
- Hudson, R.J. (1957) Genesis and depositional history of the Eaton Sandstone, Grand Ledge, Michigan. Master's Thesis, Michigan State University, East Lansing Michigan.
- Huff, B.G. (1985) Stratigraphy and depositional history of the Pennsylvanian sequence exposed at the Cagle's Mill Spillway Putnam County, Indiana. *Transactions of the Illinois Academy of Science*, 78: 33-43.
- Jackson, D.S. (1985) The petrology, porosity and permeability of the Berea Sandstone (Mississippian) Perry Township, Ashland County, Ohio. Unpublished Masters Thesis, University of Cincinnati, Cincinnati, Ohio.
- Jacobson, R.J. (1987) Fluvial-deltaic deposits (Caseyville and Abbott Formations) of early Pennsylvanian age exposed along the Pounds Escarpment, southern Illinois in Biggs, D.L. (ed.) *Centennial Field Guide Volume 3*, North-Central Section of the Geological Society of America.
- Joint Committee on Powder Diffraction Standards (JCPDS), Berry, L.G., Post, B., Weissman, S., McMurdie, H.F. and McClune, W.F. (eds.) (1974) *Selected Powder Diffraction Data for Minerals*, Joint Committee on Powder Diffraction Standards, Philadelphia, Pennsylvania.
- Kalliokoski, J. (1982) Jacobsville Sandstone in Wold, R.J. and Hinze, W.J. (eds.) *Geology and Tectonics of the Lake Superior Basin, The Geological Society of America Memoir 156*.
- Kelletat, D. (1980) Studies on the age of honeycombs and tafoni features. *Catena*, 7: 317-325.
- Kelly, W.A. (1936) Pennsylvanian System of Michigan. *Occasional Papers on the Geology of Michigan*, no. 40.
- Knight, J.E. (1977) A thermochemical study of alunite, enargite, luzonite and tennantite deposits. *Economic Geology*, 72: 1321-1336.
- La Kind, J.D. and Stone, A.T. (1989) Reductive dissolution of goethite by phenolic reductants. *Geochimica et Cosmochimica Acta*, 53, 961-971.
- Lerman, A. (1979) *Geochemical Processes: Water and Sediment Environments*. John Wiley & Sons, New York, 481 p.

- Lewis, T.L. (1988) Late Devonian and Early Mississippian distal basin-margin sedimentation of northern Ohio. *Ohio Journal of Science*, 88: 23-39.
- Li, Y.H. and Gregory, S. (1974) Diffusion of ions in sea water and in deep sea sediments. *Geochimica et Cosmochimica Acta*: 38, 703-714.
- Livingston, R.A. (1992) Report of investigation of salt-damaged sandstone from the Willard Chapel, Auburn, New York. United States Department of Commerce National Institute of Standards and Technology Report.
- Long, D.T., Fegan, N.E., McKee, J.D., Lyons, W.B., Hines, M.E. and Macumber, P.G. (1992) Formation of alunite, jarosite and hydrous iron oxides in a hypersaline system: Lake Tyrrell, Victoria, Australia. *Chemical Geology*, 96: 183-202.
- Luther, III, G.W., Kostka, J.E., Church, T.M., Sulzberger, B. and Stumm, W. (1992) Seasonal iron cycling in the salt-march sedimentary environment: the importance of ligand complexes with Fe(II) and Fe(III) in the dissolution of Fe(III) minerals and pyrite, respectively. *Marine Chemistry*, 40, 81-103.
- Mabbutt, J.A. (1979) *Desert Landforms*. MIT Press, Cambridge, Massachusetts, 340 p.
- Malcuit, R.J. and Bork, K.B. (1987) Black Hand Gorge State nature Preserve: Lower Mississippian deltaic deposits in east-central Ohio in Biggs, D.L. (ed.) *Centennial Field Guide Volume 3*, North-Central Section of the Geological Society of America.
- McArthur, J.M., Turner, J.V., Lyons, W.B. Osborn, A.O. and Thirlwale, M.F. (1991) Hydrochemistry on the Yilgarn Block, Western Australia: Ferrolysis and mineralisation in acidic brines. *Geochimica et Cosmochimica Acta*, 55: 1273-1288.
- McConnell, D. (1976) Hypothetical phyllophosphate structure for taranakite. *American Mineralogist*, 61: 329-331.
- McFarlane, M.J. (1976) *Laterite and landscape*. Academic Press, New York, 151 p.
- McGreevy, J. P. (1984) A preliminary scanning electron microscope study of honeycomb weathering of sandstone in a coastal environment. *Earth Surface Processes and Landforms*, 10: 509-518.

- (1984) The possible role of clay minerals in salt weathering. *Catena*, 11: 169-175.
- and Smith, B. J. (1982) Salt weathering in hot deserts: observations on the design of simulation experiments. *Geografiska Annaler*, 64: 161-170.
- Meierding, T.C. (1984) Marble tombstone weathering rates in the United States. *Geological Society of America Abstracts with Programs*: 16, 592.
- Merino, E. (1984) Survey of geochemical self-patterning phenomena in Nicolis, G. and Baras, F. (eds.) *Chemical Instabilities*, 305 - 328, NATO ASI Series C: Mathematical and Physical Sciences, v. 120.
- (1986) Geochemical self-organization: Feedback, textural consequences, quantitative modeling. *GSA Abstracts with Programs*, 18, 616.
- Mottershead, D.N. (1994) Spatial variations in intensity of alveolar weathering of a dated sandstone structure in a coastal environment, Weston-super-Mare, UK in Robinson, D.A. and Williams, R.B.G. (eds.) *Rock Weathering and Landform Evolution*: 151-174, John Wiley & Sons Ltd., New York.
- Mrakovich, J.V. and Coogan, A.H. (1974) Depositional environment of the Sharon Conglomerate Member of the Pottsville Formation in northeastern Ohio. *Journal of Sedimentary Petrology*, 44: 1186-1190.
- Murray, J.W. and Dietrich, R.V. (1956) Brushite and taranakite from Pig Hole Cave, Giles County, Virginia. *American Mineralogist*, 41:616-626.
- Mustoe, G. E. (1982) The origin of honeycomb weathering. *Geological Society of America Bulletin*, 93: 108-115.
- (1984) Cavernous weathering in the Capitol Reef Desert, Utah. *Earth Surface Processes and Landforms*, 8: 517-526.
- Norton, C.W. (1979) The Sharon Conglomerate in northeastern Ohio in Donahue, J. and Rollins, H.B. (eds.) *Coal Geology of the Northern Appalachians, Field Trip Guidebook, Ninth International Congress of Carboniferous Stratigraphy and Geology*.
- Ollier, C. (1984) *Weathering*. Longman, New York.
- Ortoleva, P.J. (1984a) Modeling nonlinear wave propagation and pattern formation at geochemical first order phase transitions in Nicolis, G. and Baras, F. (eds.) *Chemical Instabilities*, 329 - 340, NATO ASI Series C: Mathematical and Physical Sciences, v. 120.

- (1984b) The self organization of Liesegang bands and other precipitate patterns in Nicolis, G. and Baras, F. (eds.) *Chemical Instabilities*, 289-297, NATO ASI Series C: Mathematical and Physical Sciences, v. 120.
- , Merino, E., Moore, E. and Chadam, J. (1987a) Geochemical self-organization I. Reaction-transport feedbacks and modeling approach. *American Journal of Science*, 287, 979-1007.
- , Chadam, J., Merino, E. and Sen, A. (1987b) Geochemical self-organization II. The reactive infiltration instability. *American Journal of Science*, 287, 1008-1040.
- Price, J.R. (1994) Geochemical mass balance models of sandstone weathering in the Pennsylvanian recharge beds of south-central Michigan. Master's Thesis, Michigan State University, East Lansing, Michigan.
- Pringle, P. (1982) Geologic study sites of the Cuyahoga Valley National Recreation Area - southern section. Unpublished Masters Thesis, University of Akron, Akron, Ohio.
- Pye, K. and Schiavon, N. (1989) Cause of sulphate attack on concrete, render and stone indicated by sulphur isotope ratios. *Nature*, 342: 663-664.
- Robinson, D.A. and Williams, R.B.G. (1994) Sandstone weathering and landforms in Britain and Europe in Robinson, D.A. and Williams, R.B.G. (eds.) *Rock Weathering and Landform Evolution*: 371-391, John Wiley & Sons, New York.
- Sakae, T. and Sudo, T. (1975) Taranakite from the Onino-Iwaya Limestone Cave at Hiroshima Prefecture, Japan: A new occurrence. *American Mineralogist*, 60: 331-334.
- Simon, J.A. and Hopkins, M.E. (1966) *Sedimentary Structures and Morphology of Late Paleozoic Sand Bodies in Southern Illinois*. Field Guidebook, AAPG Semi-Centennial Convention, St. Louis Missouri.
- Smith, B.J., Magee, R.W. and Whalley, W.B. (1994) Breakdown patterns of quartz sandstone in a polluted urban environment, Belfast, Northern Ireland in Robinson, D.A. and Williams, R.B.G. (eds.) *Rock Weathering and Landform Evolution*: 131-150.
- Smith, B. J. and McGreevy, J. P. (1983) A simulation of salt weathering in hot deserts. *Geografiska Annaler*, 65: 127-133.

- Smith P.J. and Brown, W.E. (1959) X-ray studies of aluminum and iron phosphates containing potassium or ammonium. *American Mineralogist*, 44: 138-142.
- Stoffregen, R.E. and Alpers, C.N. (1992) Observation on the unit-cell dimensions, H₂O contents, and δD values of natural and synthetic alunite. *American Mineralogist*, 77: 1092-1098.
- Stumm, W and Morgan, J.J. (1981) *Aquatic Chemistry, First Edition*. John Wiley and Sons, New York, N.Y., 780 p.
- Sultan, R., Ortoleva, P., DePasquale, F. and Tartaglia, P. (1990) Bifurcation of the Ostwald-Liesegang supersaturation-nucleation-depletion cycle. *Earth-Science Reviews*, 29, 163-173.
- Takahasi, K., Suzuki, T. and Matsukura, Y. (1994) Erosion rates of a sandstone used for a masonry bridge pier in the coastal spray zone in Robinson, D.A. and Williams, R.B.G. (eds.) *Rock Weathering and Landform Evolution*: 175-192.
- Tisza, S.T. (1956) A subsurface study of the Tar Springs Formation, Union-Webster-henderson Counties, Kentucky. Unpublished Master's Thesis, University of Illinois, Urbana, Illinois.
- Treworgy, J. and Norby, R. (1989) Carboniferous Geology of the Eastern United States: Overview of the Mississippian in the Illinois Basin in Cecil, C.B. and Eble, C. (eds.) *Coal and Hydrocarbon Resources of North America*. American Geophysical Union, Washington, D.C.
- Vargas, J. (1975) Petrogenetic study of the Black Hand Member of the Cuyahoga Formation (Mississippian) in central Ohio. Unpublished Masters Thesis. Ohio University, Cincinnati, Ohio.
- Velbel, M.A. and Brandt, D.S. (1989) Sedimentology and paleogeography of the Pennsylvanian strata of Grand Ledge, Michigan: Michigan Basin Geological Society Field Trip Guidebook, 33 pp.
- Velbel, M.A., Price, J.R., Brandt, D.S. (1994) Sedimentology, paleogeography, and the geochemical weathering of the Pennsylvanian strata of Grand Ledge, Michigan. Field guide for the Eastern Section AAPG Annual Meeting Field Trip and Great Lakes Section - SEPM 24th Annual Fall Field Conference.

- Wallis, J. and Velbel, M.A. (1985) Honeycomb weathering of Pennsylvanian sandstones, Grand Ledge, Michigan. *Geological Society of America Abstracts with Programs*, 26:1330.
- Wallis, J. (1986) Honeycomb Weathering at Grand Ledge, Michigan. Unpublished Manuscript.
- Weast, R.C. (ed.) (1979) *CRC Handbook of Chemistry and Physics*. CRC Press, Inc., Boca Raton Florida, p. F-56.
- Weller, S. (1921) *Geology of the Golconda Quadrangle*. Kentucky Geological Survey, Frankfort, Kentucky.
- Wellman, H.W. and Wilson, A.T. (1965) Salt weathering, a neglected geological erosive agent in coastal and arid environments. *Nature* 205: 1097-1098.
- Wellman, H.W. and Wilson, A.T. (1968) Salt weathering or fretting, in *The Encyclopedia of Geomorphology*, Fairbridge, R.W. ed., Reinhold Book Corporation, New York.
- Wescott, W.A. (1982) Depositional history of the Tar Springs Sandstone (Upper Mississippian), southern Illinois. *Journal of Sedimentary Petrology*, 52: 353-366.
- Whaley, P.W., Hester, N.C., Williamson, A.D., Beard, J.G., Pryor, W.A. and Potter, P.E. (1979) *Depositional Environments of Pennsylvanian Rocks in Western Kentucky*. Field Guidebook, Annual Field Conference of the Geological Society of Kentucky, University of Kentucky, Lexington, Kentucky.
- Williams, P.A. (1990) *Oxide Zone Geochemistry*. Ellis Horwood, New York, 286 p.
- Williams, R.B.G. and Robinson, D.A. (1989) Origin and distribution of polygonal cracking of rock surfaces. *Geografiska Annaler*, 71A, 145-159.
- Wier, C.E. and Esarey, R.E. (1951) *Pennsylvanian Geology and Mineral Resources of West Central Indiana*. Field Guidebook Fifth Annual Indiana Geologic Field Conference, Department of Geology, Indiana University.
- Wiese, R.G., Powell, M.A. and Fyfe, W.S. (1987) Spontaneous formation of hydrated iron sulfates on laboratory samples of pyrite- and marcasite-bearing coals. *Chemical Geology*, 63: 29-38.

- Winkler, E.M. (1994) *Stone in Architecture*. Springer-Verlag, Berlin, Germany, 313p.
- (1965) Weathering rates as exemplified by Cleopatra's Needli in New York City. *Journal of Geological Education*: 13-14, 50-52.
- and Singer, P.C. (1972) Crystallization pressure of salts in stone and concrete. *Geological Society of America Bulletin*, 83, 3509-3514.
- Wright, V.P., Sloan, R.J., Valero, G.B., Garvie, L.A. (1992) Ground water ferricretes from the Silurian of Ireland and Permian of the Spanish Pyrenees. *Sedimentary Geology*, 77, 37-49.
- Young, A. R. M. (1987) Salts as an agent in the development of cavernous weathering. *Geology*, 15: 962-966.
- Zehnder, K. and Arnold, A. (1989) Crystal growth in salt efflorescence. *Journal of Crystal Growth*, 97: 513-521.

MICHIGAN STATE UNIV. LIBRA



3129301413362